ИЗВЕСТИЯ ВЫСШИХ УЧЕБНЫХ ЗАВЕДЕНИЙ.
Т 68 (2) Серия «**ХИМИЯ И ХИМИЧЕСКАЯ ТЕХНОЛОГИЯ**» 2025
V 68 (2) **ChemChemTech** 2025

DOI: 10.6060/ivkkt.20256802.7002

ОЦЕНКА ПРОГРЕССА ИССЛЕДОВАНИЙ, ТЕНДЕНЦИЙ И ПРИМЕНЕНИЯ ПЛЕНОК ЛЕНГМЮРА-БЛОДЖЕТТ НА ОСНОВЕ ЖИРНЫХ КИСЛОТ

Тхи Тхао Ву, Чи Дык Лыонг, Дык Куонг Нгуен, Ву-Тоан Ле, Тхи Тху Тхуй Буй, Дык Донг Чан, Тхи Хоа Хоанг, Зуй Минь Ву, Д.Б. Березин

Чи Дык Лыонг (ORCID 0009-0002-3503-5089)*

Университет Южной Флориды, 4202 Э. Фаулер Авеню, Тампа, Флорида, США, 33620
E-mail: luongtriduc2005@gmail.com*

Ву Тхи Тхао (ORCID 0009-0008-4021-849X), Дык Кыонг Нгуен (ORCID 0000-0001-8128-2174), Тхи Тху Тхуй Буй (ORCID 0009-0003-4823-0825), Дык Донг Чан (ORCID 0009-0008-9357-6151), Тхи Хоа Хоанг (ORCID 0009-0008-1947-9505), Зуй Минь Ву (ORCID 0009-0006-3826-3596)

Инженерно-технологический Университет Вьетнамского Национального Университета, Ханоя (VNU-UET), E3, 144 Суан Тхуи, Кау Зьай, Ханой, Вьетнам, 100000
E-mail: vtthao@vnu.edu.vn, cuongnd@vnu.edu.vn

Дмитрий Борисович Березин (ORCID 0000-0001-5814-9105)

Ивановский государственный химико-технологический университет, Шереметевский пр., 7, Иваново, Российская Федерация, 153000
E-mail: berezin@isuct.ru

Ву-Тоан Ле (ORCID 0000-0002-0078-1789)

Вьетнамский институт научных технологий и инноваций Министерства науки и технологий, улица Дай Ко Вьет, 01, Хай Ба Чынг, Ханой, Вьетнам, 100000
E-mail: toan.lv.2023@gmail.com

Метод Ленгмюра-Блоджетт привлекает значительное внимание благодаря своей способности формировать наноструктурированные пленки из многих материалов с их контролируемым составом и толщиной. Современная технология Ленгмюра-Блоджетт постоянно разрабатывает новые технические возможности и исследуемые материалы для получения тонких наноструктурированных пленок с заданными свойствами. Однако пленки Ленгмюр-Блоджетт жирных кислот считаются одними из наиболее распространенных и наиболее изученных наноматериалов, применяемых в различных областях. Несмотря на их популярность и недавние достижения, современный обобщающий обзор по этой теме не был представлен в литературе. В этом исследовании дан анализ литературы по пленкам жирных кислот с использованием библиометрического метода с привлечением данных Scopus в течение 22 лет (2002–2023 гг.). Целью публикации является предоставление всестороннего обзора данных в рассматриваемой области, тенденций ее развития и возможных применений. Приведен анализ факторов, влияющих на свойства и потенциал применения пленок Ленгмюр-Блоджетт жирных кислот, а также необходимость расширения гибридных соединений на их основе для практического применения. В обзоре отмечается тенденция к расширению международного сотрудничества в области исследований тонких пленок.

Ключевые слова: Ленгмюр-Блоджетт, жирная кислота, библиометрический анализ, тонкая пленка, наноструктурированные пленки

EVALUATION OF RESEARCH PROGRESS, TRENDS, AND APPLICATIONS OF LANGMUIR-BLODGETT FILMS OF FATTY ACIDS

Thi Thao Vu, Tri Duc Luong, Duc Cuong Nguyen, Vu-Toan Le, Thi Thu Thuy Bui, Duc Dong Tran, Thi Hoa Hoang, Duy Minh Vu, D.B. Berezin

Tri Duc Luong (ORCID 0009-0002-3503-5089)*

University of South Florida, 4202 E. Fowler Avenue, Tampa, FL, USA, 33620
E-mail: luongtriduc2005@gmail.com*

Thi Thao Vu (ORCID 0009-0008-4021-849X), Duc Cuong Nguyen (ORCID 0000-0001-8128-2174), Thi Thu Thuy Bui (ORCID 0009-0003-4823-0825), Duc Dong Tran (ORCID 0009-0008-9357-6151), Thi Hoa Hoang (ORCID 0009-0008-1947-9505), Duy Minh Vu (ORCID 0009-0006-3826-3596)

University of Engineering and Technology, Vietnam National University, Hanoi, E3, 144 Xuan Thuy, Cau Giay, Hanoi, Vietnam, 100000
E-mail: vtthao@vnu.edu.vn, cuongnd@vnu.edu.vn

Dmitry B. Berezin (ORCID 0000-0001-5814-9105)

Ivanovo State University of Chemistry and Technology, Sheremetevskiy ave., 7, Ivanovo, 153000, Russia
E-mail: berezin@isuct.ru

Vu-Toan Le (ORCID 0000-0002-0078-1789)

Vietnam Institute of Science Technology and Innovation, Ministry of Science and Technology, 01 Dai Co Viet Street, Hai Ba Trung, Hanoi, Vietnam, 100000
E-mail: toan.lv.2023@gmail.com

The Langmuir-Blodgett method has attracted significant attention due to its ability to form nanostructured films from many materials with precise film composition and thickness control. The modern Langmuir-Blodgett (LB) technique has continually developed novel methods and materials to fabricate nanostructured thin films. However, Fatty acid films fabricated by the Langmuir-Blodgett are considered one of the most common, earliest, and most studied nanomaterials applied in different fields. Despite their popularity and recent advances, a contemporary review on this topic has not been available to summarize published literature. This study reviews prior research on fatty acid film literature incorporating Bibliometric Analysis from Scopus during 22 years (2002 – 2023) to provide a comprehensive review concerning the significant contribution of the field, its trends, and applications. The results provide an overview of factors affecting the properties and application potential of fatty acids and a need for the extension of fatty acids-based hybrid compounds for practical applications. Also, the review suggests a trend in increase of the international research collaboration in the field of thin films.

Keywords: Langmuir-Blodgett, fatty acid, thin films, nanostructured films, bibliometrics analysis

Для цитирования:
Тхи Тхао Ву, Чи Дык Лыонг, Дык Куонг Нгуен, Ву-Тоан Ле, Тхи Тху Тхуй Буй, Дык Донг Чан, Тхи Хоа Хоанг, Зуй Минь Ву, Березин Д.Б. Оценка прогресса исследований, тенденций и применения пленок Ленгмюра-Блоджетт на основе жирных кислот. *Изв. вузов. Химия и хим. технология*. 2025. Т. 68. Вып. 2. С. 6–45. DOI: 10.6060/ivkkt.20256802.7002.

For citation:
Thi Thao Vu, Tri Duc Luong, Duc Cuong Nguyen, Vu-Toan Le, Thi Thu Thuy Bui, Duc Dong Tran, Thi Hoa Hoang, Duy Minh Vu, Berezin D.B. Evaluation of research progress, trends, and applications of Langmuir-Blodgett films of fatty acids. *ChemChemTech [Izv. Vyssh. Uchebn. Zaved. Khim. Khim. Tekhnol.]*. 2025. V. 68. N 2. P. 6–45. DOI: 10.6060/ivkkt.20256802.7002.

INTRODUCTION

The Langmuir-Blodgett (LB) method refers to a fabrication technique used to create thin film materials on the nanoscale, which allows film thickness to be controlled and ordered material structure to be maintained [1-4]. LB films were rooted in Pockel's early article [5] on oil surface contamination. A basic LB film is formed at the interface by the spreading of an amphiphilic molecule on the water subphase, followed by

the compression of the spread amphiphile to form a condensed film and subsequently transferred onto a substrate [6]. Complex LB films having more layers can be formed by adding the same or different material onto the pre-existing layers [7-10]. The LB method offers versatility in material choice [11-14], resulting in a wide range of applications such as sensors [14-16], semiconductors [17-19], biomaterials [8, 20, 21], batteries [22, 23] and optical applications [24-26].

Prior studies have discussed new materials for LB film formation [27-29]. Makiura [11] reviewed metal-organic frameworks (MOFs) for film fabrication, focusing mainly on preparation, isotherm characteristics, characterization (UV-Vis, infrared and X-ray spectra, atomic force microscopy (AFM)), and fabrication aspects of porphyrin and triphenylene-based nanosheets. Guo and Briscoe [30] focused on a review of LB films' bacterial-lipid monolayers, which discussed basic isotherm characteristics, permeability, film flexibility, and its potential for application as an *in vitro* membrane. Although these reviews highlighted advanced areas of film material and architectures, older film materials such as fatty acids remain highly relevant as a mainstay of the LB film and method [31-33].

Natural fatty acids are defined as aliphatic monocarboxylic acids commonly containing a carbon chain of 4 to 28 carbons that are usually unbranched [34]. It is one of the earliest materials in the LB literature, which is a form of fatty acid/lipid [5, 35]. Fatty acids can either be saturated or unsaturated, depending on the presence of double or triple bonds. The fatty acid's structure (a carboxylic group attached to a long carbon chain) confers its amphiphilic behaviors that are tied to the LB method [36]. This fundamental acid has a wide range of applications, including metal binders [37], tribological lubricants [32, 38], and structural film for different materials [39, 40].

The most recent review of fatty acids conducted by Peng [41] provides a comprehensive review of the field. The authors discussed the chain orientation, structure, substrate effects, the correlation between floating solid films and thermal effects, and the stability of fatty acid films in monolayer and multilayer forms. Since Peng's work, no specific and targeted review has been conducted to summarize recent advances in LB fatty acid films. Since Peng's publication [41], there has been no attempt at an updated summary of published fatty acid film literature, leaving a 22-year gap (2002-2023) that needs to be reviewed to provide a complete picture of the field development and its potential.

In this study, we use bibliometric analysis to analyze articles related to LB films of fatty acids between 2002 and 2023 to (i) identify key metrics such as annual scientific production, prominent authors, and international collaboration, (ii) identify and review high-impact and highly cited articles within our bibliometric database, and (iii) identify and review major and potential application areas of fatty acid films.

The bibliometric analysis uses software such as Bibliometrix and VOSviewer to extract some meaningful statistics (e.g. the number of publications, international collaboration, keyword analysis, scientific productivity, and author information), summarize existing clusters of research topics, and explore emerging research topics from collected bibliometric data (e.g authors, publication date, and total citations) from an online database (e.g. Scopus, Web of Science, Dimensions, etc.) [42, 43]. This method has emerged as a powerful tool to review and analyze a large number of scientific publications, which have traditionally been applied in the social sciences [44-46] such as environmental science [47, 48], economics [49, 50], and healthcare [51, 52]. Recently, bibliometric analysis has been employed to review literature in natural science, including chemistry [53, 54], mathematics [55], and materials science [56-60].

This work aims to answer three research questions:

Q1: What is the current state of the field?

Q2: What advances in the areas concerning film deposition, properties, and applications have been made in recent years?

Q3: What are future prospects for the field?

The first research question will be assessed by a narrative review by extrapolating data and trends from reviewed articles combined with bibliometric analysis of the published literature using available tools and software to allow for complete visualization of the state of the field.

The second research question will be answered by the bulk of the literature review within the body of this article. Finally, the third research question will be answered by the last section of this review, which discusses the literature and future prospects.

INTRODUCTION TO THE LANGMUIR-BLODGETT METHOD

History of the Langmuir-Blodgett method

The first reported sighting of a thin molecular film was reported by Benjamin Franklin in 1774 when he dropped oil into a pond and witnessed the spread of the oil. In the late 19th century, Agnes Pockels [5] experimented in her kitchen to devise a version of the modern-day Langmuir-Blodgett trough. Around the same time, Lord Rayleigh quantified Franklin's earlier experiment and calculated that the film was about one

molecule thick (around 1.6 nm). Agnes Pockels later sent a letter to Lord Rayleigh, and he supported her work, helping her publish in the journal Nature in 1891, building the foundation for further research.

However, the films and method are now named the Langmuir-Blodgett (LB) method in memory of Irving Langmuir and his assistant Katherine Blodgett's systematic studies on film materials and experimental setups. In 1932, Langmuir received a Nobel Prize in Chemistry for his work on surface science. He and Katherine continued to refine their experimental techniques, many of which are utilized today.

Since then, the LB method has been improved with better experimental apparatus and an increased understanding of film synthesis. The range of materials has expanded to include surfactants [61-63] biological compounds [64-66], ions complexes [67-69] and inorganic compounds [70-72].

Surfactants

Surfactants are molecules that reduce tension between two surfaces (liquid-gas/ liquid-liquid) due to their structural properties. The general structure of a surfactant consists of a hydrophilic and a hydrophobic part. The hydrophilic part is attracted toward the liquid, while the hydrophobic part moves away from the liquid. This machine pulls the surfactant molecule to the top surface layer, where the attraction between one surfactant molecule to the bulk material is less than the attraction between bulk material molecules. As a result, the surfactant decreases the surface tension [73].

There are three main types of surfactants [74], classified according to their hydrophilic part.

1. Non-ionic surfactants: Surfactants that carry no charge on their hydrophilic head.

2. Ionic surfactants: Surfactants that carry charge on their hydrophilic head. Further classified into anionic and cationic types according to charge.

3. Amphoteric surfactants: Surfactants that carry both anionic and cationic charges on their surface active part and exhibit properties of both anionic and cationic properties.

Surfactants are used extensively in the Langmuir-Blodgett method. The role of surfactants in the Langmuir-Blodgett method ranges from primary film material [32, 75-77] to a tool for transferring other particles onto the surface [78-81].

Fatty acids are carboxylic acids with a long carbon chain as surfactants. A complete definition of fatty acids can be found in IUPAC's documents [34]. The long carbon chain provides unique properties to fatty acids that are unobserved in short-chain carboxylic acids. One of the most important properties they exhibit is their hydrophobic tendencies due to their large molecular weight and the water-repelling carbon chain. However, their carboxyl group provides hydrophilic interactions, and as a result, these fatty acid compounds exhibit what is known as amphiphilic properties (Fig. 1).

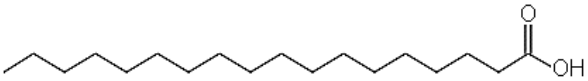

Fig. 1. Stearic acid, a common material in many Langmuir-Blodgett studies

Рис. 1. Стеариновая кислота, распространенный материал во многих исследованиях Ленгмюра-Блоджетт

LB films of fatty acids is the precursor to today's modern LB method. With pioneers like Pockels, Langmuir, and Blodgett, research into pure fatty acid films has been boosted. Since then, a wide body of literature has been published, detailing many aspects of a pure fatty acid film.

Subphase

The subphase is the liquid bulk used in Langmuir-Blodgett experiments. However, experiments are not restricted to the water subphase. The subphase can be modified to change its behavior, for example, by adding ions or changing the pH value and temperature [75, 82-90].

Additionally, the subphase provides a different pathway for film fabrication. In the case of tungsten trioxide electrochromic films, the water subphase was used to dissolve tungsten oxides, which were then collected using appropriate surfactant molecules to form a film [70].

Spreading solvent

The spreading solvent is a chemical that is used to transfer and facilitate the uniform spreading of film material on the subphase surface. In the case of most Langmuir-Blodgett experiments, the spreading solvent should fulfill two properties:

1. The ability to rise to the surface of the subphase (not miscible with subphase).

2. The ability to spread evenly on the surface

Thus, non-spreading solvents like hexane are not commonly used in experiments while chloroform is extremely popular. Additionally, the evaporation time for a solvent may be considered. There is a certain threshold for each specific solvent that when reached, will deter the solvent from effectively spreading on the subphase. This threshold is further modified by environmental and pre-existing conditions like subphase properties, surface-active agents, and the presence of ions within the subphase. A model for understanding the spreading of solvents in Langmuir-Blodgett experiments has been developed elsewhere [91].

Langmuir-Blodgett film formation

The Langmuir-Blodgett method operates on the principle of molecular attraction between molecules to fabricate a film. As the material is spread on the subphase surface, the distance between each molecule is large, preventing any meaningful attraction. The method seeks to compress, or shorten this distance, so that the molecules may form a stable film. This underlying principle is represented through the state of the film and surface pressure [92].

The surface pressure of the film is calculated by:

$$\Pi_{film} = \Pi_{subphase} - \Pi_o$$

where Π_{film} is the surface pressure of the system containing only the Langmuir-Blodgett film, $\Pi_{subphase}$ is the surface pressure of the system containing only the subphase (measured before experiments), and Π_o is the surface pressure of the system that consists of the subphase and the film. The surface pressure of the film increases when the system's pressure decreases as the layer of surfactants begins to form.

The general state of the film is shown below:

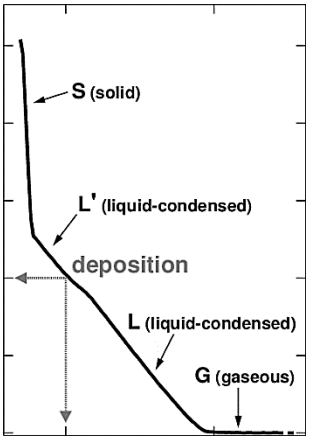

Fig. 2. Surface pressure diagram of stearic acid [93]
Рис. 2. Диаграмма поверхностного давления стеариновой кислоты [93]

At the lowest pressures, the film exists in a gaseous state (Fig. 2). As the layer gets compressed, the distance decreases as the film approaches a liquid state. At its densest concentration, the film exists in a solid state. Past this solid state, the film enters its collapsed form, where the 2D structure is disrupted due to film tension affecting film integrity, forming micelles, 3D structures, and crystals [94].

Langmuir-Blodgett and Langmuir-Schaefer deposition

The film forming solution (usually a volatile organic compound that evaporates quickly and has good spreading capabilities [91] containing the film material) is first spread on the subphase surface. After the solvent has mostly evaporated, the mechanism begins to move the barrier(s) toward the center of the Langmuir-Blodgett trough. As the barrier moves, the space between molecules becomes compressed. The subphase surface tension decreases as the degree of compression increases due to fewer subphase molecules occupying the surface layer. At the desired degree of compression, the barrier movement will be stopped and deposition can begin. Note that immediately after film compression ceases, the film will begin to reorient to minimize energy and a change in surface pressure may be noticed.

There are two popular method of film deposition: Langmuir-Blodgett (vertical) and Langmuir-Schaefer (horizontal) (Fig. 3). In addition, the technology of transferring floating layers to the solid substrate by roll-to-roll has recently been developed (Fig. 4). As the substrate is lowered into the film, the barrier moves correspondingly and the film is pushed onto the substrate in the case of Langmuir-Blodgett deposition. The barrier stays constant during a Langmuir-Schaefer deposition [1]. After drying, the end result is a film made of the chosen material on the substrate surface.

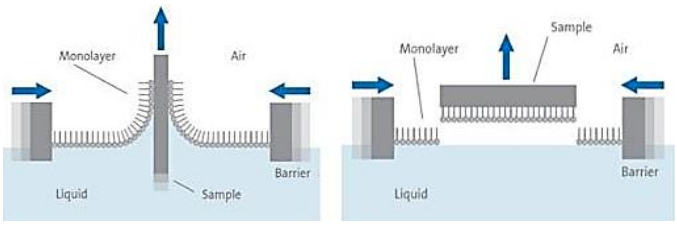

Fig. 3. Deposition of a floating monolayer onto a hydrophilic solid substrate
Рис. 3. Нанесение плавающего монослоя на гидрофильную твердую подложку

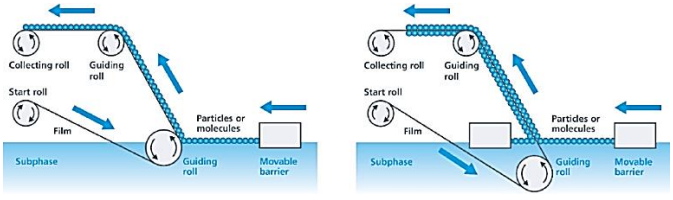

Fig. 4. Roll-to-roll deposition
Рис. 4. Нанесение рулонного материала

Common characterization techniques and equipment

Langmuir-Blodgett films can be characterized during floating layer formation by using built-in tools on many systems such as the Brewster Angle Microscope (BAM) built-in on some KSV Nima systems and through a universal surface pressure and molecular area isotherm that is universal for all studies within the field.

For further characterization, tools like the scanning electron microscope (SEM) and the atomic force microscope (AFM) offer great insights into film morphology. If one wishes to study the spectral properties of the film, tools like the UV-Vis spectra and Fourier-transform infrared spectroscopy (FTIR) are available. For special films that contain crystalline phases, it is possible to utilize many X-ray techniques to ascertain the structure. While the techniques mentioned here are the most commonly seen, this is by no means comprehensive (Table 1).

Table 1

Method for characterization floating layer and solid film obtained by Langmuir-Blodgett technique

Таблица 1. **Метод характеризации плавающего слоя и твердой пленки, полученной методом Ленгмюра-Блоджетт**

Floating layers	Solid LB thin film
Thermal analysis (Pi-A)	Morphology: scanning electron microscope (SEM), Field emission scanning electron microscope (FE-SEM), transmission electron microscope (TEM), atomic force microscope (AFM)
Brewster Angle Microscopy (BAM)	Optical: Ultraviolet-visible spectroscopy UV-Vis, Photoluminescence Spectroscopy (PL), Fourier-transform infrared spectroscopy (FTIR), Polarized optical microscopy (POM)
Surface Potential Sensor	Thermal: Differential scanning calorimetry (DSC), Differential Thermal Analysis (DTA)
Interfacial Shear Rheometer (ISR Flip)	Hydrophilic & hydrophobic surface: Contact angle
	Structure: X-ray diffraction (XRD)
	Elastic modulus (E): estimated from isotherm

BIBLIOMETRIC REVIEW

Methodology

Employment of the bibliometric analysis enables large volumes of published literature to be reviewed [95, 96], to identify trends and patterns of a topic over a long period [97, 98]. This approach offers a clear article search methodology to improve credibility and replication [99], which consists of three sequential steps: data collection, data extraction, and data analysis [98]. First, Elsevier's Scopus database with a huge amount of natural science publications was selected due to its extensibility and reliability [100-103]. Second, clean extracted data was inputted into Bibliometrix (R Studio, version 4.1.3), and VOSviewer (version 1.6.19) [104-107]. Besides that, VOSviewer and Bibliometrics were used to graph data, and Excel 2019 was used to screen data. Finally, the extracted graphs were converted into meaningful charts and graphics for data analysis by following the general analysis guideline applied in prior high-impact articles in the field of natural sciences [56, 108].

Data collection and extraction

With Scopus as the chosen database, the time period for the search was narrowed to the period between 2002 and 2023 considering Peng's review [41] in 2001. We limited the document type and language to English research articles only to ensure a quality and accurate understanding of the reviewed material. We excluded research areas that are out of the scope of this study as follows [109]:

(EXCLUDE (SUBJAREA, "VETE") OR EXCLUDE (SUBJAREA, "NURS") OR EXCLUDE (SUBJAREA, "MATH") OR EXCLUDE (SUBJAREA, "NEUR") OR EXCLUDE (SUBJAREA, "SOCI") OR EXCLUDE (SUBJAREA, "HEAL") OR EXCLUDE (SUBJAREA, "COMP") OR EXCLUDE (SUBJAREA, "BUSI") OR EXCLUDE (SUBJAREA, "PSYC") OR EXCLUDE (SUBJAREA, "ECON") OR EXCLUDE (SUBJAREA, "EART")).

To ensure the data relevancy to this study scope, the final sample of 1,229 articles was mass-filtered in Excel 2019 using the Find function to highlight all articles with "fatty acid" and "carboxylic acid" in their titles or abstracts. All articles that do not contain "fatty acid" were removed, resulting in 430 articles remaining, which subsequently were manually reviewed in terms of title and abstract to ensure strict adherence to the LB fatty acid film topic. This manual process led to 129 irrelevant articles being removed, and 301 articles retained for bibliometric analysis.

Results

Publication volume

The study of LB fatty acids appears to be less attractive to scholars, having a negative annual growth rate of 8.85% from 2002 to 2023 (Fig. 5). This field experienced a gradual increase in publications for the 2002-2010 period with a total of 161 articles accounting for 53.49% of the total articles, especially in 2007 and 2010 with 24 articles published. However, the number of articles gradually decreased between 2011 and 2023 with the highest number of publications in 2014 (15 articles), which possibly indicates falling interest towards fatty acid films in the last decade.

Publications by country

The LB method and LB fatty acid films specifically have spread widely across the world, excluding

Africa. Fig. 6 shows the countries with a higher number of publications in the field of fatty acids in deeper blue. The leading countries in the field of fatty acids are the United States, France, Spain, China, India, and Japan.

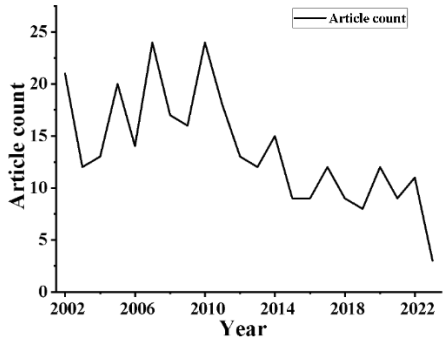

Fig. 5. Annual scientific production
Рис. 5. Годовой объем научной продукции

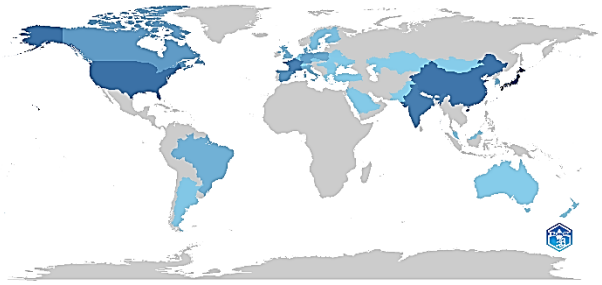

Fig. 6. Scientific production world map
Рис. 6. Карта мира научного производства

Regarding total publication, Japan was ranked first with 182 articles, followed by the United States with 129 articles, then China with 123 articles while the British authors published only 33 articles. Articles of American authors were cited the most with total citations of 624, which was much higher than that of Japanese researchers, and nearly doubled total citations of Chinese ones (Table 2).

Table 2

Leading countries in the field of LB films of fatty acids
***Таблица 2.* Страны-лидеры в области ЛБ-пленок жирных кислот**

Country	Total publications	Total citations
Japan	182	479 (#2)
USA	129	624 (#1)
China	123	330 (#5)
India	110	189 (#7)
France	104	278 (#6)
Spain	77	180 (#9)
Canada	69	455 (#3)
Germany	59	156 (#10)
Poland	48	426 (#4)
UK	33	183 (#8)

Leading authors

10 well-known authors in the field of fatty acids field since 2002 are shown in Fig. 7. Paige F. Matthew from the University of Saskatchewan had the highest publication volume on fatty acids with 10 articles. His work is concerned with Langmuir films and surface science [110, 111], Gemini surfactant films [112], and the effect of perfluorotetradecanoic acid on a phospholipid monolayer on the air-water interface [113].

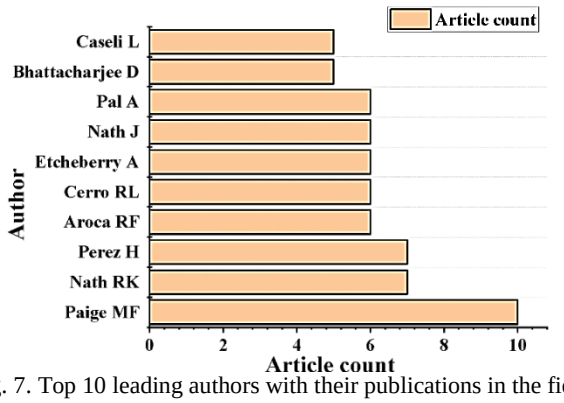

Fig. 7. Top 10 leading authors with their publications in the field of fatty acids
Рис. 7. Топ-10 ведущих авторов с публикациями в области жирных кислот

The only two authors who published articles recently (2020-2023) were Paige MF and Caseli L (Fig. 8). These 10 authors still stay in the LB films, but they show their interest in more complex organic nanostructured film [114-117].

Leading journal in the field of fatty acids

The top 5 leading journals publishing fatty acids research have an H-index ranging from 8 to 18. The highest-ranked journal is Langmuir (H-index = 18), which has traditionally been well-known for its influential publications in general surface science, polymers, and overall physical/chemical engineering of materials at interfaces with 48 articles. Other journals on the list are also dedicated to surface materials such as Thin Solid Films (H-index = 7) with 17 articles, Colloids and Surfaces A (H-index = 12) with 23 articles, and Journal of Colloid and Interface Science (H-index = 8) with 16 articles. Outside of surface science, only general chemistry journals such as Journal of Physical Chemistry B (H-index = 15) with 26 articles. Since 2020, only Langmuir and the Journal of Colloid and Interface Science maintained their average publication related to fatty acids per year (about 3 articles for the former and about 1 article for the latter). Other journals appear to publish fewer articles on LB films of fatty acids than before 2020 (see Fig. 9).

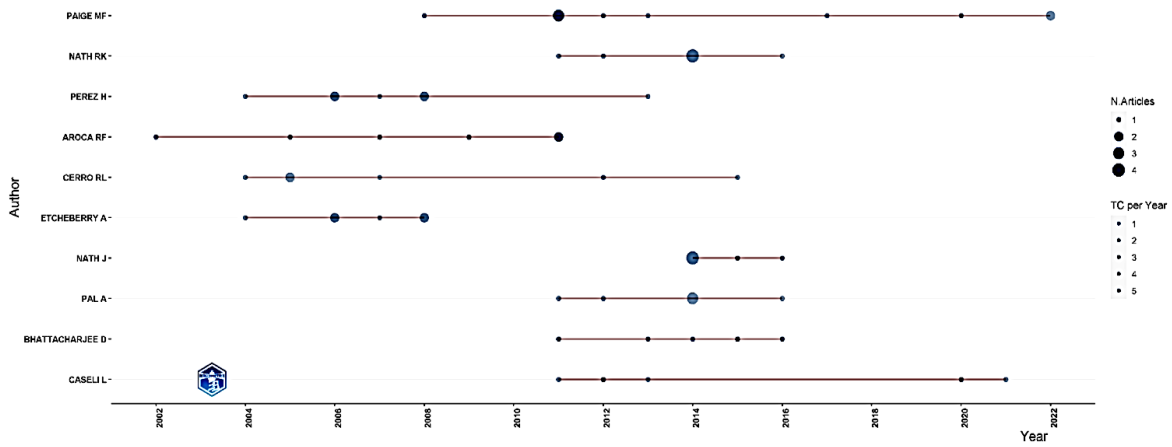

Fig. 8. Publications of leading authors by years
Рис. 8. Публикации ведущих авторов по годам

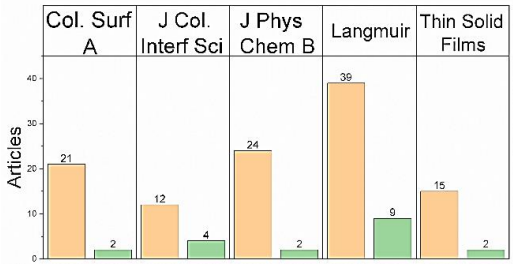

Fig. 9. Five leading journals in LB films of fatty acid research (before 2020 in orange, from 2020 in green, https://ctj-isuct.ru/article/view/6239/3617)
Рис. 9. Пять ведущих журналов в области исследований жирных кислот в LB-пленках (до 2020 г. выделены оранжевым цветом, с 2020 г. – зеленым, https://ctj-isuct.ru/article/view/6239/3617)

International collaboration

Collaborations between countries in terms of their strengths are presented in Fig. 10. Leading countries tend to build their networks of collaborations. American researchers frequently collaborated with Spain, Canada, Poland, and Brazil (red cluster) while France maintains its collaborations with India, Israel, and Russia (green cluster). Japan has built its research network with China, the United Kingdom, and South Korea (blue cluster) while Germany mainly collaborated with Denmark (yellow cluster).

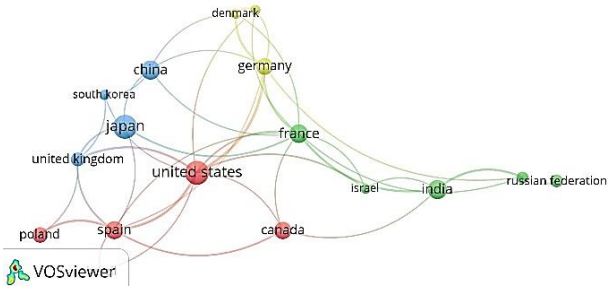

Fig. 10. Collaboration between countries exported from VOSviewer
Рис. 10. Сотрудничество между странами, экспортированными из VOSviewer

Author co-citation network

The co-citation network of authors with 50 minimum citations is shown in Fig. 11. Co-citation is when articles are cited together in another publication; connected items on the co-citation network are cited together more. Authors who are cited together often work on similar themes, divided into clusters.

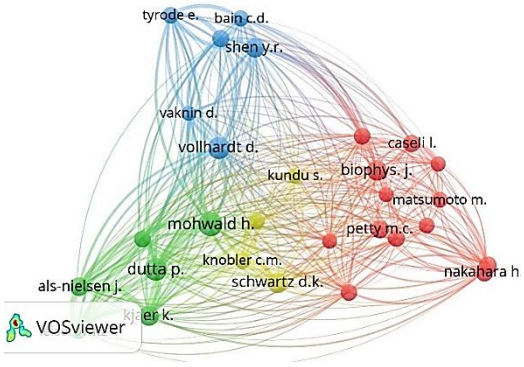

Fig. 11. Network of author co-citation
Рис. 11. Сеть авторского социтирования

In the graphic, we can observe four distinct clusters: red, yellow, green, and blue. The red cluster contains key authors Petty MC and Oliveira Jr., who published many fundamental reviews and books on LB film technology [1, 92, 118-121], thus they are often cited together. In the yellow cluster, DK Schwartz publishes reviews of the LB technique [122-125] and other fundamental aspects of LB films of fatty acids [126-128] while CM Knobler publishes on fundamental experiments and LB film theory [129-131]. The blue cluster contains key authors D Vollhardt, who publishes fundamental aspects of LB films [132-134], and YR Shen, who publishes on interface science, specializing in surface vibrational spectroscopy and sum-frequency generation [135-138]. YR Shen, who can be considered the pioneer for sum-frequency generation and vibrational

techniques in surface science and LB fields in particular, had multiple of multiple highly-cited articles of which [135] on second-harmonic and sum-frequency generation for surface science achieved over 2800 citations. Finally, the green cluster contains key authors, nasmely H Mohwald and P Dutta, who published on basic metal ions such as iron [139], lead and cadmium [140], and magnesium [141]. H Mohwald who publishes reviews on LB films, and concerning metal ions in LB films [89, 142-144]. P Dutta publishes on metal ions [139, 140], and organic molecules [145, 146].

Author keywords co-occurrence analysis

Fig. 12 shows the analysis of the author keywords via co-occurrence (i.e. analysis by the degree that keywords appear together), divided into 4 clusters. The yellow cluster contains basic fatty acid film materials together with basic characterization "contact angles" and "surface free energy". The blue cluster contains the central keyword "langmuir monolayers" and also contains film material "linoleic acid" as well as methods "brewster angle microscopy" and "photopolymerization". The green and red clusters show some overlap, possibly due to the similar composition of the two clusters. Both clusters contain characterization methods "xps", "afm" and film materials "perfluorocarbon", "palmitic acid", and "lipid bilayer".

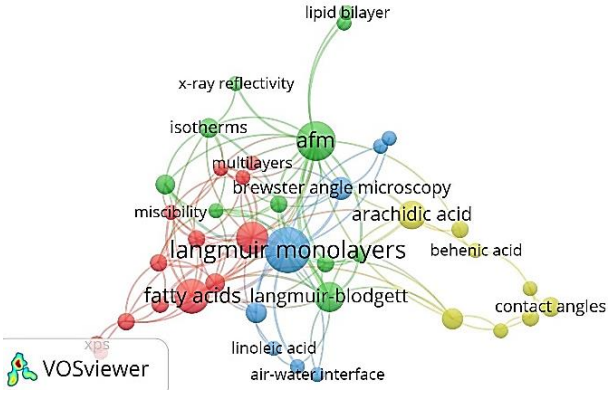

Fig. 12. Author keywords co-occurrence network
Рис. 12. Авторская сеть совпадения ключевых слов

Fig. 13 shows the time overlay for Fig. 12. The central keyword "langmuir monolayers" is a light green color, indicating the time value of approximately 2014 and demonstrating the recent relevancy of the general topic. The red cluster in Fig. 12 has a range of keywords throughout time, with nodes such as "xps" standing for old characterization methods, "fatty acids" as a general topic with a time value of approximately 2012, and newer keywords such as "palmitic acid" and "perfluorocarbon". The variety of keyword time values indicates an established research area in the dataset. A similar trend is seen in the green cluster, where there is a good mix of old concept keywords "phase separation" and newer keywords "isotherms". Another notable feature is the yellow node in Fig. 12, which is deep blue in Fig. 13. We speculate that the yellow cluster relates to fundamental studies in fatty acid films, which explains the old age of the cluster.

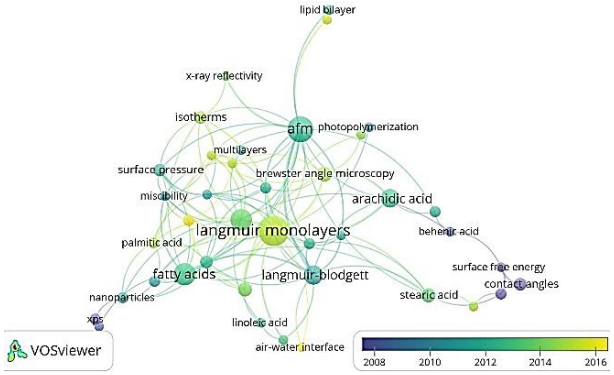

Fig. 13. Author keywords co-occurrence network over time
Рис. 13. Сеть повторения ключевых слов авторов во времени

Table 3 presents a complete list of keywords, date ranges, and topics for each cluster shown in Fig. 12. Clusters 1 and 4 appeared relatively early (2005 and 2003) while clusters 2 and 3 appeared in the 2010s (2011 and 2010). All clusters continued to be researched in recent years (2014 to 2017), showing a degree of interest by researchers. No keywords later than 2017 appeared in VOSviewer, probably due to their novelty and low citation count, which was filtered out by VOSviewer when applying the analysis parameters.

There are overlaps between clusters in terms of keywords. Common overlaps include:

i - BAM – Brewster angle microscope/microscopy: A characterization technique used for viewing the films during formation, available as an add-on in some Langmuir trough models such as KSV NIMA.

ii - Different types of fatty acids (arachidic, behenic, stearic, linoleic, palmitic acid): Similar long-chain carboxylic acids with the ability to form stable LB films.

Fig.14 shows the most cited articles during the period (2002-2023).

These most cited articles are classified into 04 clusters (Table 3) as follows:

Red cluster: This cluster focuses on DPPC and perfluorocarbons. The highest cited publication was an article entitled "Chitosan as a lipid binder: A Langmuir monolayer study of chitosan-lipid interactions" written by Wydro [147], discussing the properties and interactions of chitosan on fatty acid and lipid Langmuir layers. The surface-pressure area isotherm showed limited film expansion due to chitosan molecules. Stearic acid has the lowest limit, while linoleic and alpha-linoleic

films exhibited the highest values. Compression modulus was affected by chitosan, decreasing for stearic acid and cholesterol while slightly increasing for all linoleic and oleic films. The authors provide four possible factors contributing to the observed effects: electrostatic interactions between amine and carboxylic groups, insertion of chitosan molecules, changing lipid conformations, and hydrogen bonds between chitosan and cholesterol.

Table 3

Clusters in Fig. 12 (https://ctj-isuct.ru/article/view/6239/3617)
***Таблица 3*. Кластеры на рис. 12 (https://ctj-isuct.ru/article/view/6239/3617)**

Cluster ID	Cluster keywords	Year range	Topics
1 - Red	Bam (brewster angle microscope, dipalmitoyl phosphatidylcholine (DPPC), fatty acids, langmuir-blodgett technique, miscibility, monolayers, multilayers, nanoparticles, palmitic acid, perfluorocarbon, phospholipids, surfactant, xps (x-ray photoelectron spectroscopy)	2005-2017	DPPC and perfluorocarbons
2 - Green	Afm (atomic force microscopy), isotherms, langmuir-blodgett, lipid bilayer, mixed monolayers, phase-separation, pressure-area isotherm, surface potential, surface pressure, surface roughness, x-ray reflectivity	2011-2015	Characterization methods
3 - Blue	air-water interface, biosensors, brewster angle microscopy, cholesterol, langmuir monolayers, linoleic acid, photopolymerization, polydiacetylene	2010-2016	Biosensing and photopolymerization for diacetylene molecules
4 - Yellow	Aggregates, arachidic acid, behenic acid, contact angles, langmuir-blodgett method, quartz crystal microbalance, stearic acid, surface free energy	2003-2014	Film materials and quartz crystal microbalance

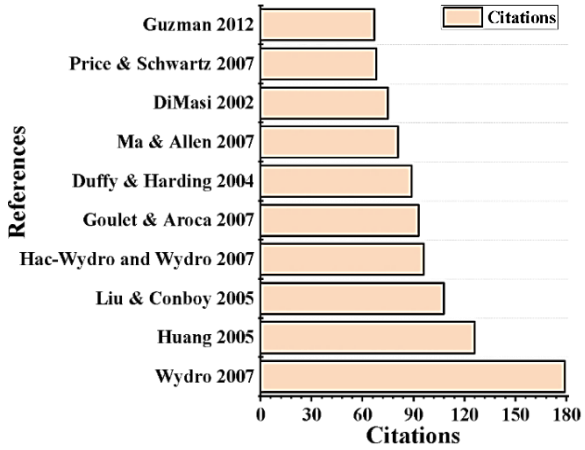

Fig. 14. The most cited articles in the field of fatty acids
Рис. 14. Наиболее цитируемые статьи в области жирных кислот

A different perspective on DPPC layers was provided by Guzman [148] which investigated the effect of silica nanoparticles on the DPPC/palmitic films. For DPPC films, silica nanoparticle incorporation causes the contraction of the film, while in palmitic acid films, a large concentration of silica nanoparticles can cause failures in monolayer formation. A decrease in quasi-static dilational elasticity for DPPC and DPPC/palmitic acid films is observed when incorporating silica nanoparticles. The suggested mechanism for this effect is nanoparticle-lipid complexes and interactions, similar to the ideas brought up by Wydro [147].

In contrast to Wydro's work[147], in which large molecules of chitosan's effect on fatty acid layers were studied, Hac-Wydro [149] investigated the effect of fatty acids on model membranes of cholesterol/DPPC using stearic acid, oleic, and alpha-linoleic acid. For cholesterol/fatty acid films, fatty acids cause cholesterol films to condense, shown as a shift towards smaller film areas on the isotherm, interacts repulsively with saturated fatty acids (stearic acid) and attractively with unsaturated fatty acids (oleic and alpha-linoleic) and decreases the compression modulus. For DPPC/fatty acid films, DPPC is condensed by fatty acids and forms attraction interactions with the strongest attraction with alpha-linoleic acid at approximately 0.5 fatty acid molar ratio; the compression modulus was reduced by fatty acids. Similar behavior is observed in cholesterol/DPPC/fatty acid films.

Ma's paper [150] reported a similar effect to Hac-Wydro [149] when investigating the effect of palmitic acid on DPPC layers. Isotherm analysis suggests miscibility between palmitic acid and DPPC and that palmitic acid catalyzes more ordered chains in DPPC, causing the molecular to become more compact or condensed. The possibility of a hydrogen bond between

palmitic acid's carboxylic group and the phosphate group of DPPC is also suggested through vibrational sum frequency generation spectroscopy.

Blue cluster: This cluster focuses on biosensing and photopolymerization for diacetylene molecules. Huang's work [67] describes the effects of metal ions on a film of 10,12 - tricosadiynoic acid (TDA), a photopolymerizable diacetylene fatty acid. Analysis of the surface-area isotherm indicated that TDA appears to not form complexes with calcium and nickel ions, while copper and cadmium ions greatly expanded the molecular area, silver and zinc ions might have catalyzed the transition from monolayers to multilayers in the TDA film. Photopolymerization under UV light of the metal-organic films yielded different results. Silver-containing films could not be photopolymerized, zinc-containing films showed thermochromism reversible at 90-160 °C but not reversible above 180 °C, possibly due to the irreversible damage caused by the heat to the zinc-carboxylate complex. Copper-containing films showed highly stable chiral structures. Goulet [151] used arachidic acid as a spreading solvent salPTCD and R18 dyes for use in surface-enhanced resonance Raman spectroscopy (SERRS). At high concentrations, the dyes are highly miscible and demonstrate uniform spectral characteristics while at single-molecular concentrations, the spectral profile differed, which was attributed to single-molecule detection. However, it was cautioned that more research should be considered before reaching a definitive answer to the possibility of single-molecule detection with SERRS.

Green cluster: This cluster focuses on characterization methods. A sum-frequency vibrational spectroscopy study determined the alkyl chain tilt angles for DSPC lipids at 12 ± 4 degrees on the silica substrate and the phosphocholine tilt at 66 ± 4 degrees [152]. In addition, the contact angle was determined to be hydrophobic for solid deposited DSPC and hydrophilic for DSPC on water. Analysis of the lipid structure indicated no effect of subphase/substrate variation on the core alkyl lipid chains. Furthermore, the nature of the deposition itself (Langmuir-Blodgett or Langmuir-Schaefer) does not affect the film structure. Low variance between phosphocholine tilt is attributed to weak coupling between lipids and the charged silica substrate.

Yellow cluster: This cluster focuses on film materials and quartz crystal microbalance. Duffy and Harding [153] described calcite crystals on stearic acid monolayers. The degree of film ionization and crystal/substrate interactions were identified as major factors influencing nucleation. Specifically, higher substrate ionization increases crystal adhesion which is conducive to growth; crystal/substrate interactions affect the number of grown faces of the crystal. A revision of the simple "lock and key" model to account for complex crystal/fatty acid film interactions is suggested. Similar to Duffy and Harding [153], Patel [154] described the growth of a calcite material on an arachidic acid film. However, Patel utilized poly(acrylic acid) to model biological systems. The factors affecting crystal growth were noted to be polymer weight and carbon dioxide escape rate (related to the ionization of fatty acid films and carbonate ions). Price's work [155] investigated the phases of fatty acids using nematic liquid crystals for octadecanoic, eicosanoic, and docosanoic acids. A positive correlation between the number of methyl groups and triple point temperature was found, and it was suggested that the liquid crystals play a role in forming the fatty acid layer structure.

FACTORS AFFECTING LANGMUIR-BLODGETT AND LANGMUIR-SCHAEFER FILMS OF FATTY ACID AND THEIR DERIVATIVES

Factors affecting Langmuir-Blodgett films

There are many factors affecting the end property of Langmuir-Blodgett films. We propose a division into three main groups:

1. Pre-fabrication factors
2. In-fabrication factors
3. Post-fabrication factors

Each factor can affect the film on multiple properties, for example, submerging the film into an ionic solution creates holes of varying sizes that directly affect the mechanical properties of the resulting layer [156].

Pre-fabrication factors pertain to the procedures carried out prior to transferring the film onto the subphase for compression. This commonly includes material and solvent quality, equipment status and cleaning, experimental setups, etc. These factors should be checked prior to every experiment.

In-fabrication factors are the largest group. This group refers to all the processes during film fabrication. This includes mechanical factors like compression speed, trough stability, deposition, method of film collection, physical qualities of subphase, temperature, moisture, dust, and material properties (some materials are more flexible during compression) as well as chemical factors such as the presence of substances in subphase and pH value [86, 87, 157-159].

Post-fabrication factors refer to processes after the film has been fabricated. This includes additional modifications to film morphology through various

means, film stability outside of trough, oven temperature (for films that require heating at high temperatures such as metal oxides), and more [160].

The combination of factors from those abovementioned three groups grants each film a unique property, making Langmuir-Blodgett films highly versatile for both research and applied uses.

Subphase ions

Among Langmuir-Blodgett and Langmuir-Schaefer fatty acid films and their derivatives, subphase ions play an important role in film formation. These ions in the secondary phase can interact with molecules at the air-water interface, thereby affecting the organization and order of the membrane.

Several studies have shown the effects of subphase ions as inducing electrochemical effects: interactions between fatty acid molecules and these ions. This can alter the surface properties of the monolayer film and affect the dispersion and reorganization of fatty acid molecules on the air-water interface. The ions in the subphase can induce ionic interactions with fatty acid molecules, resulting in the formation of complex molecular structures. For example, metal ions in the subphase can form complexes with fatty acid molecules, altering the self-organizing properties of the LB membrane. At the same time, the ions in the subphase can induce specific interactions with fatty acid molecules, increase the roughness of the monolayer film, and create specific interaction complexes between the ions and the fatty acid molecules. This may affect the structure and properties of Langmuir-Blodgett membranes.

J.A. Zasadzinski [126] and his team investigated and showed the effect of incorporating divalent metal cations and fatty acids of different chain lengths into films deposited on both mica and amourphous oxidized silicon substrates. The difference between the lattice parameters limiting for multilayer films must be due to the effect of cations although the symmetry of the buffer layer is determined by the alkane chain buffer. Surface potential measurement shows that Ba ion and other alkaline earth metals electrostatically interact with fatty acids by screening negative charges in a nonspecific manner, whereas Cd, Mn, and transition metals interact more specifically through covalent bonding. In the case of CdA_2, the team had previously concluded that the head–head group interface was necessary for order stabilization. While this appears to be true for cadmium and barium, it is true to a lesser extent for manganese and does not appear to be true for lead. Molecular order can also be stabilized by the interaction of the membrane with a specific substrate. However, even in these cases, the specific structure formed by monolayer membranes is significantly different and more extensive than that of multilayer structures.

In addition, the work of F. Mugele [156] and colleagues showed that the effects of Ca^{2+} and Na^+ ions were compared by varying their concentrations in the subphase.

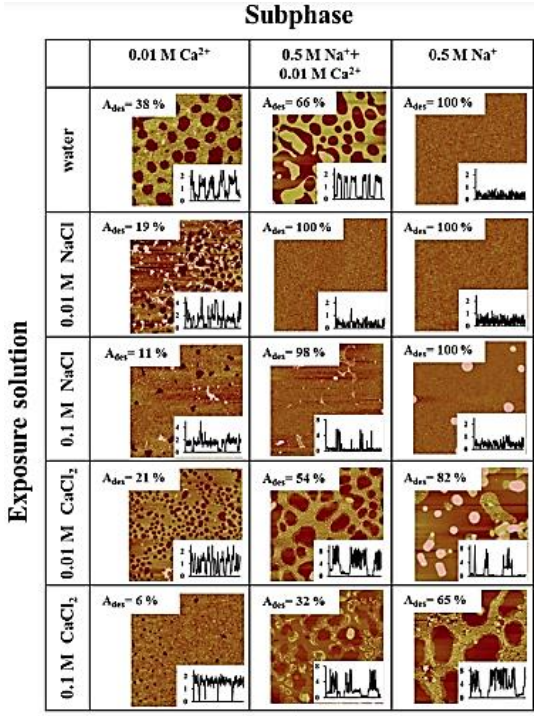

Fig. 15. AFM images of LB films prepared with all combinations of sub-phases after exposure to water and liquid preparations. Image size: 5×5μm^2. The Ades desorption region represents the area of the exposed bare substrate. The inset shows representative cross-sections. Vertical scale: in nm. Horizontal scale: 5 μm [156]
Рис. 15. АСМ-изображения пленок LB, приготовленных со всеми комбинациями субфаз после воздействия воды и жидких препаратов. Размер изображения: 5×5 мкм^2. Область десорбции Ades представляет собой площадь экспонированной голой подложки. На вставке показаны репрезентативные поперечные сечения. Вертикальный масштаб: в нм. Горизонтальный масштаб: 5 мкм [156]

The AFM image shows almost intact films with a few circular holes exposing the bare substrate when prepared in the secondary phase in the presence of Ca^{2+} while the Na^+-containing fractions result in a large area of the substrate bare after contact with water (Fig. 15).

Partial stabilization of the layers in contact with purified water suggests that some adsorbed Ca^{2+} is present and can stabilize the LB membrane. However, this stabilization is clearly not as strong as in the case of pure 0.01 M $CaCl_2$ fractionation. The competition between the more strongly bound Ca^{2+} ions and the 50-fold more concentrated Na^+ ions in the secondary phase leads to a mixed association of R– and SiO–

with the two cations (Fig. 16). When exposed to pure NaCl solution, the chemical potential gradients of Ca^{2+} and Na^{+} seem to lead to complete destabilization of the membrane, suggesting that initially the Ca^{2+} and/or $SACa^{+}$ ions that stabilize the LB membrane can be exchanged with Na^{+} ions from the large contact solution leading to complete decomposition of the layer. The behavior in contact with pure Ca^{2+} solution again reveals ion exchange between the bulk solution and the loosely bound portions of the LB monolayer [156].

Thus, it can be seen that the ions in the subphase in the Langmuir-Blodgett and Langmuir-Schaefer films, especially for fatty acids and their derivatives, play an important role in determining molecular organization, stability and propagation behavior of the monolayer on the sub-phase surface. Their presence affects important aspects of LB engineering, ultimately influencing the fabrication of thin films.

Nature of surfactant

The surfactants used in the Langmuir-Blodgett (LB) deposition technique are amphiphilic molecules such as fatty acids, amines, lipids, etc. They participate in the formation of floating films on the water-air interface in the form of a single element or a complex (mixed with many other surfactants). Participating fatty acids used to fabricate membranes by Langmuir-Blodgett technology are usually fatty acids with hydrophobic long-chain carbon chains and hydrophilic heads of COOH functional groups. Because of their surfactants, they can be used to reduce the surface tension between two immiscible phases, such as oil and water. During LB deposition, a monolayer of fatty acid surfactants is first formed at the air-water interface. This single layer is then carefully transferred onto a solid substrate, resulting in the formation of a thin film. The arrangement of fatty acid molecules in the monolayer can be controlled by manipulating experimental parameters such as compressive pressure, temperature, and the nature of the fatty acid – the nature of the surfactant. The choice of fatty acid surfactant depends on the specific application and the desired properties of the thin film. Recently, scientists have focused on making Langmuir - Blodgett thin films from hybrid materials with fatty acids instead of studying monolayer films of fatty acids as before. The results of the Langmuir - Blodgett thin film fabrication studies of fatty acids and fatty acid hybrid materials are listed in Table 4.

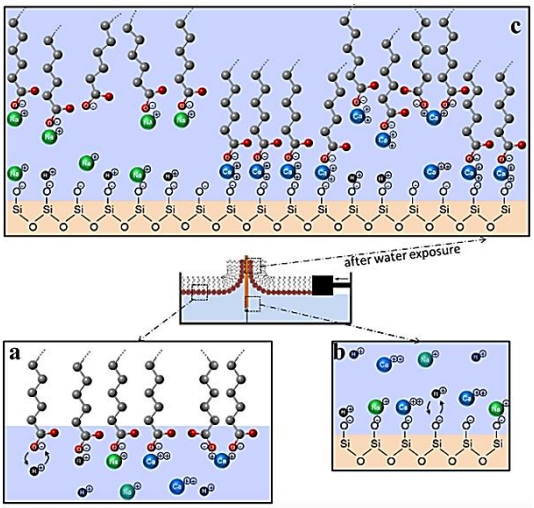

Fig. 16. Schematic illustration of monolayer adsorption-desorption process (a) formation of salt complexes with dissociated fatty acid at air–water interface (b) negatively charged substrate dipped under subphase (c) desorption of monolayer after water exposure [156]
Рис. 16. Схематическая иллюстрация процесса адсорбции-десорбции монослоя (a) образование солевых комплексов с диссоциированной жирной кислотой на границе раздела воздух–вода (b) отрицательно заряженный субстрат, погруженный в субфазу (c) десорбция монослоя после воздействия воды [156]

Table 4

Research results on the fabrication of Langmuir - Blodgett thin films of fatty acids and fatty acid hybrid materials
***Таблица 4.* Результаты исследований по получению тонких пленок Ленгмюра-Блоджетт из жирных кислот и гибридных материалов на основе жирных кислот**

Surfactant	Result	Reference
1	2	3
VitaminC/SA	Structure of LB film depends on the mole fraction of VitC and the nature of the substrate	[161]
PPV/SA	1-layer: Roughness 3.14 nm 3-layer: Roughness 4.05 nm	[162]
Cl-PPV/SA	1-layer: heterogeneity with some valleys 9-layer: homogeneous	[163]
$NiPc(OBu)_8$/SA	The bands of the absorbance spectra: Q band (~760 nm) and B band (~317 nm)	[164]
PyB/SA (PyY/SA)	The size of the cluster in PyB (150×120- 280×210 nm) and PyY 250x350 ± 5×10 nm^2	[165]
Saponit/SA	Saponite layers was largely affected by the subphase $MgCl_2$ concentration.	[166]
GOx/SA	A smooth morphology, containing domains of various contrast. Thickness:10-11,5nm.	[167]

continuation of the table

1	2	3
Chitosan/SA	Structure strongly dependent on chitosan mole fraction and deposition pressure	[168]
P3OT/SA	High conductivity and roughness	[169]
PheDH/SA	1-layer: 2.5-5nm 5-layer: 10-12 nm	[40]
PQ/SA/ $RE(PMo11)_2$	Uniform monolayer, creating a smooth surface	[170]
C60/SA	The nanoparticles have joined with each other and form a kind of ordered aggregation, which like a net	[171]
P3HT/SA	The coverage increased at π = 35mM/m	[172]
Imidazole Derivative/SA	The width and height of the nanoballs are nearly 100 nm and 4.5 nm respectively	[173]
PNVK/SA/ urease	Urease can be immobilized onto these PNVK/SA LB monolayers	[174]
DPPC–Palmitic acid, DPPC, Palmitic acid	The π–A isotherm of DPPC–Palmitic acid, DPPC, Palmitic acid at the same film forming conditions shows the difference in the area per molecule and surface and molecular structure at the time of thin films	[148]
Stearic Acid	The observed average thickness of ~2 nm is consistent with the length of SA molecules and thus with the expected molecular structure as sketched in the inset	[156]
Arachidic and Stearic Acids	5-layer stearic acid film has a developed morphology. The islands with a diameter of about 0.4–0.8 μm and a height of 2–6 nm can be distinguished in the film structure	[175]

Through comparison, it can be seen that the nature of the surfactant has an influence on the thin film formation, which is expressed through the Π-A isotherm of the film forming process and properties of solid thin films. Under the same experimental conditions, the nature of the surfactant changed, leading to a different time of film formation. It can be seen that the nature of the surfactant is the most important factor determining the properties of Langmuir - Blodgett, and Langmuir - Schaefer films formed by their different chemical structures. From there, it is possible to select a single or hybrid material of fatty acids to form suitable membranes for the desired applications.

pH levels

The pH level has a significant influence on the properties and stability of Langmuir-Blodgett (LB) and Langmuir-Schaefer (LS) fatty acid films and their derivatives. Fatty acids, consisting of a carboxylic acid group, react with different pH values and alter membrane properties [176]. Several studies have shown that pH has a significant effect on Langmuir-Blodgett (LB) film formation of fatty acids. To investigate the influence of pH on the LB and LS membranes of fatty acids, the work of K. Dopierala [88] and research team was particularly useful, describing the transformation of the oleic acid monolayer from apo-α-lactalbumin protein in milk is pH dependent, the interaction between oleic acid (OA) monolayers when penetrated by apo-bovine α lactalbumin (BLA III) in media with different pH (Fig. 17).

Changes in pH can lead to structural changes in the monolayers of fatty acids and cause essential changes in protein interactions. Under conditions of higher pH, the electrostatic force governs the adsorption of proteins. The interaction between the oleic acid monolayer and apo-α-lactalbumin at pH 2 is mainly the result of hydrophobic forces, the film forming stably.

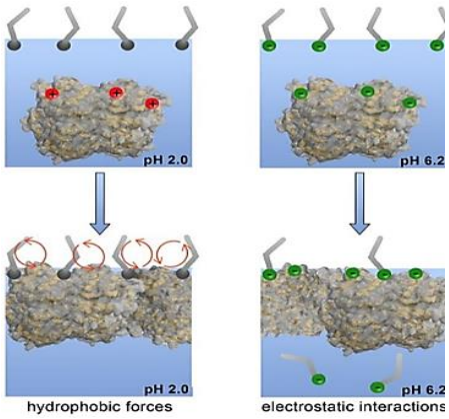

Fig. 17. Schematic depiction of the influence of pH on the formation of mixed monolayers of OA and BLA III [88]

Рис. 17. Схематическое изображение влияния pH на образование смешанных монослоев OA и BLA III [88]

The research of K.H. Kang [177] and colleagues presents the fabrication process of Langmuir-Blodgett (LB) films deposited at different subphase pHs. In the π-A isotherm in Fig. 18, the monolayer on the air/air interface water has different limiting regions

per molecule and shows more condensate with increasing pH of the secondary phase. When the palmitic acid LB film is deposited, the change in resonant frequency is proportional to the deposition layer, and there is more resonant frequency change in the case of a higher pH range as expected. In the resonant frequency range response for pumping organic gas, the frequency matching has been improved in the case of LB membranes fabricated in the lower subphase pH range and dependent on the molecular weight of the organic gas.

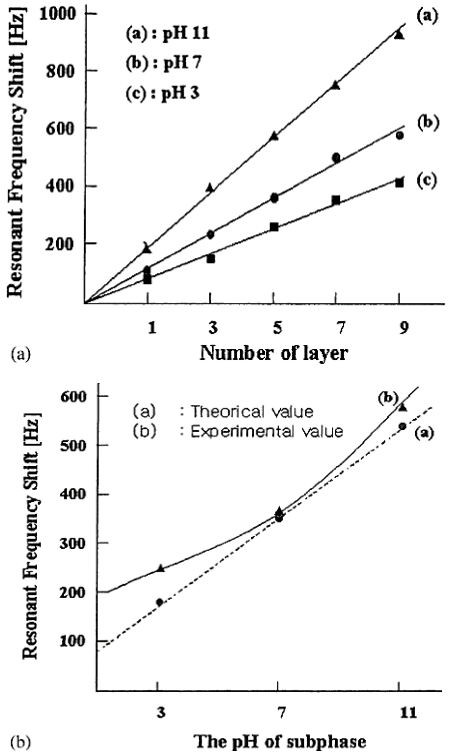

Fig. 18. The resonant frequency shift depending on deposition of LB film (a) and pH relationship (b) [177]

Рис. 18. Сдвиг резонансной частоты в зависимости от осаждения пленки LB (a) и соотношения pH (b) [177]

In summary, pH directly affects the ionization state of fatty acids and thus affects the intermolecular interactions and their surface morphology in the Langmuir–Blodgett membrane.

Ionization is the process by which a fatty acid molecule loses or gains a proton (H^+), forming a negative ion (acid) or a positive ion (salt). According to studies, the pH value of a fatty acid solution can affect the quantity and properties of acid ions and salt ions in the solution. This can impact the ability to form LB films and the properties of the formed films. For example, in some cases, low pH can produce more acidic ions in solution, increasing the hydrophobic and film-forming properties of fatty acids. However, at high pH, the ratio of salt ions increases and can reduce the film-forming capacity and hydrophobic properties of the films. Therefore, pH control during fatty acid LB film formation is crucial to achieve a thin film of desired properties and structure.

Temperature

Langmuir - Blodgett film formation of fatty acids depends on temperature stability [178]. In the work of Katarzyna Dopierala [88], the effect of temperature on binding in fatty acids by α-lactalbumin was investigated. The obtained results show that in the investigated thermal ranges, the thin film formed at the temperature of 36.6 gives the most stable and uniform film results. At other temperatures, the molecules tend to move in a chaotic manner, and the film shrinks unevenly.

Concentration

Concentration plays an important role in the formation of Langmuir – Blodgett (LB) and Langmuir – Schaefer (LS) fatty acid films and their derivatives. Both LB and LS techniques involve the deposition of organic monolayers. There have been many studies on Langmuir - Blodgett and Langmuir - Schaefer films of fatty acids and their derivatives, investigating the film formation at different fatty acid concentrations or referring to specific concentrations. Solution concentrations of fatty acids or derivatives can influence interactions with the Langmuir plane (water-air interface). A study by G.B. Talapatra [179] and colleagues studied the interaction between oval albumin (OVA) and stearic acid layers, which showed significant differences in isotherms when different concentrations were tested (Fig. 19).

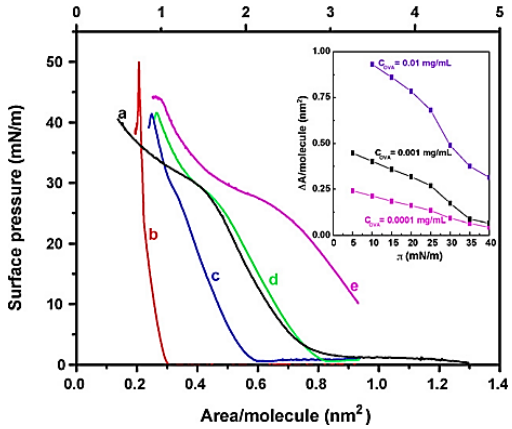

Fig. 19. Surface pressure–area isotherms at room temperature (26 ◦C) of (a) pure OVA, (b) pure SA, and (c–e) SA with different concentrations (0.0001, 0.001, and 0.01 mg/mL) of OVA in pure water subphase, respectively. The inset shows the change in area (A)/molecule vs. surface pressure plot of the SA–OVA monolayer [179]

Рис. 19. Изотермы поверхностного давления–площади при комнатной температуре (26 ◦C) (a) чистого OVA, (b) чистого SA и (c–e) SA с различными концентрациями (0,0001, 0,001 и 0,01 мг/мл) OVA в чистой водной субфазе соответственно. На вставке показано изменение площади (A)/молекулы в зависимости от поверхностного давления монослоя SA–OVA [179]

The π–A isotherm at the concentrations of SA investigated gives different results. When the concentration is increased, the formation of LB film will take place earlier, the area for a molecule at the time of thin film formation is also different, leading to different surface morphology of the obtained film.

Similarly, the work of Luciano Caseli [180] clarified the effect of surfactant concentration on galactose oxidase immobilized in the Langmuir-Blodgett stearic acid membrane.

Through this study, it is possible to understand how fatty acid concentration affects the interaction and properties of Langmuir–Blodgett floating films. Studying the fatty acid concentration during this process helps to better understand the relationship between fatty acid concentration and the properties of the thin film produced. Fatty acid concentrations in the Langmuir-Blodgett process can affect the thickness and uniformity of the thin films. Too high a concentration of fatty acids can lead to the formation of a multilayer film that occurs before the compression begins, or to produce a thicker and more heterogeneous thin film. Meanwhile, lower concentrations of fatty acids can lead to thinner and more uniform thin films. In addition, fatty acid concentrations can also affect the chemical and structural properties of thin films. Properties such as adsorption capacity, elasticity, strength and surface properties of films can vary with fatty acid concentration. Therefore, thin film formation by the Langmuir-Blodgett method is a sensitive process for fatty acid concentrations. This highlights the importance of adjusting fatty acid concentrations to achieve thin films with desired properties.

Compression speed

During Langmuir-Blodgett (LB) film formation, the compression rate is determined by the travel speed of the barrier (barrier) during the adjustment of the surface area of the LB thin film on the water–zero interface. Studies have shown the difference in thin films formed upon varying the compression rate (Table 5).

The compression rate actually plays an important role in the formation and properties of Langmuir-Blodgett (LB) and Langmuir-Schaefer (LS) fatty acid films and their derivatives. When these films are formed at the right compression rate, it allows a more organized and controlled encapsulation of molecules at the air-water interface, allowing the molecules enough time to spontaneously form, resulting in a stable and tightly structured membrane [181]. This can result in enhanced film quality and improved properties such as increased stability, uniformity, and reproducibility. When the compression speed is too slow, this does not affect the film formation too much, but it makes the experiment time longer, productivity, and efficiency decrease. In contrast, when the compression rate is too fast, the molecules do not have enough time to properly arrange themselves, resulting in a poorly organized and uneven membrane structure. This can result in films with lower stability, increased roughness, and reduced uniformity. Therefore, controlling the compression rate is very important to achieve the desired film characteristics.

Table 5

Compression speed affecting Langmuir-Blodgett and Langmuir-Schaefer films of fatty acid and their derivatives
***Таблица 5.* Скорость сжатия, влияющая на пленки Ленгмюра-Блоджетт и Ленгмюра-Шефера жирных кислот и их производных**

Surfactant	Compression speed	Result
GOx/SA	Vn = 3.5 mm/min,	A smooth morphology, containing domains of various contrasts. Thickness:10-11,5nm [167]
Chitosan/ SA	Vc = 10 mm/min	Structure strongly dependent on chitosan mole fraction and deposition pressure [168]
PheDH/SA	Vc = 1 mm/min	1-layer: 2.5-5nm 5-layer: 10-12 nm [40]
C60/SA	Vc = 10 mm/min	The nanoparticles formed ordered aggregation, which resembles a net [171]
Imidazole Derivative/SA	Vc = 5 mm/min	The width and height of the nanoballs are nearly 100 nm and 4.5 nm respectively [173]
PNVK/SA/ urease	Vc = 5 mm/min	Urease can be immobilized onto these PNVK/SA LB monolayers [174]

Transfer pressure

Surface tension was measured using the Willhelmy method [182], in which the Willhelmy plate was connected to a strain gauge and intercepted at the air-water interface. During the formation of the Langmuir–Blodgett floating film of fatty acids and their derivatives, when the surfactant is compressed by the barrier, the molecules move and there is a change in the

induced force. Surface tension plays a very important role in this process as it helps to determine the packing density and orientation of the molecules on the substrate. During the compression phase, the pressure will gradually increase until the thin film formed is in a steady state. The stability of the LB membrane requires a balance between the passive interaction of the fatty acid molecules with the water surface and the interaction between the fatty acid molecules. The Langmuir - Blodgett floating film will be transferred onto the solid substrate by the Langmuir - Schaefer method, the pressure at this time is called transfer pressure.

Transfer pressure plays an important role in the formation and quality of Langmuir-Blodgett (LB) and Langmuir-Schaefer (LS) fatty acid films and their derivatives. The work of Satyajit Hazra [172] on the development and structural evolution of poly(3-hexylthiophene) (P3HT) Langmuir and Langmuir–Blodgett (LB) blended with stearic acid provides Results on the influence of Transfer pressure on LB film formation by observing AFM images of membranes obtained at different Transfer pressure (Fig. 20). Due to the weak polar nature and strong intermolecular bonds of pure P3HT, it often agglomerates right on the surface of the water. Therefore, it is difficult to fabricate stable multilayer P3HT by superimposing ordered monolayers on a solid substrate. Fatty acids mixed with P3HT according to the appropriate molar concentration will reduce the hardness, and greatly improve and increase their polarity when put on the water-air interface.

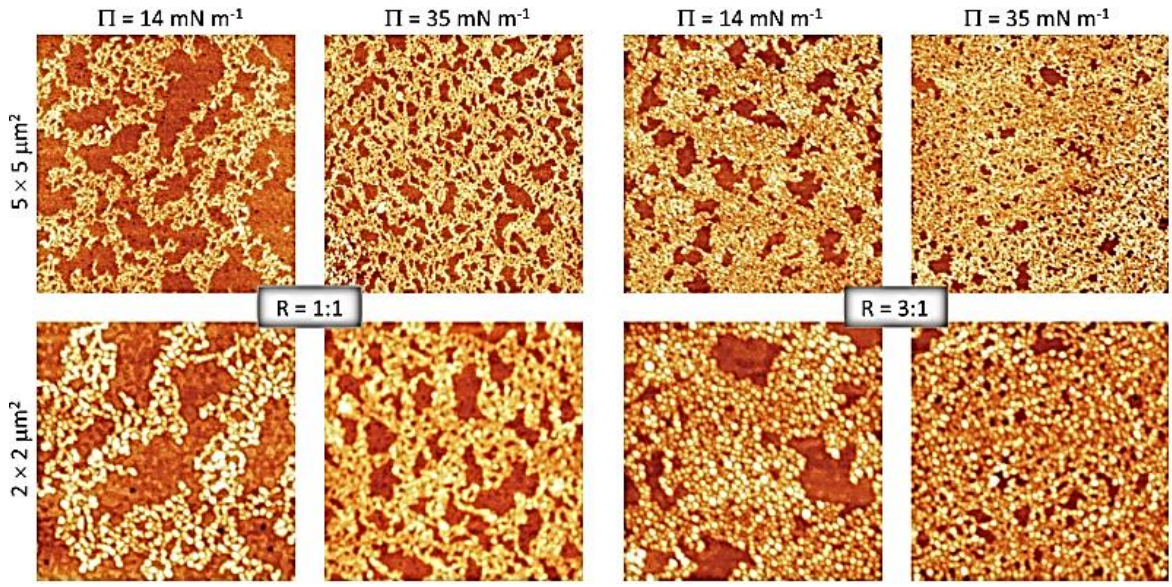

Fig. 20. AFM images in two different scan sizes for the mixed P3HT–SA LB films deposited at two different compositions (R) and at two different pressures (P) [172]

Рис. 20. АСМ-изображения в двух различных размерах сканирования для смешанных пленок P3HT–SA LB, осажденных при двух различных составах (R) и при двух различных давлениях (P) [172]

Thus, it can be concluded that the compressive pressure at the time of thin film collection is an important factor in the formation process as well as the surface structure, morphology, and thickness of LB and LS film of fatty acids and their derivatives.

Orientations of deposited substrates

The process of forming supernatant films of surfactants by the Langmuir-Blodgett method depends on many parameters as mentioned in sections 3.1-3.6. After the stable embossed monolayers are formed, they can be transferred onto the substrate to obtain solid films. The film deposition floats onto the solid substrates in a direction perpendicular to the water-air interface (a Langmuir-Blodgett film will be obtained) and in a parallel direction (a Langmuir-Schaefer film will be obtained). In each method of transferring the membrane to the substrate according to LB or LS depends on the membrane embedding speed, substrate nature, number of embedding monolayers, transfer pressure and especially orientations of substrates. Studying the LB film of stearic acid when changing the tilt angle (direction) of the embedding substrate in the direction of membrane compression at values of $\theta = 0$, 45, 90° showed the difference in molecular orientation, roughness and shape of obtained film state (Fig. 21).

PROPERTIES OF LANGMUIR-BLODGETT FILMS

Molecular orientation

On pure carboxylic acid films, Tao's work was particularly informative, providing information on the structure of carboxylic acids with varying chain lengths from 4 to 20 and a 24-carbon carboxylic acid

[184]. In this study, Tao reported a chain tilt from 15 degrees to 25 degrees for films on a silver substrate, while films on a copper and aluminium substrate stayed relatively perpendicular. This finding is in accordance with an earlier study by Chollet [185] which found behenic acid at around 25 degrees of tilt from the normal. Later research expanded this survey of molecular orientation to salts of fatty acids. A common theme in many fatty acid salt studies concludes that the position of the film molecule remains perpendicular to the surface with a high degree of stability. A recent study [75] corroborated the reported findings by performing investigations on copper arachidate. However, it would be an overstatement to say that all works agree with this proposition. Outka, Stöhr et al. 1988 concluded that calcium arachidate molecules exhibit 33 degrees of tilt. An extensive survey on metal derivatives of behenic acid [186] conducted ellipsometry measurements to determine the thickness of the deposited film.

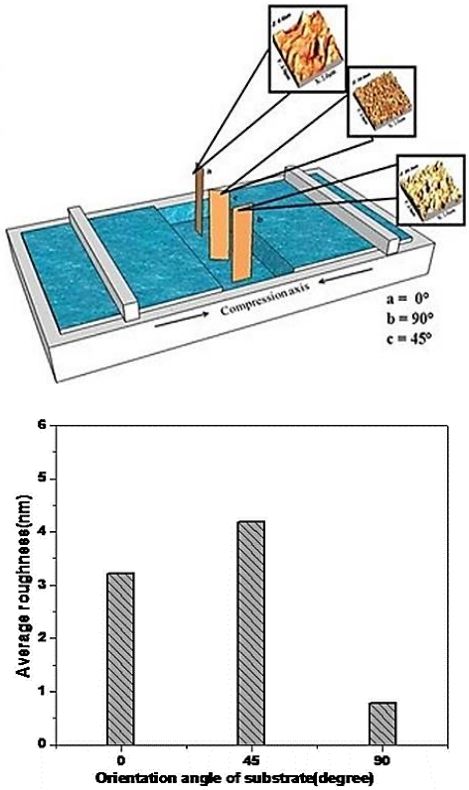

Fig. 21. Schematic diagram of Langmuir trough with three substrates to be at different orientation angles with respect films to the compression axis (θa = 0°, θb = 90°, θc = 45°) (left) and Average roughness of LB stearic acid at different 15 mN/m with orientation angles of the substrates with respect to the compression direction (θ) [183]

Рис. 21. Схематическая диаграмма ванны Ленгмюра с тремя подложками, находящимися под разными углами ориентации по отношению к пленкам к оси сжатия (θa = 0°, θb = 90°, θc = 45°) (слева) и средняя шероховатость стеариновой кислоты LB при разных 15 мН/м с разными углами ориентации подложек по отношению к направлению сжатия (θ) [183]

Table 6

Thickness of various film systems measured by ellipsometry methods

***Таблица 6.* Толщина различных пленочных систем, измеренная методами эллипсометрии**

System	Thickness in Å	Reference
Stearic acid*	21	[82]
Behenic acid*	32	[186]
Sodium stearate	22	[82]
Sodium behenate	30	[186]
Copper stearate**	19	[82]
Copper behenate**	23	[186]
Manganese stearate	24.5	[187]
Manganese behenate	30	[186]

Note: * Thickness determined from monolayers on acidic subphases (HCl 10^{-2} mol/L)
** Mean values from inhomogenous monlayers
Reproduced from [186]. All credits to the original authors.
Примечание: * Толщина определена из монослоев на кислых субфазах (HCl 10^{-2} моль/л)
** Средние значения из неоднородных монослоев
Воспроизведено из [186]. Все кредиты принадлежат первоначальным авторам

We observe that several film systems containing various ions like copper, sodium, or manganese have a thickness less than that of the original film. The logical expectation for a film that has substituted its hydrogen for a larger ion is that the film thickness will increase, and although not explicitly mentioned in the original study, assuming homogenous and good quality film deposition with minimal loss of film material at the time of measurement, we can theorize that a less than perpendicular angle is exhibited by the film molecules. Another work applies a more novel ion in the form of uranyl arachidate [188] and surveyed the film thickness over many pH levels (Fig. 22).

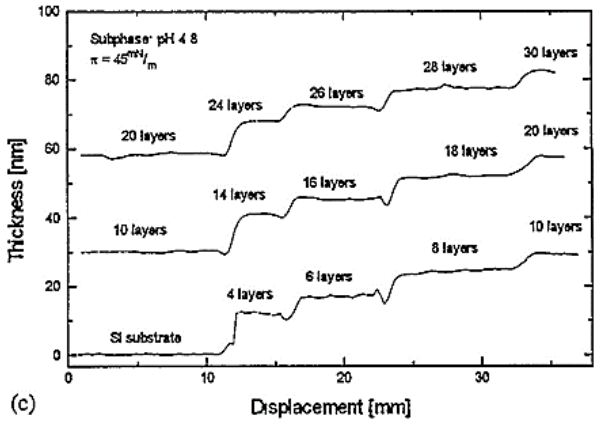

Fig. 22. Thickness survey of uranyl arachidate

Рис. 22. Исследование толщины уранил-арахидата

It can be inferred that the average film thickness per layer is around 3 nme. The thickness of an arachidic acid film has been reported in literature [175]

at 2.5 nm. When comparing this increase to the values reported in Table 6, we see that despite the uranyl ion possessing a size significantly larger than that of sodium or other reported ions, the change in film thickness is relatively similar. This can be theorized as a deviation from the normal orientation of the film molecules assuming other variables carry minimal impact. Regarding the anisotropy in the film layers, studies differ in their results. A mathematical model using ellipsometry has been proposed to investigate anisotropy [189].

A recurring theme in some studies states that subphase pH is a major factor in determining film properties [75, 188]. Lower pH results in less ion exchange between the film molecule and subphase, resulting in a higher molecular tilt due to unequal intermolecular forces. At higher pH, the ions are exchanged more and the tilt degree is less. This difference between pH levels can be explained via the disassociation of the fatty acid film. As pH decreases, the number of fatty acid molecules that do not disassociate increases and vice versa. A more detailed description of the effect of subphase pH levels is discussed elsewhere in this review article. There are also mentions of substrate effects on film orientation, such as the differing film material using silver, copper, and aluminium [184] and this variable's effect will also be discussed in this article.

Regarding mathematical models, earlier works [190-192] contain formulas and methods for the calculation of film parameters.

Interestingly, an article slightly unrelated to fatty acid films details an amphiphilic polymer molecule of polyacrylate with azobenzene side groups that exhibit thermotropic properties and can reorient using UV light or annealing [193]. This finding can be translated to studying fatty acid films hybridized with azobenzene groups and surveying it for similar reorientation patterns, creating a potential method for manipulation of film structure.

Morphology

Araujo F fabricated beta-galactosidase (β-gal, an enzyme that catalyzes hydrolysis) film in LB film of stearic acid and poly[(9,9-dioctylfluorene)-co-thiophene] (PTPF) conjugated polymers for application in biosensors [194]. LB is the optimal method to immobilize enzymes and protect the structure of lipids and polymers in membranes. Using atomic force microscopy (AFM) it is shown that the film with different thicknesses is shown by contrast in Fig. 23. F. Araujo [194] investigated the surface roughness by varying the film composition: (A) stearic acid and enzymes, (B) stearic acid and polymers, (C) polymers and enzymes, (D) stearic acid, enzymes, and polymers. The results showed that film (B) had the highest surface roughness and the most pronounced morphological heterogeneity. The film (C) shows defects such as ridges, protrusions, and deep grooves. Film (D) is evaluated as defects on the film surface are minimized, but the roughness on the membrane surface is still recorded due to the nature of the components present in the film.

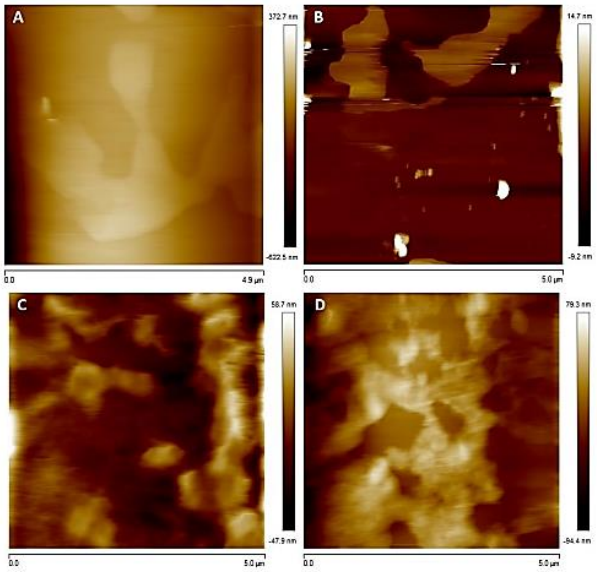

Fig. 23. AFM atomic force microscopy images of membrane surfaces based on different composition, (A) stearic acid and enzymes, (B) stearic acid and polymers, (C) polymers and enzymes, (D) stearic acid, enzymes, and polymers [194]

Рис. 23. Изображения мембранных поверхностей, полученные с помощью атомно-силовой микроскопии АСМ, на основе различного состава: (A) стеариновая кислота и ферменты, (B) стеариновая кислота и полимеры, (C) полимеры и ферменты, (D) стеариновая кислота, ферменты и полимеры [194]

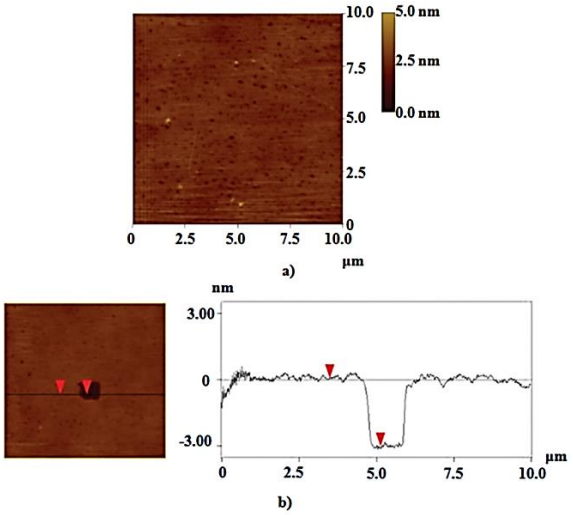

Fig. 24. OCA Surface morphology image of OCA and monolayer OCA cross-section [32]

Рис. 24. Изображение морфологии поверхности OCA и поперечное сечение монослоя OCA [32]

Silicone is widely used in MEM microstructure devices. However, this is a less durable material, very prone to damage, and has no natural lubricant. To extend the life of MEM devices, Akulova et al. used a monolayer film as a protective coating [32]. The monomolecular film made from octacosanoic acid (OCA), a naturally occurring fatty acid used as a protective coating for silicon, was investigated for its strength, wear resistance, and low toxicity.

The surface morphology of the OCA monolayer shown in Fig. 24 shows that the voids on the OCA-coated surface occur during the fatty acid film transition from the aqueous phase to the substrate. The results of AFM image analysis show that the average surface roughness of the OCA layer is 0.52 nm and the square root roughness (RMS) is 1.4 nm. The AFM image shows the formation of a uniform OCA coating on the silicon with a film thickness of 3.2 nm. The abrasion resistance survey results of the OCA film showed in Fig. 25. That the OCA-coated silicon surface was abraded after 780 ± 15 sliding cycles with 1N load. Fatty acid molecules have a weak bond with the substrate, so they can easily move between the contact surfaces to help slow down the wear process.

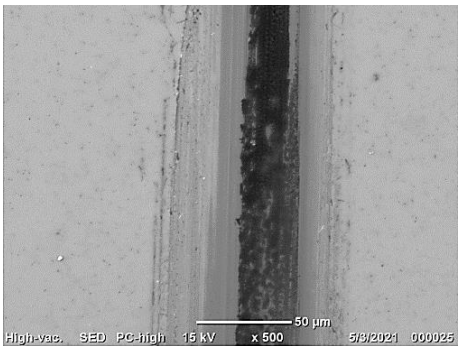

Fig. 25. SEM image–of abrasion stain on silicon surface coated by OCA monolayer [32]

Рис. 25. Изображение СЭМ – абразивное пятно на поверхности кремния, покрытой монослоем OCA [32]

Paul et al. have fabricated monolayer films of fatty acid (arachidic acid)-based gold nanoparticles for application in metal–insulator–semiconductor (MIS) structures. Transmission electron microscopy image of a single layer of Au nanoparticle LB transferred onto a carbon-coated microscope grid is shown in Fig. 26. The nanoparticles have a tight arrangement, good order, and uniform distribution on the membrane. The average particle diameter is about 8 nm and covers the membrane surface [195].

Thus, it can be seen that the LB film has good coverage, high compaction capacity, surface uniformity and high degree of directional order [196]. Depending on the different film composition, it is possible to create a film with different smoothness and surface roughness. It is also possible to change the thickness control for specific applications from a single test layer to the desired thickness by embedding different layers onto the substrate. The fatty acid LB film can also create holes on the surface of the material for application in superhydrophobic materials.

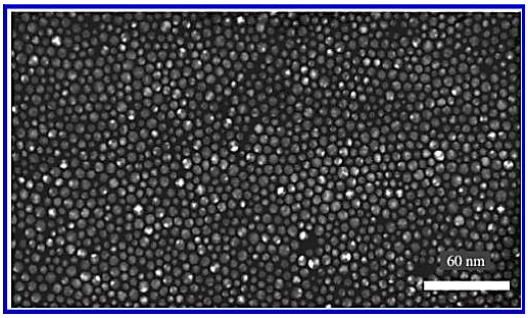

Fig. 26. Transmission electron microscopy of a single layer of LB Q-Au transferred onto a carbon-coated microscope grid [195]

Рис. 26. Просвечивающая электронная микроскопия одного слоя LB Q-Au, перенесенного на покрытую углеродом сетку микроскопа [195]

Stability

Stability is a major issue for LB membrane applications. The LB films of fatty acids are evaluated to have poor heat resistance and can change their properties and structure over time [196]. Therefore, in addition to the notes in the manufacturing process, it is also necessary to choose an appropriate membrane protection environment. Kobayashi et al investigated the thermal stability of Langmuir-Blodgett (LB) films of icosanoic acid by Fourier transform infrared absorption spectroscopy (FTIR) and scanning electron microscopy [197] Kobayashi used scanning electron microscopy to examine the film surface at different temperatures. Based on the SEM image (Fig. 27), it can be seen that a few holes were observed on the membrane surface even below the bulk melting point, possibly due to surface fluctuations and desorption occurring for the icosanoic acid film. This allows the acid molecules to move from lower to higher positions in the membrane and form holes on the surface of the LB membrane. The analysis results show that the LB film of icosanoic acid has chaos and displacement of acid molecules when the temperature increases, making the film unstable even at the mass melting point.

Fig. 28 shows the temperature dependence of the FTIR RAS spectra of the icosanoic acid LB film. FTIR in combination with DTA shows that the intensity of CH_2 oscillations increases with temperature and increases most strongly at 76 °C which is the sub-melting temperature, slight shift, and spectral expansion can be observed. When cooled to a temperature of 30 °C, the

film had structural reorientation, but the original room temperature spectrum was not obtained.

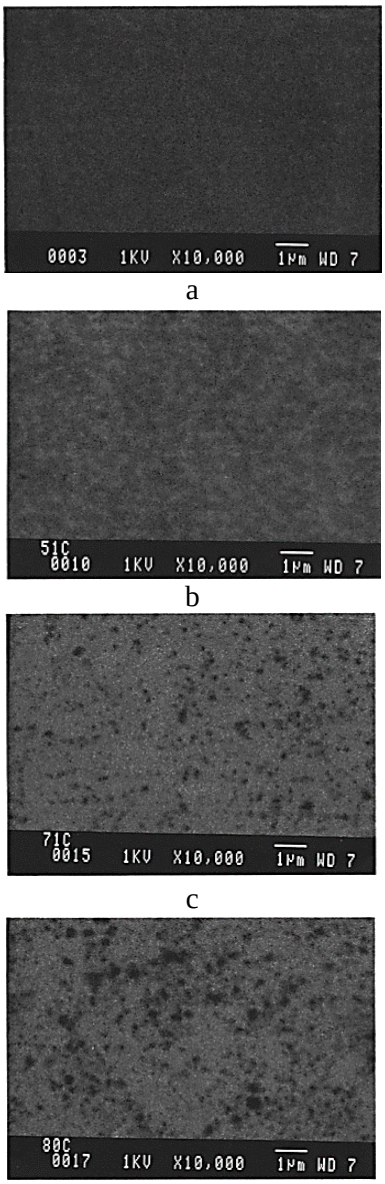

Fig. 27. Scanning electron microscopy images of LB icosanoic acid films at different temperatures: (a) 25 °C; (b) 51 °C; (c) 71 °C; (d) 80 °C [197]

Рис. 27. Сканирующие электронные микроскопические изображения пленок LB икозановой кислоты при различных температурах: (a) 25 °C; (b) 51 °C; (c) 71 °C; (d) 80 °C

Zhang [198] also had a similar experiment using FTIR spectra of 21-layer stearic acid LB films recorded at high temperatures from 20° to 80 °C, in different wavenumber regions to show optical changes in Fig. 29. The temperature-induced spectrum is more obvious. The results show that the IR spectrum of the film is in the CH_2 region at high temperature. 2916 and 2850 cm^{-1} in the 20 °C spectrum are assigned to symmetric CH_2 stretching oscillations, respectively, of unchanged frequency (2916 and 2850 cm^{-1}, respectively) up to 62 °C. Then, upon a sudden increase in the temperature range of 62-68 °C, and finally reaching constant values (2923 and 2854 cm^{-1}, respectively) above 68 °C indicating the frequency of the stretching bands of CH_2 is very sensitive to the structure of the hydrocarbon chain. The values of 2916 and 2850 cm^{-1} for CH_2 symmetric stretching bands are characteristic of a highly ordered hydrocarbon chain structure. It can be seen that the structure of the stearic acid film cannot be restored when it is returned to room temperature.

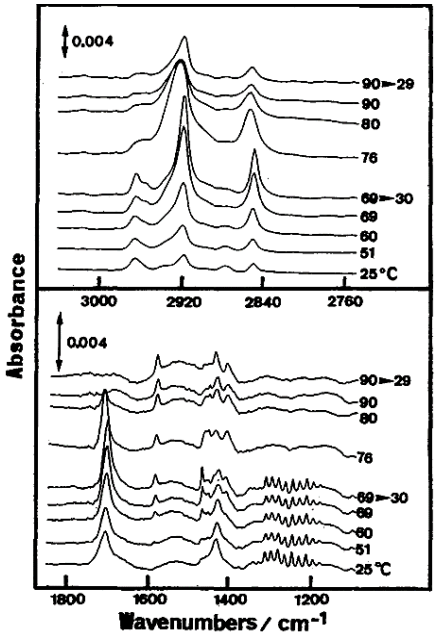

Fig. 28. FTIR spectra of icosanoic acid dependent on temperature [197]

Рис. 28. Спектры ИК-Фурье икозановой кислоты в зависимости от температуры [197]

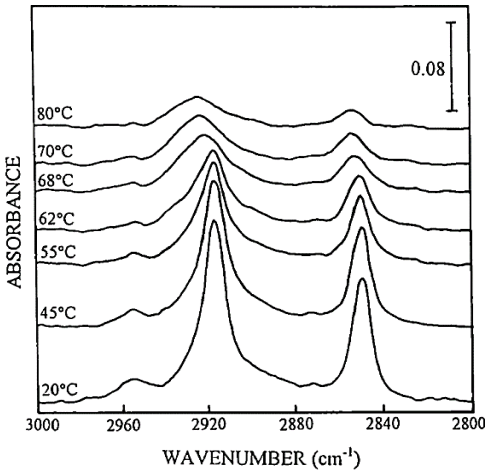

Fig. 29. Infrared spectra of a 21-layer stearic acid LB film in the high-temperature CH_2 extension region

Рис. 29. Инфракрасные спектры 21-слойной пленки стеариновой кислоты LB в области высокотемпературного расширения CH_2

Goto et al. [79] have developed a poly(p-phenylene vinylene) (PPV) block copolymer film immobilized in a Langmuir–Blodgett (LB) stearic acid (HSt) film, and incorporated with glucose-stabilized palladium nanoparticles. oxidase (GOx-PdNP) to enhance their electrical conductivity and luminescence properties.

Nanobiocomposites, based on HSt, PPV, and GOx-PdNP, were transferred from the air-water interface onto solid supports using the LB technique. These films are characterized by surface pressure area isotherms, polarization-modulated infrared reflectance-absorption spectroscopy, fluorescence spectroscopy, and conductivity measurements. The results indicate that the incorporation of GOx-PdNP in the PPV-HSt LB film enhances the luminescence and electrical conductivity of PPV. Based on the higher conductivity and emission obtained with hybrid LB membranes and the ability to modulate the molecular-level interactions between membrane components by varying the experimental conditions, thus allowing optimal Further chemistry, one can envision applications for these films in optical and electronic devices, such as organic light-emitting diodes. In addition, fatty acids used in the fabrication of hydrophobic films show that they can be used to protect materials from corrosion, against physicochemical agents, and prolong the life of the material. The corrosion tests of Zhu J showed that the stearic acid film can resist chemical agents to protect magnesium from corrosion after a chemical corrosion test [199]. Zhu J also studied the chemical stability of superhydrophobic surfaces by using acids to investigate the contact angle of the film. The contact angle of the droplet with pH 1 and 2 has a contact angle greater than 150° which is lower than the contact angle of water. Thus, it can be seen that the surface of the film can be destroyed under strong acid conditions, and the superhydrophobic surface can be lost.

Structure

Amphiphilic molecules of fatty acids can form molecular monolayers on the surface of water. Changing the surface pressure can change the structure of the membrane. The film structure of stearic acid shows X-ray diffraction patterns of 21 monolayer films of stearic acid deposited at different migration rates of the glass substrate. Based on the graph Fig. 30, there are two series of diffraction peaks [200]. The values at $2\theta = 4.41°$, 6.58° and 11.0° are due to the reflections (002), (003), and (005) of the C crystal with long spacing of 3.99 nm, respectively. The peaks at $2\theta = 5.70°$ and 9.53°, on the other hand, are assigned to reflections (003) and (005), respectively, in crystal form with a long spacing of 4.64 nm. Several studies have shown that the structural arrangement of fatty acid films can change from hexagonal to rhombic at a thickness greater than that of the monolayer [196].

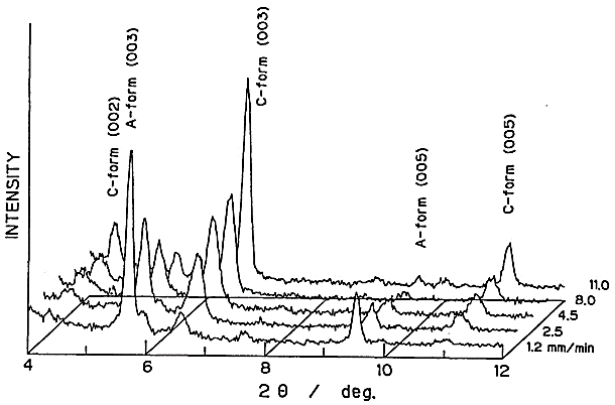

Fig. 30. X-ray diffraction pattern of 21-layer stearic acid film on a glass substrate [200]

Рис. 30. Рентгеновская дифракционная картина 21-слойной пленки стеариновой кислоты на стеклянной подложке [200]

By controlling the desired thickness, the LB film can create a porous membrane structure through a corrosion mechanism [201]. After forming the stearic acid film by LB method on mica substrate, the film was etched by soaking in salt solution to create a porous structure. The AFM image of SA monolayer film shows a uniform surface with rare defects (Fig. 31A) and its high-resolution image (Fig. 31B). However, the area of defects accounts for only a small percentage of the total area. These SA LB membranes on mica were able to maintain their structure for several days. These types of porous materials can be used in many fields such as life sciences, catalysis and optics. In addition, with the single-layer film making mechanism, the thickness of the film can be completely controlled and the desired thickness is obtained.

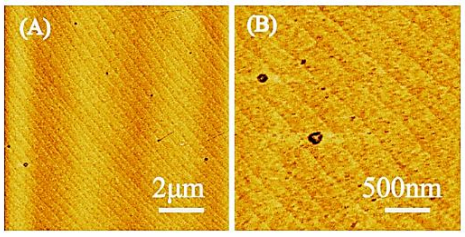

Fig. 31. AFM image of SA monolayer (B) High resolution image of SA monolayer [201]

Рис. 31. Изображение монослоя SA, полученное с помощью АСМ (B). Изображение монослоя SA с высоким разрешением [201]

Optical

The graph presented a survey on the various parameters that affect the optical properties of mixed DBPI/PMMA or DBPI/Stearic acid films. As we can observe from the dotted line in both a) and b), a minor

red shift occurred when comparing the original material in chloroform to the annotated lines with molar fractions (Fig. 32). Although small, this indicates a change in the material structure.

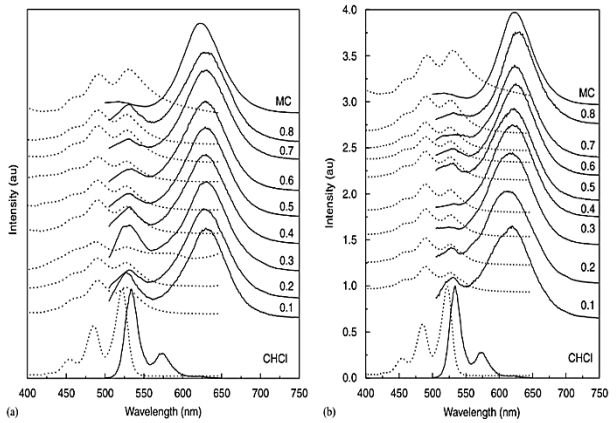

Fig. 32. UV-Vis absorption spectra (dotted line) of N,N-bis (2,5-di-tert-butylphenyl)-3,4,9-perylenedicarboximide (DBPI) in polymethyl methacrylate (PMMA) and Stearic acid [157]
Рис. 32. Спектры поглощения в УФ-видимой области (пунктирная линия) N,N-бис(2,5-ди-трет-бутилфенил)-3,4,9-перилендикарбоксимида (DBPI) в полиметилметакрилате (ПММА) и стеариновой кислоте [157]

From a perspective of the exciton model [202], exchanges between molecular dipoles can cause an exciton band with specific energy to materialize. This specific energy can be different or equal to the monomer's value. A formula is used to calculate the change in energy:

$$\Delta E = 2M^2(1 - 3cos^2\theta)/r^3$$

where M represents the dipole moment, θ represents the angle between the dipole and the r vector, and r is the length of the vector between the two centers of the dipole. Depending on the θ value, the change in energy can be positive, negative, or none. At the angle of 54.7 degrees, no shift is observed, while for angles less than 54.7 the sign of E is negative, meaning the band is formed below the monomer's level thus creating a red shift. On the opposite end, angles above 54.7 degrees up until 90 degrees cause the formation of an exciton band above the original monomer's band, prompting the molecule to accept shorter wavelengths thus causing a blue shift.

Earlier studies have found that aggregation causes shifts in the spectra [203]. It is worth noting that in this case, the aggregation of film molecules caused the exciton band energy to fall below the original monomer band, thus prompting the material to absorb light towards the red end of the visible spectrum (longer wavelengths – less energy). These aggregates are called J-aggregates. Note that while the studies mentioned red shift, it is by no means comprehensive and the opposite can occur, which is a blue shift. A blue shift is the absorption of shorter wavelengths, or increased energy light towards the blue end of the visible spectrum. This is caused by the exciton band energy moving higher than the original monomer band energy. These aggregates are called H-aggregates.

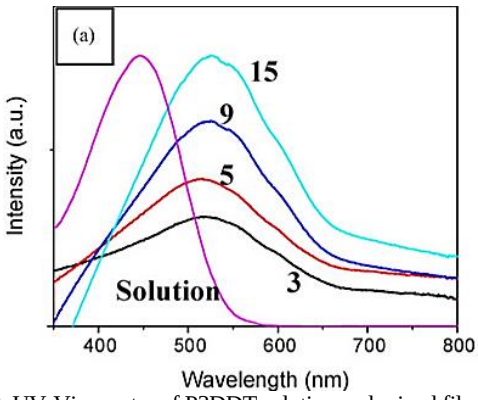

Fig. 33. UV-Vis spectra of P3DDT solution and mixed films [204]
Рис. 33. УФ-видимые спектры раствора P3DDT и смешанных пленок [204]

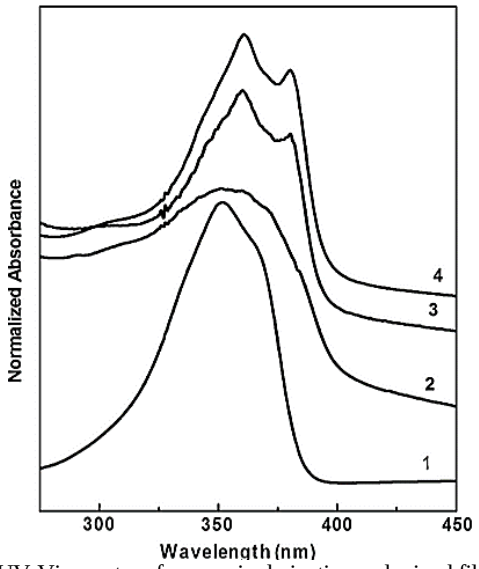

Fig. 34. UV-Vis spectra of coumarin derivative and mixed films [205]
Рис. 34. УФ-видимые спектры производных кумарина и смешанных пленок [205]

Similar conclusions can be drawn from Fig. 33 and Fig. 34 as we observe a significant red shift in the UV-Vis spectrums. All of the articles attribute this to the creation of aggregates causing the delocalization of electrons and lowering the energy required for the excitation of the material. However, existing literature on LB films that exhibit blue shift behavior is not uncommon. Blue shifts for azobenzene-containing fatty acids, stilbene amphiphiles, and pyrenes were also reported [206-208].

Changing film parameters seems to have mixed effects based on film architecture. Fluorescence spectra showed small shifts from the influence of molar fractions, but significant changes dependent on layer count and pressure [157]. In this article, increasing layer count or pressure causes an increase in excimer emission and a decrease in monomeric emission, explained by the increase in molecular density/distance, causing a higher rate of formation for excimers and thus increasing excimer emission on the spectra. Molar fractions do not produce visible changes in spectra except a specific molar fraction of 0.8 carbazole/PMMA produces a spectra similar to that of carbazole in a microcrystal state [158]. It appears that this molar fraction creates a stable environment for the formation of similar structures. Higher layers of the film appear to cause a reversal in the fluorescence spectra characteristics. At lower layer counts, emission within the longer wavelengths is higher relative to the shorter end, while at higher layer count this appearance is reversed. The paper only provides speculations on this phenomenon, attributing it to changes in electronic structure caused by additional layers. Further study is needed to clarify this observation. Pressure does not have a significant effect. The effect of changing film parameters are better discussed elsewhere within this review article.

In general, optical properties of LB films and LB films of fatty acids are highly diverse and dependent on the properties of the compounds chosen by researchers. Apart from the red/blue shift phenomenon observed in the articles, we have not found many trends or themes within the optical properties of LB films of fatty acids.

APPLICATIONS POTENTIALS OF FATTY ACIDS

Sensing and biosensing

Sensing and biosensing can be considered one of the key applications for LB films of fatty acids with over 1400 articles [1] (see Table 3 for the keyword "biosensors" in cluster 3). Recently, these films have been applied in surface-enhanced Raman scattering (SERS), which enables biomolecules to become highly sensitive sensors when FRaman scattering is enhanced thanks to surface modification [209]. Early studies highlighted the basic gas sensing applications into (i) gas sensors, (ii) ion sensors, and (iii) biosensors and immunosensors [210]. For gas sensors, the device that incorporates LB films takes advantage of the high ratio of film area to film volume property of thin films. Due to the high surface area, when the film is exposed to a sensitive molecule, a reaction quickly begins and changes the film's properties. This change can be measured and output the type of molecule and concentration. For ion sensors, there are ion-sensitive layers or ion-sensitive field-effect transistors (ISFET) [210]. In these devices, ions form complexes with film material, which then is measured using a quartz crystal microbalance (QCM) [211], or the device has a measured change in voltage when exposed to ion concentrations in ISFETs [212]. Immunosensors operate in the same manner as ion sensors, with biomolecules causing measured changes in film properties [210].

A biosensor measures biological or chemical reactions by generating signals proportional to the concentration of the analyte in the reaction [213]. Biosensors have been widely studied and applied in most fields from monitoring the impact of environmental pollution, in the food and textile industries to their application in medicine and biology [214]. Thanks to their short response times and small form factor, biosensors exhibit the capability to function in a variety of environments and temperatures. Nonetheless, the crucial element impacting the sensitivity of these sensing systems is the presence of identification units characterized by optimized surface density, excellent contact ability, long lifetime, high stability, and high reliability. Molecular assemblies in a thin-film model that meet the requirements of biosensors can be fabricated using the Langmuir - Blodgett (LB) and Langmuir - Schaefer (LS) techniques [215, 216], which allows thin layers of lipids to be stacked atop one another. By optimizing the parameters, these techniques can fabricate thin films of amphoteric molecules, which have suitable properties for immobilizing adsorbent molecules with biological activity [217].

Gas sensor is a device that can detect and give the concentration of various gasses such as toxic gas, explosive gas, volatile organic compounds or moisture [218]. Gas sensors are generally divided into two types: reversible sensors that can be used continuously and repeatedly and the second type are non-reverse sensors that can give a quick warning of toxic gasses but can only be used once. However, it is important for most gas sensors to select a sensitive material that can respond quickly [219]. Ding Hanming et al. previously reported the results of gas sensing using LB membrane fatty acid salts to detect H_2S gas [220]. According to previous evidence, H_2S gas has a direct impact on humans, causing high levels of olfactory fatigue. At low concentrations from 0 to 150 ppm, H_2S gas can be irritating and when exposed to 5 minutes at concentrations of 800 ppm they can be fatal to humans [221]. Extensive research has been conducted on providing early warnings for detecting H_2S gas even in low concentrations. However, the applicability of most commercial

gas sensors is restricted due to their reliance on inorganic materials and the necessity to operate at high temperatures. In recent studies, organic thin films have shown outstanding advantages in terms of low-temperature operation, rapid fabrication process, and material availability [123, 222]. Among these materials, fatty acids are commonly employed, particularly salts of stearic, arachidic, behenic acids, and others. These substances exhibit rapid and facile reactions with H_2S molecules. Moreover, the LB thin film possesses a structural advantage attributed to its extensive surface area, facilitating easy diffusion of gas molecules into the thin film. As a result, fatty acid LB thin films have the potential to serve as sensitive materials for gas sensors [220].

Thickness shear mode (TSMs) biosensors have many potential applications in pharmaceutical science. They can accurately measure mass in the nanogram range, film thickness, viscosity, and shear modulus. The application of these biosensors to measure the drug partition coefficient has opened up new potential applications in the field of medicine [223]. Previous publications have described the principle of fatty acid multilayer films as a suitable chemical modeling system, displacement, and spectral properties of three fatty acid film layers coated on the sensor by the Langmuir-Blodgett method [41]. The results indicate that the frequency change is non-linear at low fatty acid counts and the viscosity in the film becomes higher at a large number of film layers. An inverse relationship was observed between sequence length and frequency change which was attributed to the influence of the morphology of the sensing surface [223]. This shows the importance of accurately and fully describing the properties of lipid multilayer membranes so that they can be applied in sensors drug delivery coefficient [223].

A surface acoustic wave (SAW) sensor for the detection of odorants was also presented earlier by S.M. Chang by applying the Langmuir-Blodgett technique [224]. Through the deposition of various phospholipids and fatty acids onto the surface of the SAW device, the characteristics of this device operating at 310 MHz coated with phosphatidylcholine were analyzed. It is shown that the identification of these odorants depends on the type of lipid used for the coating [224]. Since then, many studies have been developed to discuss and compare their normalized resonant frequency shift patterns.

Tribological applications

The lubricating properties of LB fatty acid film surfaces have been applied in tribological applications [32, 225, 226]. When comparing the wear reduction efficiency of octacosanoic acid (OCA) LB monolayers to other self-assembly films, namely octadecanoic (OA) and octadecyl trichlorosilane (OTS), OCA has 7.5 times the resistance of OA films and about 27 times the resistance of OTS films [32]. The large difference between OCA and OTS films is explained via the nature of the interaction between the film and the material. OTS forms covalent bonds while OCA and OA form weak bonds with the material. This weak bond allows molecules to navigate between surfaces, thus reducing the wear and stress on the material. However, the difference in wear reduction efficiency between OA and OCA films (both fatty acids) was not elucidated. Other fatty acids and fatty acid derivative materials should be investigated, especially a mechanism explaining the difference in the lubricating quality of different fatty acids [227].

Model membranes

Recent studies of LB fatty acid films for biomedical applications were focused on tear films for dry eye disease [228-231], and model membranes [232-237]. The application of LB fatty acid films can be expanded into the biomedical field by fulfilling other requirements, namely biocompatibility, low corrosion, and tissue integration [238]. Although it is evident that fatty acid films satisfy biocompatibility, we have limited data on the low corrosion and tissue integration ability of fatty acid films [7, 239, 240]. We speculate that LB fatty acid films are likely to be used as short-term materials and surfactants in biomedical fields such as tear film layers.

Fatty acids which are major components of biologically relevant structures such as cell membranes have been the subject of many studies due to their biocompatibility and potential applications. Solid-state lipid layers can be used as model membranes for the study of lipid ligand-binding proteins, cell identification, insertion of proteins into membranes, and other biofilms-related studies [241]. Proposed by Prof. Marcio Francisco Colombo and validated by Prof. João Ruggiero Neto, the utilization of Langmuir monolayer membranes emerged as a fitting approach to understanding the molecular-level functions of biomolecules within cells [242].

Applying the Langmuir monolayer membrane technique in studying the interactions between molecules and simulating cell membranes [243, 244], thereby applying them to medicine is a trend that is of great interest to researchers. Studies on the effects of unsaturated fatty acids (UFAs) and plant sterols/stanols on biofilms modeled as cholesterol/DPPC systems [245] showed that the hypoglycemic agents studied changing the physiological properties of the model membrane, directly affecting the fluidity and interactions between

the membrane components [246]. By applying the Langmuir monolayer membrane technique to study the intermolecular interactions, the above study showed that not only cholesterol but also its oxidized derivatives oxyterol [247, 248] are involved in the formation of atherosclerotic plaques in the artery wall. Moreover, the close association between oxyterol and cholesterol on the same cell membrane is closely related to each other and plays an important role in vascular remodeling, and is associated with atherosclerosis. Therefore, the interaction between unsaturated fatty acids and cholesterol with oxyterol has been studied through the monolayer LB membrane technique [246]. The report of Giuseppe Vitiello et al [249] used omega-3 fatty acids to reduce the risk of developing Alzheimer's disease (AD) by modulating the properties and dynamics of nerve cells. Results of studying the effects of lipids omega 3 and 1,2-didocosahexaenoyl-sn-glycero-3-phosphocholine [22:6(cis)PC] on the physiological properties of the lipid bilayer and their interactions with the amyloid peptide fragment A (25-35) has been shown to interact selectively with the cholesterol-rich (Chol) and sphingomyelin (SM) classes. [22:6(cis)PC] increases the A(25-35) interaction with the membrane and aids in the internalization of peptides between lipid acyl chains [249], thereby helping to prevent the process of causing Alzheimer's disease. It can be seen that the application of Langmuir membrane technology together with fatty acids is increasingly being studied for the simulation of cell membranes and their application in the treatment of diseases, which further promotes the development of cell membranes techniques in biomedical and cellular fields.

Environmental science

Applications of fatty acid films in environmental science have emerged. This emergence is rooted in applications of LB films for the detection of harmful substances such as heavy metals [250, 251], pharmaceutical waste [252], and harmful peroxides [253]. This future research direction was evidenced by [254] who described a thin film of poly(piperazine-amide)/sulfonated graphene oxide (SGO)/magnetite-decorated SGO via the electrospray interfacial polymerization method for dye/saltwater separation. The thin film was characterized by hydrophilicity, roughness, porosity, and permeation properties. Similarly, Ma [255] used a thin-film composite polyamide through the electrospray method and highlighted the film's features, namely porosity, surface charge, permeability, and heavy metal ion adsorption. The LB method can replicate similar materials [254, 255] through porosity and surface roughness modification to allow for ion adsorption. Fabricated LB polyimide/fatty acid films have been reported as structurally similar to our speculative polyamide/fatty acid film [256, 257], in which fatty acid incorporation can render unstable film-forming materials such as polyamides viable for thin film fabrication. In our opinion, we consider using LB films of fatty acids for environmental purposes to be highly potential and feasible for researchers to conduct.

Metal ion adsorption is a viable research direction that has a basis in current LB fatty acid film literature [258]. Heavy metal ions such as cadmium, lead, chromium, and arsenic are highly toxic to biological life and must be purified from water sources. Fatty acid films solve this predicament via the ion adsorption mechanisms of cadmium ion [127, 259-261], lead ion [262-265], and chromium ion [266]. Although the theoretical possibility has been established, this area remains unexplored despite its potential.

Chitosan and carbon material

Yan's work [267] described chitosan microspheres produced via precipitation with promising ion adsorption properties. Considering the recent interest in chitosan-based LB films [268, 269], researchers can consider incorporating the chitosan microspheres from Yan's work into their LB film research. Other works have detailed chitosan/fatty acid films, demonstrating the uses of this material [147, 168, 235]. Li's work [270] demonstrated a hydrogel material formed from polymers and amylose exhibiting dye absorption properties. While forming hydrogel is not practical using LB techniques, researchers have historically investigated amylose-containing LB films such as mixed amylose/esters films [271, 272], and amylose/dye films [273].

Alvarez's work [274] demonstrated that ozonation of granular activated carbons (GACs) affected adsorption strength towards phenolic compounds of the material. Since LB technology allows for the fabrication and modification of surface characteristics, films containing GACs can be considered a potential material for investigation. However, the large size of GACs prevents them from practical applications in experiments and application. Thus, we recommend a similar alternative: powdered activated carbon (PACs). According to a manufacturer, the median perimeter of PACs is 15 to 30 μm [257]. If these micron-sized particles can be incorporated into LB films, probably by using a support layer such as fatty acids, we can realize a novel research area that has not been previously done before.

Solar cells

Along with the development of renewable energy, thin film solar cells have received more and more attention in recent times due to their outstanding optical properties and high energy conversion efficiency

[275]. The use of fatty acid thin films in thin film solar cells has been proposed, which can be anti-reflective coatings or act as an absorbent layer, or can be combined with other materials to passivate defects, which enhances the efficiency of solar cells [275, 276].

Almost all of the semiconductors commonly used for solar cells such as silicon or gallium arsenide have a high refractive index ($n > 3.0$), which leads to a deterioration in their efficiency [277]. As previously published, a common method to reduce the reflection of solar cells is to add an anti-reflective (AR) coating at the end of the battery processing. In addition to acting as an anti-reflective coating, this material must also meet the requirements for use as a protective cover for solar cells [278]. In order to overcome the weaknesses of materials used as protective covers for solar cells today such as glass, silicon, polymer coatings, etc., organic films of long-chain fatty acids have applied in this area [277]. The use of fatty acid films based on the L-B method as coatings on the glass surface of solar panels has been reported since the early 1940s, but the application of both AR and protective coatings is a matter of ongoing research. The research conducted by S.L. Buckner and V.K. Agarwal has shown that fatty acid L-B films can grow films of high quality with controllable thickness, whose refractive index can be adjusted to a limited extent through the CH_2 group. integrated in molecular chains or by replacing H^+ ions with metal ions [277]. In addition, the hydrophobic -CH_3 group in the molecule can be used to maintain the outermost layer, which is responsible for inhibiting water absorption, the use of polydiacetylene membranes [$CH_3(CH_2)_n$-C≡C-C≡C-$(CH_2)_m$-COOH] as a photopolymer will provide thermal stability and mechanical stiffness corresponding to the panel protection material. The use of fatty acid films such as stearic acid films on silicon solar cells as an antireflection and protective coating has been presented and studied recently, showing a decrease of 10-30% in the reflectance on commercial solar cells. The refractive index of stearic acid films in the range of 1.42-1.48 is suitable for the efficient use of fatty acid thin films in the field of solar cells [277].

The enhancement of the efficiency of solar cells using a new material that combines inorganic materials and fatty acids has been demonstrated previously. This helps to limit the surface defects of the material, enhance the transport of charge carriers and increase the light absorption capacity of the solar panels [278]. In the report of Yifang Qi et al., the passivation technique was used to improve the performance of perovskite solar cells (PSC) [279]. Accordingly, a new material was fabricated, using fatty acids-polyamidoamine-COOH (FPC) with sixteen long alkyl chains and eight carboxylic acid functional groups, which can passivate Pb defects at the surface and grain boundaries, which play an important role with recombination at the interface between the perovskite layer and $PC_{61}BM$ (Phenyl-C61-butyric acid methyl ester) in PSC. The energy conversion efficiency of PSC modified by fatty acid-polyamidoamine-COOH (FPC) can be increased to 21.01% with J_{SC} = 23.74 mA/cm^2, V_{OC} = 1.09 V, and FF = 81.16%. Furthermore, the hydrophobic long alkyl chains improve the stability of the device, which can maintain 82% of the original PCE value in ambient at 305 °C for 30 days [279].

In another study, the combination of ionic liquids from the products of organic acids and organic amines with inorganic thin films was also presented [276]. Accordingly, an easy and environmentally friendly approach is developed to deposit $Cu_2ZnSn(S,Se)_4$ thin films by adding the important n-butylammonium butyrate ionic liquid in the solution. deposition of thin films, they can dissolve some metal oxides such as Cu_2O, ZnO và SnO, and various metal chlorides. Then, n-butylammonium butyrate was completely removed by thermal decomposition using a low-temperature sintering process, forming a high-quality Cu_2ZnSnS_4 nanoparticle thin film. Thin-film solar cells using the above material give an energy conversion efficiency of 8.79%, showing the potential for making solar cells using green methods with an easy process [276].

To improve the efficiency and longevity of photovoltaic devices, electrodes made of fullerenes and derivatives combined with ionic liquid electrolytes have been used in solar cells (DSSCs) [280]. In Katayanagi's study, Hideki et al. produced carbon electrodes suitable for applications in solar cells using LB technique and sulfonated fullerenes as substrates [281]. Accordingly, monolayer and multilayer films with sulfonyl-based fullerene/fatty acid and non-fullerene mixtures have been investigated [281].

Conductor

The growing fascination with organic thin films possessing conductive and semiconductor characteristics stems from their potential applications in electronic devices that demand a molecular-level structure. The fabrication of a nanometer-sized organic conductive film has opened up many applications such as in solar cells, sensors, or light-emitting diodes [282]. However, the fabrication of thin films with molecular structures with high order level, well-controlled size and growth direction is still one of the difficulties in this field. To solve that problem, the LB technique pro-

vides precise control over the layer-by-layer deposition and orientation of the molecule. Even so, since the polycrystalline structure of LB thin films leads to heat-activated charge transport causing their conductivity to degrade, improvement of the crystal structure is essential to achieve a highly conductive LB film [283]. According to previously published studies, LB membranes of mixed fatty acid molecular systems have been shown to exhibit metallic conductive properties [282]. The charge transport and structural properties of these films were investigated as a function of the alkyl chain lengths of fatty acid molecules at different molar ratios [282]. T. Minakata et al. successfully fabricated polyacene thin films with the fatty acid diacetylene (22,24-pentacosadynoic acid: ω-PDY) used as a monomer [284]. Among them, the polymerization of 3,4 polyethynylacetylene mainly occurred in the LB process, then the C=C bond was formed by irradiation with an excimer laser or an electron beam. The formation of aromatic structures in the LB film increases electrical conductivity. The results of nanostructured TTF-TCNQ (tetrathiafulvalene-7,7,8,8-tetracyanoquinodimethane) films exhibit a conductivity of 2.10^{-2} S/cm, which is six times greater than that of PDA (10,12-pentacosadiynoic acid) multilayer [284]. Another study successfully fabricated polyaniline and polypyrrole conductive films by the LB method combined with stearic acid (PAN-B/SA) to form stable films at the air-water interface [285]. The alkyl chains of the stearic acid molecules are randomly distributed in the LB membrane which minimizes influence on the electrical properties of polyaniline. These films are then converted to multilayer films with a conductivity of about 1 S/cm when doped with hydrochloric acid [285].

Leonid M. Goldenberg fabricated a tetrabutylammonium-Ni(dmit)$_2$ complex film at the air-water surface with various substrates from the supernatant containing different concentrations of tricosanoic acid [286]. The morphological, electrochemical, and photoelectrochemical properties of the conductive thin films show that the conductivity value measured at room temperature is 10^{-2} S·cm^{-1}, thermal activation energy ΔE = 0.08 – 0.1 eV over a temperature range of 100-300 K, by electrochemical doping after deposition with four different anions and by chemical doping with iodine. The electrochemical doping method during LB film deposition showed a conductivity value of 10^{-3} S.cm^{-1} [286].

Smart windows

In daily life, heat absorption through transparent surfaces such as windows can lead to an increase in temperature in buildings, offices, cars, or enclosed spaces which makes the heating process, cooling, and artificial lighting consume a lot of energy [287]. With the advancement of nanotechnology, it is possible to create materials with unique structural properties that are capable of reducing energy consumption in a certain area. In buildings or cars, these materials can be applied to smart windows. Smart windows can reduce energy consumption by controlling the absorption of solar radiation at will in different weather conditions based on the principle of phase change [288, 289]. Paneliya and colleagues have successfully fabricated paraffin coated with silica mixture as an organic phase change material with ultrathin coating using Langmuir-Blodgett technique [290]. Due to low thermal conductivity, paraffin is coated with fatty acids to increase heat conduction during phase transformation (solid-liquid), the phase transition temperature is reduced from 0.6-2.5 °C, melts at 54.72 °C and condenses at 52.09 °C. Paraffins combined with fatty acids can induce van der Waals interactions that cause chaotic crystalline domains at the surface of materials or monolayers [290]. The film of epoxy monomer diglycidylether of bisphenol A (DGEBA) is double-coated with stearic acid and methacrylic monomer which crystallizes at temperatures below 40 °C and melts at 45 °C. The process of investigating the transmittance of the film according to the heating/cooling cycle at 20 °C/min shows that at 48 °C, the film has an almost 100% transmittance and drops to only 35% below 37 °C because of crystallization in the membrane. The process is repeatedly reproducible with optical transmittance unaffected by the cooling rate.

Battery

Fatty acids are not only studied and applied in the field of sensing, medicine or biology but also in the field of energy storage such as in batteries or capacitors. They are used mainly as a coating that improves electrical conductivity and increases the electrochemical performance of the battery. In any chemical reaction, the surface of the material plays a very important role, the choice of coating for the anode and cathode materials in the electrochemical cell greatly increases the conductivity and shortens the diffusion time. ions [291]. Accordingly, a mixed negative electrode material of $LiFePO_4$/C was synthesized by sol-gel technique using long-chain fatty acids such as lauric, myristic and oleic acids as surfactants for the carbon coating [292]. Although $LiFePO_4$ possesses the outstanding properties of cathode materials, it is limited by its poor electronic conductivity, resulting in high impedance, low capacity, and ion diffusion rate. This makes the application of large Li-ion batteries in electric vehicles limited. Furthermore, the surface properties of $LiFePO_4$

are indeterminate, whether it is polar or nonpolar, hydrophobic or hydrophilic all depends on the synthesis technique and the nature of the material used for coating [292]. An organic material with many functional groups such as a surfactant that can favorably interact with the complex surface of $LiFePO_4$ is commonly used as a carbon material such as C_{12} and C_{14} fatty acids and in some studies, oil olive oil, soybean oil, and butter were used for the $LiFePO_4$ carbon coating [291]. Survey results of $LiFePO_4$/C composite materials using lauric acid ($C_{12}H_{24}O_2$) and myristic acid ($C_{18}H_{34}O_2$) as surfactants show that the Li-ion diffusion coefficient is higher, the discharge capacity is 155 $mAh \cdot g^{-1}$ at C/3 rate and cyclic stability relative to the starting material [292]. Another report fabricated an ultra-stable zinc-metal positive electrode thanks to a stable fatty acid-zinc interface layer [293]. In situ complexation of saturated fatty-zinc acid can produce an extremely thin layer of zinc compounds, thereby modulating Zn nucleation and deposition kinetics. Furthermore, the multifunctional surface of the hydrophobic carbon chains of fatty acids acts as an effective protective layer to exclude water molecules from the surface and inhibit the corrosion of the zinc surface. The results show that the anode by fatty acid-zinc layer gives a cycle life of more than 4000 h at $5mA.cm^{-2}$. In addition, the fully assembled Zn/V_2O_5 cells have excellent performance and long-cycle stability [293].

Superhydrophobic coating

Long-term dusty material surfaces can cause loss of aesthetics and above all reduce the efficiency of devices such as solar cells or glass doors. Superhydrophobic surfaces can prevent the accumulation of dust and water due to their self-cleaning ability. Thanks to the low contact angle delay and nanometer rough surface of the solid substrate, water droplets can easily slide across the surface of the material and wash away dirt. The lower surface roughness results in less contact area between the material surface and the water droplet. Combined with the air in the pores on the surface of the porous material, the contact angle of the water droplet is higher. Razavi et al [294] functionalized sepiolite or meerschaum ($Mg_4Si_6O_{15}(OH)_2.6H_2O$) nanoparticles with naturally derived alkyls (cinnamic acid ($C_9H_8O_2$) and myristic acid (($C_{14}H_{28}O_2$) to fabricate superhydrophobic surfaces water by dipping the substrate in solution. The results show a contact angle of 150°. In addition to hydrophobicity, the surfaces also show antibacterial and anti-biofouling properties formed from a fatty acid-metal-carboxylate mixture and coated on the surface of the material [295]. The water contact angles with the metals for use as coatings are different, respectively: nickel (150.2±1.88°), cobalt (151.0±1.68°), copper (151.1±0.98°), iron (150.5±1.88°), zinc (152.2±1.08°) and sliding angles are all less than 5°. Coatings with a combination of metals that can create hydrophobic surfaces of various colors: copper (blue), nickel (light blue), iron (brown), cobalt (purple), and zinc (white). Furthermore, the metal carboxylate is highly stable, and can be maintained for at least 6 months without fading or losing its superhydrophobicity.

Protection of Steel

Corrosion is the main cause of deterioration in the quality and service life of steel. Annual costs for maintenance and repair are very large. Therefore, finding a method to solve the problem of steel corrosion is an urgent issue. In particular, using coatings to prolong the protection time of steel is a popular trend today. A protective coating that covers the entire surface of the material can help isolate the steel surface from the surrounding environment, thereby minimizing the impact of the environment on the surface of the steel. Environmentally friendly fatty acid-based coatings, which are less toxic to the environment, are preferred over synthetic ones [32]. The Langmuir–Blodgett method of film formation is suitable for forming films with monomolecular fatty acids without requiring a vacuum and high temperature. W. Xing et al investigated the corrosion resistance of stearic acid coating to iron [296]. The corrosion resistance of the stearic acid film was tested by electrochemical measurement in 0.5 M potassium ferricyanide ($K_3Fe[CN]_6$). The results showed that as the number of stearic acid film layers increased, the peak current decreased. When iron is surrounded by 9 layers of stearic acid, the value of the peak current is almost no longer recorded. That shows the ability of the stearic acid coating to protect iron from corrosion almost completely from the electrochemical corrosion reaction. In addition, Sacilotto et al also used stearic acid to investigate the protection ability of stainless steel (AISI 304) and evaluated by electrochemical method in 0.1 mol/L NaCl with aeration at pH 6 [297]. The results after 96 hours of continuous immersion in NaCl show that the steel surface treated with stearic acid has higher corrosion resistance. The steacic acid coating acts as a protective barrier separating the sample surface from the Cl- ions that tend to come into contact with the sample surface. Sacilotto also showed that, when the surface of the sample is smooth, it contributes to uniformity with the stearic acid coating, which further enhances the protection of the coating material.

Immobilized luminescent polymers

Polymer luminescent materials (PLEDs) have increasingly asserted their importance in the fields of

lighting, displays, and devices requiring precise optical properties [298]. However, the reflective performance of these materials is hindered by the interaction between the polymer chains and the undesirable thickness of the material [299]. With the advantage of being able to control the thickness and structure of thin film materials, the Langmuir-Blodgett technique has been used for applications in producing luminescent polymer films and improving the current density of materials [162]. Due to the limitations of polymer film formation during propagation on the air-water interface of the LB technique, polymers mixed with an amphoteric substance such as phospholipids and fatty acids have been investigated to solve the above problems [300].

In order to apply the above technique to create luminescent polymer films, Andrei Sakai used a mixture of PPV (poly(p-phenylene vinylene)) with stearic acid to obtain ultrathin films from hybrid materials using the LB method [162]. Accordingly, stearic acid acts as a substrate to form Langmuir films that are stable to PPV. When comparing the fluorescence spectra of the polymer in solution in the form of a casting film and an LB film, the emission bands of the LB film are narrower and appear at lower wavelengths. Thereby, polymer thin films from the above method can be applied in most optical devices, typically the coating of organic light-emitting diodes (OLEDs) [162]. From reports for lighting applications, flat panel displays that polyfluorene and fluorene-based conjugate polymers have been intensively studied. A quinoline-fluorene-based polymer (QFC) using the LB membrane synthesis technique was investigated. The transfer of this material onto a solid substrate by the LB technique showed strong fluorescence emission. In which the emission spectrum at the peak of 405 nm is due to the luminescence of benzyl and pyridyl groups, for quinoline-free copolymers, the maximum emission is only 380 nm [301]. Membrane emission can be affected by intermolecular species (aggregates and excimers), much more strongly than in solution and up to 425 nm, as previously demonstrated by Mikroyanidis [302]. Another study also showed that a composite film consisting of fatty acids could help the polymerization of pentacosadiynoic acid and perfluoro tetradecanoic acid to be deposited on glass substrates, helping to form oriented polydiacetylene luminescent polymer materials. The results show that the membrane has a heterogeneous structure, consisting of many oriented fibers and polarized photopolymer arrays [303]. The orientation in the film is attributed to the combination of phase separation of the two immiscible surfactant components together with the mechanical force resulting from the deposition action on the substrate. The determination of the orientation properties of the fibers in the polymer film shows that their optical properties are the basis of the conversion between the blue polymer which does not fluoresce and the red polymer which is highly visible [303]. The application of fatty acids to the process of creating luminescent polymer films has been exploited in many applications, this is also a potential area for the development of LB technology.

Selective filter

Oil-water separation filtration is one of the important fields. Certification is not only used in laboratories but also in practical applications such as the oil and gas industries, food industry, oil spills and environmental protection. The moisture content of the material plays an important role in the oil separation process. Materials with high moisture content provide better oil separation performance. Shama Perween et al. have developed a composite membrane based on polyvinyl alcohol (PVA), polydimethylsiloxane (PDMS), and stearic acid by electrospinning which has the ability to effectively filter and separate oil [304]. The combination of stearic acid produces a solution with suitable viscosity and high homogeneity for nanofiber fabrication. In addition, it also helps to bind PVA and PDMS fiber molecules through Van-der-Waals binding force to help control the hydrophilic, hydrophobicity of the membrane. Membranes can become selective filters by becoming selectively permeable when in contact with an emulsion in oil. The increased proportion of PDMS in the film also showed an increase in the hydrophobicity and lipophilicity of the film, which can be used to separate the emulsion in oil. Through the color of the film after the oil refining survey, the film has a color close to the color of the original oil used as the emulsion. The test results show that the nanofiber composite film has good selective permeability to oil and can successfully separate emulsion in oil. This is also the scientific basis for making nontoxic, environmentally friendly membranes capable of refining oil with different types of fatty acids.

Stable magnetic fluid

Nanoscale magnetic materials have more special properties than bulk materials. Magnetic beads with a diameter of less than 15 nm make it easy to disperse in solution or in sol-gel form. Such dispersions of magnetic nanoparticles in the form of sol-gels are called magnetic liquids, they are kept intact even in the presence of high magnetic fields. Due to its unique superparamagnetic, triboscopic, thermal and mechanical properties, this material is widely used in the industrial field [305, 306]. However, in order to minimize the agglomeration of magnetic nanoparticles, the magnetic

nanoparticles were combined with surfactants or different polymers adsorbed on the surface. To maintain the dispersion of the magnetic nanoparticles in the solution, Wang Y et al. used oleic acid together with Tween 80 to coat the surface of the Fe_3O_4 nanoparticles [307]. The results show that Tween 80 is well compatible with oleic acid and forms a double-layer structure. Tween 80's hydrophilic head makes Fe_3O_4 nanoparticles well dispersed, suspended in water even when diluted. Investigation of magnetic properties of Fe_3O_4 nanoparticles by vibrating sample magnetometer at room temperature showed that the saturation magnetization of bare Fe_3O_4 and Fe_3O_4 coated with oleic acid and Tween 80 were 37 and 29 emu/g, respectively. L.Shen et al. used gamma irradiation to improve the stability against agglomeration of magnetic liquids when coated with unsaturated surfactants such as 10-undecenoic acid [308]. The magnetic thin films of Fe3O4 nanoparticles fabricated by the Langmuir-Blodgett method can have a thickness of only the molecular monolayer [63]. Fe_3O_4 nanoparticles surrounded by fatty acids (oleic acid and stearic acid) were maximally separated and showed uniform distribution on the membrane surface. Ultra-thin magnetic films are considered to have potential applications in electronics, especially magnetic recording applications, for magnetic recording densities in the range of 100 Gb/in^2 to 1 Tb/in^2.

In Smart Water Flood

The demand for energy in the world is increasing, which requires an increase in production from oil reservoirs. However, due to the deterioration of oil reservoirs, the amount of recovered oil is reduced. Many different methods have been tested and proposed, but the method of spraying water into lakes has not been evaluated as the most effective due to its feasibility and low cost. Some research results have shown that using brine and water salinity has a great influence on oil recovery, helping to increase oil recovery efficiency [309]. Mg^{2+}, Ca^{2+}, SO_4^{2-} ions present in salt water change the moisture content of the rocks in the reservoir to reduce their wetting ability and are called smart water [310]. By means of intelligent flooding method will create a pressure difference, and remove naphthenic acid which changes the rock surface moisture. When using fatty acids (stearic acid), it is possible to create an adhesion layer on the surface of the stone by strong fatty acid bonds, causing less sand to be produced. Interactions between stearic acid and ions at the surface can affect the mechanism that controls the stability and aggregation of droplets. Low salinity is also one of the factors that increase the interaction between stearic acid and ions and minimize the possibility of particle agglomeration [311]. The combination of nanoparticles at the rock surface that makes the rock less exposed to the environment also contributes to minimizing the amount of sand generated.

Catalytic performance

The creation of Langmuir-Blodgett (LB) thin films from lipid acids or enzymes shows the remarkable advantage of being able to control the size and structure at the molecular level. In previous work, control of the enzyme's catalytic activities showed that lipid interactions at the air-water interface in the form of a Langmuir monolayer film provide the enzyme with a soft environment that helps it to retain moisture. have secondary and tertiary structures [64, 312]. This allows the lipid-enzyme mixture to be deposited onto the solid film while their catalytic activity is still partially conserved. Although the catalytic capacity has been reduced compared with the homogeneous medium, at the molecular size, they can preserve the catalytic activity after a long time [313]. To demonstrate that, Luiz Henrique and colleagues carried out adsorbed carbon nanotubes (CNTs) on a LB monolayer of stearic acid as a substrate for the incorporation of asparaginase with the target. to enhance the catalytic performance [314]. Although asparaginases are non-surfactants due to their high hydrophilic properties [66], when they are inserted under the Langmuir layer of SA, they become adsorbents in the monolayer, where SA exhibits an isotherm with gas phase (or gas-liquid transition) up to 30 Å ^{2}/molecule. When the supramolecular structure is formed by asparaginase, SA and CNT are stabilized [314]. In the presence of CNTs in the enzyme-lipid LB membrane, they not only regulate the catalytic activity but also help to preserve the activity and increase the catalytic site of the enzyme. Not only that, this study also shows the feasibility of applying fatty acid LB membranes combined with carbon nano and enzymes for biosensors [314]. Another study also showed the influence of alkyl chains of linear -olefins on the catalytic performance of Ti-containing hierarchical macroporous silica (Ti-MMS) [315]. Accordingly, Ti-MMS was successfully prepared by solvent evaporation using organic surfactants. The results show that Ti-MMS exhibits higher catalytic activity in linear -olefin epoxidation compared with Ti-containing silica without macropores (Ti-MS) because of the advantages of interfacial coupling. porous and hierarchical macrostructure [315]. Not only that, with the aim of replacing precious metals in the catalysis process, fatty acids have been noticed and studied extensively. Accordingly, carbon-coated FeNi nanoparticles were prepared through an in situ decarbonization process using dou-

ble metal cyanide at different temperatures for the deoxidation of stearic acid [316]. Among the studied catalysts, FeNi@C-800 exhibits the greatest catalytic efficiency with selectivity up to 76.8% for heptadecane, moreover, the catalyst can maintain stable catalytic efficiency. determined through a protective carbon shell [316]. The application of fatty acid catalysts through LB thin films opens up a potential research direction to replace expensive metal catalysts.

In Vitro Anticancer Evaluation

Cancer is one of the leading causes of death worldwide, and research to limit and prevent them is of great interest. It has been shown that a diet rich in fiber and complex carbohydrates can prevent many types of cancer [317]. Short-chain acids (SCFAs) formed during the anaerobic bacterial fermentation of fiber and starch form the main products acetate, propionate, butyrate, valerate, hexanoate, ... with the ability to act as an agent. chemopreventive agents by slowing growth and activating cancer cell death [318]. To expand the applicability of fatty acids in the treatment of cancer, microplastics from fatty acids containing iron oxide nanoparticles and paclitaxel (PAX) have been proposed for the treatment of lung cancer [319]. Accordingly, microplastics, when introduced into the body as a dry powder, can be directed to selected locations using an external magnetic field and activated by increasing body temperature. At this time, the composition of microplastic particles is released and transferred to albumin and lipid bilayer [319]. The study also showed that the drug release effect depends mainly on the fatty acid composition of the microparticles, after being loaded with paclitaxel, the microparticles suppressed cell growth in human lung (A549) of malignant origin (IC50 for both lauric acid-based and myristic/palmitic microplastics containing paclitaxel are below 0.375 μg/mL) [319, 320].

In order to take advantage of the hydrophobicity of fatty acids, drug carriers based on these compounds are also used with the advantages of low melting point, low viscosity and high flexibility, etc. administered through injection or implantation [321]. As a result, fatty acids such as OA and CA are often used as surface modifiers of chitosan. OA is a saturated fatty acid, usually an omega-9 fatty acid, and CA is a polyphenol known as an antioxidant [322]. The bonding between them and chitosan helps to form the inner membrane of the nanocapsules thanks to the fatty acid molecules. Therefore, the nanocapsules will be able to hold the drug thanks to an outer hydrophobic membrane. Applying that, a new conjugated CS was investigated from OA and CA as an effective anticancer drug delivery nanocarrier. The results show that the encapsulation of the anti-cancer drug methotrexate (MTX) in CS nanocapsules occurs at pH = 5 after 90 min with a concentration of 60 ppm reaching an efficiency of up to 62.25%. Thereby, nanocarriers for MTX administration were first created by modifying the surface of CS with fatty acids [322].

DISCUSSION AND CONCLUSIONS

Summary of current research

Factors affecting fatty acid film

Ions play an important role in fatty acid film formation and synthesis, as they can interact with particles at the air-water interface and modify film architecture. Ions can affect films through electrostatic interactions, and there is evidence of a difference in these interactions in published works [126]. The concentration of ions, specifically calcium and sodium positive ions, are presented in [156] and it can be inferred that high concentrations of ions cause destructive effects on film morphology. It should also be noted that ions cause changes in film molecule orientation, but the degree of change is not universal.

pH is an important factor for film synthesis, even more so for fatty acid films. Since most fatty acids have weak disassociation in the water subphase, pH levels can directly affect the degree of disassociation and thus affect the received film.

Thermal and concentration parameters causes noticeable changes on the isotherm, owing to modified molecular behavior at different concentration and temperature levels. Compression speed is a rarely surveyed parameter, and most articles do not go into detail on this variable, but it can be noted from practical experience that compression at high speeds can cause a negative effect on the film structure, presumably due to the fast compression disallowing the film molecules to orient and form intermolecular attractions.

Transfer pressure affects film structure and deposition, and transferring at pressure too low can affect deposition quality, since the film has not fully formed. Studies demonstrating this effect can be found in literature [172, 179].

Properties of fatty acid films

Molecular orientation highly dependent on film composition. Pure fatty acid films exhibit a tilt of around 15 to 25 degrees [184], while fatty acid with subphases containing ions are highly variable. Various models developed for fatty acid films are noted in the section 4.1. An interesting case for fatty acid films is films containing azobenzene. Owing to the unique property of this group, films that incorporate this group can change their orientation via annealing and UV light [193].

Regarding surface morphology, if the conditions are of high quality, then films of fatty acids transferred onto substrates will be highly uniform with low surface roughness. However, depending on additional materials attached to the film or the role of the fatty acid within the film, surface morphology can change accordingly.

However, film thermal stability is a big drawback for fatty acid films. Due to their chemical composition, they tend to decompose and lose structure at high temperatures [197, 323]. This low thermal stability is demonstrated with microscopic images in [197]. Additionally, fatty acid films exhibit low reversibility and restructuring capability after exposure to high heat [197, 198].

Regarding the optical properties of fatty acid films, mixed fatty acid films exhibit shifts in UV-Vis spectras toward both end of the spectrum. This is theorized to be due to the formation of excimers and the resulting shift is dependent on the energy level of the formed excimer relative to the original energy level of the monomer [202].

Films of fatty acids have been incorporated for use in gas sensing devices, solar cells, biomembranes, conductors, batteries, enzymes, and even anti-cancer applications. Detailed reviews of these articles are found in the application potential section of this article.

CONCLUSIONS

Bibliometric analysis of 301 relevant articles suggests research into fatty acid films has recently slowed down even though international collaboration remains diverse and evenly spread. Despite lessened interest, fatty acid films continue to have applications in sensors, tribological, and biomedical applications. Moreover, environmental science and new materials have been highlighted as potential areas of application. Further studies should examine fatty acid films' performance relative to other film materials within the Langmuir-Blodgett field to point out new opportunities and directions for future researchers.

SUGGESTED FUTURE RESEARCH QUESTIONS

The future of the field lies in the application of mixed fatty acid films. Pure films have been heavily studied, and further studies, although highly encouraged, are likely to corroborate previous studies rather than produce new breakthroughs and knowledge. However, mixed fatty acid films are a recent development in Langmuir-Blodgett film technology, and there are many existing and undiscovered avenues of research available to aspiring researchers and scientists. Many of the mixed film studies show only preliminary results concerning the properties of mixed films and have not deeply investigated the factors affecting the properties of the films. Factors like concentration, pH or temperature, and ions mentioned in this article can be guidelines for future research.

Research into film formation factors for mixed LB films of fatty acids can provide key insights. For example, take a research project about fatty acid/carbon nanotubes [314]. The article surveyed different factors of the asparaginase, but not the fatty acid, which in this case, is stearic acid. Although standalone stearic acid is well-known, its properties can vary depending on the film architecture it is used in. Thus, we can develop the existing publications by asking these sample questions:

What is the effect if we deposit the stearic acid mixed film at different pressures?

What will happen if an ion is introduced into the subphase?

Does increasing layer numbers affect the property of the asparaginase/carbon nanotube film?

The results generated from these questions can then be applied to other research and be generalized, thus contributing to the overall development of the Langmuir-Blodgett field.

ACKNOWLEDGMENTS

This research was funded by the research project QG.23.38 of Vietnam National University, Hanoi. [Tran Duc Dong] and [Bui Thi Thu Thuy] were funded by the Master, PhD Scholarship Programme of Vingroup Innovation Foundation (VINIF), codes [VINIF.2023.ThS.035] and [VINIF.2023.ThS.134], respectively.

Данное исследование поддержано проектом QG.23.38 Вьетнамского национального университета, Ханоя. [Дык Донг Чан] и [Тхи Тху Тхуй Буй] финансировались стипендиальной программой для магистров и докторов наук Инновационного фонда Vingroup (VINIF), коды [VINIF.2023.ThS.035] и [VINIF.2023.ThS.134], соответственно.

CONFLIC OF INTEREST

Авторы заявляют об отсутствии конфликта интересов, требующего раскрытия в данной статье.

The authors declare the absence a conflict of interest warranting disclosure in this article.

REFERENCES
ЛИТЕРАТУРА

1. **Oliveira O.N., Jr., Caseli L., Ariga K.** *Chem. Rev.* 2022. V. 122. N 6. P. 6459-6513. DOI: 10.1021/acs.chemrev.1c00754.
2. **Choudhury S., Kanth S., Saxena V., Gupta J., Betty C.A.** *J. Mater. Chem. C.* 2023. V. 11. N. 34. P. 11620-11630. DOI: 10.1039/D3TC01561K.

3. **Liu J.-H., Tu T., Shen Y.-L., Tu B., Qian D.-J.** *Langmuir*. 2023. V. 39. N 13. P. 4777-4788. DOI: 10.1021/acs.langmuir.3c00166.
4. **Bhullar G.K., Kaur R., Raina K.K.** *Thin Solid Films*. 2023. V. 782. P. 140023. DOI: 10.1016/j.tsf.2023.140023.
5. **Pockels A.** *Nature*. 1892. V. 46. N 1192. P. 418-419. DOI: 10.1038/046418e0.
6. **Hussain S.A., Dey B., Bhattacharjee D., Mehta N.** *J. Heliyon.* 2018. V. 4. P. e01038. DOI: 10.1016/j.heliyon.2018.e01038.
7. **Gorbachev I., Smirnov A., Ivanov G.R., Venelinov T., Amova A., Datsuk E., Anisimkin V., Kuznetsova I., Kolesov V.** *Sensors.* 2023. V. 23. N 11. P. 5290. DOI: 10.3390/s23115290.
8. **Jurak M., Szafran K., Cea P., Martín S.** *J. Phys. Chem. B.* 2022. V. 126. N 36. P. 6936-6947. DOI: 10.1021/acs.jpcb.2c03300.
9. **Dotor L., García-Pinilla J.M., Martín S., Cea P.** *Nanoscale*. 2023. V. 15. N 6. P. 2891-2903. DOI: 10.1039/D2NR06631A.
10. **Mukherjee N., Blanchard G.** *J. Phys. Chem. B.* 2023. V. 127. N 14. P. 1520-6106. DOI: 10.1021/acs.jpcb.3c00236.
11. **Makiura R.** *Coord. Chem. Rev.* 2022. V. 469. P. 214650. DOI: 10.1016/j.ccr.2022.214650.
12. **Scholl F.b.A., Siqueira Jr J.R., Caseli L.** *Langmuir*. 2022. V. 38. N 7. P. 2372-2378. DOI: 10.1021/acs.langmuir.1c03410.
13. **Miura Y.F., Akagi Y., Hishida D., Takeoka Y.** *ACS Omega*. 2022. V. 7. N 51. P. 47812-47820. DOI: 10.1021/acsomega.2c05626.
14. **Li N., Wang C., Li L., Hao Z., Gu J., Wang M., Jiao T.** *Colloid. Surf. A: Physicochem. Eng. Asp.* 2023. V. 663. P. 131067. DOI: 10.1016/j.colsurfa.2023.131067.
15. **de Barros A., de Freitas A.d.S.M., Maciel C.C., Ferreira M.** Electrochemical sensors based on carbon nanomaterial using Langmuir–Blodgett and layer-by-layer thin films for chemical and biological analyses, in Electrochemical Sensors Based on Carbon Composite Materials: Fabrication, properties and applications. 2022. IOP Publishing Bristol, UK. p. 12-1. DOI: 10.1088/978-0-7503-5127-0ch12.
16. **Capan I., Capan R., Erdogan M., Bayrakci M., Ozmen M.** *Sens. Actuator. A: Phys.* 2022. V. 347. P. 113947. DOI: 10.1016/j.sna.2022.113947.
17. **Ito M., Yamashita Y., Tsuneda Y., Mori T., Takeya J., Watanabe S., Ariga K.** *ACS Appl. Mater. Interfaces*. 2020. V. 12. N 50. P. 56522-56529. DOI: 10.1021/acsami.0c18349.
18. **Su L., Xu F., Chen J., Cao Y., Wang C.** *New J. Chem.* 2020. V. 44. N 15. P. 5656-5660. DOI: 10.1039/D0NJ00560F.
19. **Alvarez-Venicio V., Arcos-Ramos R.O., Hernández-Rojas J.A., Guerra-Pulido J.O., Basiuk V.A., Rivera M., Carreón-Castro M.d.P.** *J. Nanosci. Nanotechnol.* 2019. V. 19. N 11. P. 7244-7250. DOI: 10.1166/jnn.2019.17129.
20. **Skrzypiec M., Weiss M., Dopierała K., Prochaska K.** *Mater. Sci. Eng.: C.* 2019. V. 105. P. 110090. DOI: 10.1016/j.msec.2019.110090.
21. **Qassime M.M., Mohammed M.T., Travkova O.G., Glukhovskoy E.G.** *J. Phys.: Conf. Ser.* 2021. V. 1853. N 1. P. 012035. DOI: 10.1088/1742-6596/1853/1/012035.
22. **Fang C., Yoon I., Hubble D., Tran T.-N., Kostecki R., Liu G.** *ACS Appl. Mater. Interfaces.* 2022. V. 14. N 2. P. 2431-2439. DOI: 10.1021/acsami.1c19064.
23. **Divagar M., Ponpandian N., Viswanathan C.** *Mater. Sci. Eng.: B.* 2021. V. 270. P. 115229. DOI: 10.1016/j.mseb.2021.115229.
24. **Chae I., Ngo D., Chen Z., Kwansa A.L., Chen X., Meddeb A.B., Podraza N.J., Yingling Y.G., Ounaies Z., Kim S.H.** *Adv. Mater. Interfaces.* 2020. V. 7. N 9. P. 1902169. DOI: 10.1002/admi.201902169.
25. **Joshi A., Gayakwad A., Manjuladevi V., Varia M.C., Kumar S., Gupta R.K.** *J. Molec. Liq.* 2022. V. 364. P. 120071. DOI: 10.1016/j.molliq.2022.120071.
26. **Nayak P., Viswanath P.** *Opt. Mater.* 2022. V. 125. P. 112069. DOI: 10.1016/j.optmat.2022.112069.
27. **Zhao T., Wang R., Li L., Jiao T.** *Nano Futures.* 2023. V. 7. N 2. DOI: 10.1088/2399-1984/acca56.
28. **Periasamy V., Jaafar M.M., Chandrasekaran K., Talebi S., Ng F.L., Phang S.M., Kumar G.G., Iwamoto M.** *Nanomaterials.* 2022. V. 12. N 5. P. 840. DOI: 10.3390/nano12050840.
29. **Ariga K.** *J. Porph. Phthalocyan*. 2023. V. 27. N 07n10. P. 924-945. DOI: 10.1142/S1088424623300045.
30. **Guo X., Briscoe W.H.** *Curr. Opin. Colloid. Interface Sci.* 2023. V. 67. P. 101731. DOI: 10.1016/j.cocis.2023.101731.
31. **Possarle L.H.R.R., Junior J.R.S., Caseli L.** *Colloid. Surf. B: Biointerfaces.* 2020. V. 192. P. 111032. DOI: 10.1016/j.colsurfb.2020.111032.
32. **Akulova V., Salamianski A., Chishankov I., Agabekov V.** *Soft Mater.* 2022. V. 20. N 2. P. 161-167. DOI: 10.1080/1539445X.2021.1933034.
33. **Saha S., Dutta B., Ghosh M., Chowdhury J.** *ACS Omega.* 2022. V. 7. N 32. P. 27818-27830. DOI: 10.1021/acsomega.1c07321.
34. **Moss G.P., Smith P.A.S., Tavernier D.** *Pure Appl. Chem.* 1995. V. 67. N 8-9. P. 1307-1375. DOI: 10.1351/pac199567081307.
35. **Rayleigh L.** *Proceed. Royal Soc. London.* 1889. V. 47. P. 364-367. DOI: 10.1098/rspl.1889.0099.
36. **Muller P.** *Pure Appl. Chem.* 1994. V. 66. N 5. P. 1077-1184. DOI: 10.1351/pac199466051077.
37. **Sthoer A., Adams E.M., Sengupta S., Corkery R.W., Allen H.C., Tyrode E.C.** *J. Colloid. Interface Sci.* 2022. V. 608. P. 2169-2180. DOI: 10.1016/j.jcis.2021.10.052.
38. **Salamianski A.E., Agabekov V.E.** *Int. J. Nanosci.* 2019. V. 18. N 03n04. P. 1940068. DOI: 10.1142/S0219581X19400684.
39. **Çapan R., Ray A.K.** *J. Mater. Sci.: Mater. Electron.* 2021. V. 32. P. 8798-8806. DOI: 10.1007/s10854-021-05551-z.
40. **da Silva R.L.C.G., Sharma S.K., Paudyal S., Mintz K.J., Leblanc R.M., Caseli L.** *Langmuir*. 2021. V. 37. N 25. P. 7771-7779. DOI: 10.1021/acs.langmuir.1c00934.
41. **Peng J.B., Barnes G.T., Gentle I.R.** *Adv. Colloid Interface Sci.* 2001. V. 91. P. 163-219. DOI: 10.1016/s0001-8686(99)00031-7.
42. **Donthu N., Kumar S., Mukherjee D., Pandey N., Lim W.M.** *J. Business Res.* 2021. V. 133. P. 285-296. DOI: 10.1016/j.jbusres.2021.04.070.
43. **Aria M., Cuccurullo C.** *J. Informetr*. 2017. V. 11. N 4. P. 959-975. DOI: 10.1016/j.joi.2017.08.007.
44. **Le T.-V., Pham H.-H.** *J. Scientometr. Res.* 2022. V. 11. N 2. DOI: 10.5530/jscires.11.2.23.
45. **El Akrami N., Hanine M., Flores E.S., Aray D.G., Ashraf I.** *IEEE Access.* 2023. V. 11. P. 78879-78903. DOI: 10.1109/ACCESS.2023.3298371.
46. **Amiri A.M., Kushwaha B.P., Singh R.** *J. Small Bus. Enterp. Dev.* 2023. V. 30. N 3. P. 621-641. DOI: 10.1108/JSBED-04-2022-0206.
47. **Zhang Z., Hu G., Mu X., Kong L.** *J. Environ. Manag.* 2022. V. 322. P. 116087. DOI: 10.1016/j.jenvman.2022.116087.
48. **Islam M.M., Chowdhury M.A.M., Begum R.A., Amir A.A.** *Environ. Sci. Pollut. Res.* 2022. V. 29. N 39. P. 59300-59315. DOI: 10.1007/s11356-022-20028-0.
49. **Alsmadi A.A., Shuhaiber A., Alhawamdeh L.N., Alghazzawi R., Al-Okaily M.** *Sustainability.* 2022. V. 14. N 17. P. 10630. DOI: 10.3390/su141710630.

50. **Kapoor P., Kar S.** *Int. Econom. Econom. Policy*. 2023. V. 20. P. 279–302. DOI: 10.1007/s10368-023-00557-w.
51. **Pei Z., Chen S., Ding L., Liu J., Cui X., Li F., Qiu F.** *J. Control. Release*. 2022. V. 352. P. 211-241. DOI: 10.1016/j.jconrel.2022.10.023.
52. **Liu C., Yu R., Zhang J., Wei S., Xue F., Guo Y., He P., Shang L., Dong W.** *Front. Immunol*. 2022. V. 13. P. 972079. DOI: 10.3389/fimmu.2022.972079.
53. **Palmblad M., van Eck N.J., Bergquist J.** *TrAC Trends Analyt. Chem*. 2022. V. 159. 116899. DOI: 10.1016/j.trac.2022.116899.
54. **Liu X., Zhao S., Tan L., Tan Y., Wang Y., Ye Z., Hou C., Xu Y., Liu S., Wang G.** *Biosens. Bioelectron*. 2022. V. 201. P. 113932. DOI: 10.1016/j.bios.2021.113932.
55. **Petcu M.A., Ionescu-Feleaga L., Ionescu B.-Ș., Moise D.-F.** *Mathematics*. 2023. V. 11. N 2. P. 365. DOI: 10.3390/math11020365.
56. **Mohammadpour J., Lee A., Timchenko V., Taylor R.** *Energies*. 2022. V. 15. N 9. P. 3426. DOI: 10.3390/en15093426.
57. **Guerrero-Gironés J., Forner L., Sanz J.L., Rodríguez-Lozano F.J., Ghilotti J., Llena C., Lozano A., Melo M.** *Clin. Oral Investig*. 2022. V. 26. N 9. P. 5611-5624. DOI: 10.1007/s00784-022-04605-8.
58. **Lam W.H., Lam W.S., Lee P.F.** *Materials*. 2023. V. 16. N 1. P. 401. DOI: 10.3390/ma16010401.
59. **Naseer M.N., Zaidi A.A., Dutta K., Wahab Y.A., Jaafar J., Nusrat R., Ullah I., Kim B.** *Energy Rep*. 2022. V. 8. P. 4252-4264. DOI: 10.1016/j.egyr.2022.02.301.
60. **Colombo B., Gaiardelli P., Dotti S., Caretto F.** *J. Compos. Mater*. 2022. V. 56. N 19. P. 3063-3080. DOI: 10.1177/00219983221109877.
61. **Pienpinijtham P., Han X.X., Ekgasit S., Ozaki Y.** *Phys. Chem. Chem. Phys*. 2012. V. 14. N 29. P. 10132-10139. DOI: 10.1039/c2cp41419h.
62. **Bu W., Fan H., Wu L., Hou X., Hu C., Zhang G., Zhang X.** *Langmuir*. 2002. V. 18. N 16. P. 6398-6403. DOI: 10.1021/la020085c.
63. **Lee D.K., Kim Y.H., Kim C.W., Cha H.G., Kang Y.S.** *J. Phys. Chem. B*. 2007. V. 111. P. 9288-9293. DOI: 10.1021/jp072612c.
64. **Girard-Egrot A.P., Godoy S., Blum L.J.** *Adv. Colloid. Interface Sci*. 2005. V. 116. N 1-3. P. 205-225. DOI: 10.1016/j.cis.2005.04.006.
65. **Scholl F.A., Caseli L.** *Colloids Surf. B: Biointerfaces*. 2015. V. 126. P. 232-236. DOI: 10.1016/j.colsurfb.2014.12.033.
66. **da Rocha Junior C., Caseli L.** *Mater. Sci. Eng.: C*. 2017. V. 73. P. 579-584. DOI: 10.1016/j.msec.2016.12.041.
67. **Huang X., Jiang S., Liu M.** *J. Phys. Chem. B*. 2005. V. 109. N 1. P. 114-119. DOI: 10.1021/jp046500m.
68. **Gao L.-H., Wang K.-Z., Cai L., Zhang H.-X., Jin L.-P., Huang C.-H., Gao H.-J.** *J. Phys. Chem. B*. 2006. V. 110. N 14. P. 7402-7408. DOI: 10.1021/jp054525v.
69. **Supian F.L., Richardson T.H., Deasy M., Kelleher F., Ward J.P., McKee V.** *Langmuir*. 2010. V. 26. N 13. P. 10906-10912. DOI: 10.1021/la100808r.
70. **Kondalkar V.V., Mali S.S., Kharade R.R., Mane R.M., Patil P.S., Hong C.K., Kim J.H., Choudhury S., Bhosale P.N.** *RSC Adv*. 2015. V. 5. N 34. P. 26923-26931. DOI: 10.1039/C5RA00208G.
71. **Li X., Zhang L., Wang X., Shimoyama I., Sun X., Seo W.-S., Dai H.** *J. Am. Chem. Soc*. 2007. V. 129. N 16. P. 4890-4891. DOI: 10.1021/ja071114e.
72. **Li X., Zhang G., Bai X., Sun X., Wang X., Wang E., Dai H.** *Nature Nanotechnol*. 2008. V. 3. N 9. P. 538-542. DOI: 10.1038/nnano.2008.210.
73. **Rosen M.J., Kunjappu J.T.** Surfactants and interfacial phenomena. John Wiley & Sons. 2012. 600 p. DOI: 10.1002/9781118228920.
74. **Porter M.R.** Handbook of surfactants. Springer. 2013. 227 p.
75. **Capistran B.A., Blanchard G.J.** *Langmuir*. 2019. V. 35. N 9. P. 3346-3353. DOI: 10.1021/acs.langmuir.9b00022.
76. **Das N.M., Roy D., Gupta M., Gupta P.S.** *Phys. B: Condens. Matter*. 2012. V. 407. N 24. P. 4777-4782. DOI: 10.1016/j.physb.2012.08.035.
77. **Лутфуллина Г.Г., Фатхутдинова А.А.** Синтез и исследование свойств неионогенного поверхностно-активного вещества на основе жирных кислот кукурузного масла и диэтаноламина. *Изв. вузов. Химия и хим. технология.* 2022. Т. 65. Вып. 11. С. 20-26. **Lutfullina G.G., Fatkhutdinova A.A.** *ChemChemTech [Izv. Vyssh. Uchebn. Zaved. Khim. Khim. Tekhnol.]*. 2022. V. 65. N 11. P. 20-26. DOI: 10.6060/ivkkt.20226511.6640.
78. **Costa A.S., Imae T.** *Langmuir*. 2004. V. 20. N 20. P. 8865-8869. DOI: 10.1021/la049088a.
79. **Goto T.E., Sakai A., Iost R.M., Silva W.C., Crespilho F.N., Péres L.O., Caseli L.** *Thin Solid Films*. 2013. V. 540. P. 202-207. DOI: 10.1016/j.tsf.2013.05.106.
80. **Mitamura K., Imae T.** *Trans. Mater. Res. Soc. Jpn*. 2003. V. 28. P. 71-74.
81. **Zhavnerko G., Agabekov V., Gallyamov M., Yaminsky I., Rogach A.** *Colloid. Surf. A: Physicochem. Eng. Asp*. 2002. V. 202. P. 233-241. DOI: 10.1016/S0927-7757(01)01085-8.
82. **Gabrielli G., Puggelli M., Ferroni E., Carubia G., Pedocchi L.** *Colloid. Surf*. 1989. V. 41. P. 1-13. DOI: 10.1016/0166-6622(89)80036-8.
83. **Nabok A., Ray A.K., Iwantono, Hassan A., Simmonds M.** *IEEE Trans. Nanotechnol*. 2003. V. 2. N 1. P. 44-49. DOI: 10.1109/TNANO.2003.808514.
84. **Geue T., Schultz M., Englisch U., Stoemmer R., Pietsch U., Meine K., Vollhardt D.** *J. Chem. Phys*. 1999. V. 110. P. 8104-8111. DOI: 10.1063/1.47871
85. **Mukherjee N., Blanchard G.** *J. Phys. Chem. B*. 2023. V. 127. N 14. P. 1520-6106. DOI: 10.1021/acs.jpcb.3c00236.
86. **Buhaenko M.R., Grundy M.J., Richardson R.M., Roser S.J.** *Thin Solid Films*. 1988. V. 159. N 1-2. P. 253-265.
87. **Hasegawa T., Kamata T., Umemura J., Takenaka T.** *Chem. Lett*. 1990. V. 19. P. 1543-1546. DOI: 10.1246/CL.1990.1543.
88. **Martyna K., Dopierała K., Marek W., Prochaska K.** *Langmuir* 2019. V. 35. N 8. P. 3183-3193. DOI: 10.1021/acs.langmuir.8b04153.
89. **Tippmann-Krayer P., Kenn R., Möhwald H.** *Thin Solid Films*. 1992. V. 210. P. 577-582. DOI: 10.1016/0040-6090(92)90346-D.
90. **Wang W., Lu X., Xu J., Jiang Y., Liu X., Wang G.** *Phys. B: Condens. Matter*. 2000. V. 293. N 1-2. P. 6-10. DOI: 10.1016/S0921-4526(00)00516-0.
91. **Large M., Ogilvie S., King A., Dalton A.** *Langmuir*. 2017. V. 33. N 51. P. 14766–14771. DOI: 10.1021/acs.langmuir.7b03867.
92. **Petty M.C.** Langmuir-Blodgett Films. Cambridge University Press. 1996. 234 p. DOI: 10.1017/CBO9780511622519.
93. **Fazio V.S.U., Komitov L., Radüge C., Lagerwall S.T., Motschmann H.** *Eur. Phys. J. E*. 2001. V. 5. N 3. P. 309-315. DOI: 10.1007/s101890170062.
94. **Birdi K.S., Vu D.T.** *Langmuir*. 1994. V. 10. N 3. P. 623-625. DOI: 10.1021/la00015a004.
95. **Liu X., Sun R., Wang S., Wu Y.J.** *Library Hi Tech*. 2020. V. 38. N 2. P. 367-384. DOI: 10.1108/LHT-01-2019-0024.
96. **De Bellis N.** Bibliometrics and citation analysis: from the science citation index to cybermetrics. Scarecrow Press. 2009. 450 p.

97. **Chen Y., Lin M., Zhuang D.** *Chemosphere*. 2022. V. 297. P. 133932. DOI: 10.1016/j.chemosphere.2022.133932.
98. **Yousef B.A.A., Mahmoud M., Aljaghoub H., Abdelkareem M.A., Alami A.H., Olabi A.G.** *Therm. Sci. Eng. Prog*. 2023. V. 45. P. 102082. DOI: 10.1016/j.tsep.2023.102082.
99. **Leopizzi R., Palmi P., Di Cagno P.** *Utilities Policy*. 2023. V. 84. P. 101651. DOI: 10.1016/j.jup.2023.101651.
100. **Alviz-Meza A., Orozco-Agamez J., Quinayá D.C.P., Alviz-Amador A.** *Chem. Eng*. 2023. V. 7. N 1. P. 2. DOI: 10.3390/chemengineering7010002.
101. **Kamaruzzaman W.M.I.W.M., Nasir N.A.M., Hamidi N.A.S.M., Yusof N., Shaifudin M.S., Suhaimi A.M.A.A.M., Badruddin M.A., Adnan A., Nik W.M.N.W., and Ghazali M.S.M.** *Arab. J. Chem.* 2022. V. 15. N 4. P. 103655. DOI: 10.1016/j.arabjc.2021.103655.
102. **Prochaska C., Gallios G.** *Processes*. 2021. V. 9. N 7. P. 1177. DOI: 10.3390/pr9071177.
103. **Nandiyanto A.B.D., Ragadhita R., Fiandini M., Al Husaeni D.N., Aziz M.** *Moroc. J. Chem.* 2023. V. 11. N 04. P. 11-4. DOI: 10.48317/IMIST.PRSM/morjchem-v11i04.41591.
104. **Nandiyanto A.B.D., Al Husaeni D.N., Al Husaeni D.F.** *J. Eng. Sci. Technol*. 2021. V. 16. N 6. P. 4414-4422.
105. **Kurniati P.S., Saputra H., Fauzan T.A.** *Moroc. J. Chem.* 2022. V. 10. N 3. P. 10-3. DOI: 10.48317/IMIST.PRSM/morjchem-v10i3.33061.
106. **Fauziah A.** *Indones. J. Multidicip. Res.* 2022. V. 2. N 2. P. 333-338. DOI: 10.17509/ijomr.v2i2.43341.
107. **van Eck N.J., Waltman L.** *Scientometrics*. 2010. V. 84. N 2. P. 523-538. DOI: 10.1007/s11192-009-0146-3.
108. **Chen Y., Yeung A.W.K., Pow E.H.N., Tsoi J.K.H.** *J. Prosthet. Dent*. 2021. V. 126. N 4. P. 512-522. DOI: 10.1016/j.prosdent.2020.08.012.
109. **Takahashi R., Kaibe K., Suzuki K., Takahashi S., Takeda K., Hansen M., Yumoto M.** *Scientometrics*. 2023. V. 128. P. 3507–3534. DOI: 10.1007/s11192-023-04711-8.
110. **Yeboah A., Muhammad S., Yan D., Singh S.K., Moreno B., Paige M.F.** *Colloid. Surf. A: Physicochem. Eng. Asp.* 2022. V. 654. P. 130109. DOI: 10.1016/j.colsurfa.2022.130109.
111. **Yan C., Paige M.F.** *Colloid. Surf. A: Physicochem. Eng. Asp.* 2022. V. 645. P. 128937. DOI: 10.1016/j.colsurfa.2022.128937.
112. **Singh S.K., Yeboah A., Bu W., Sun P., Paige M.F.** *Langmuir*. 2022. V. 38. N 51. P. 16004-16013. DOI: 10.1021/acs.langmuir.2c02462.
113. **Yeboah A., Paige M.** *J. Surfactants Deterg.* 2023. V.26. N 6. P. 779-787. DOI: 10.1002/jsde.12700.
114. **Majumdar S., De J., Pal A., Ghosh I., Nath R.K., Chowdhury S., Roy D., Maiti D.K.** *RSC Adv.* 2015. V. 5. N 31. P. 24681-24686. DOI: 10.1039/C5RA01618E.
115. **Santiago J.S., Cerro R.L., Scholz C.** *Polym. Int.* 2021. V. 70. N 1. P. 41-50. DOI: 10.1002/pi.6142.
116. **Debnath P., Chakraborty S., Deb S., Nath J., Bhattacharjee D., Hussain S.A.** *J. Phys. Chem. C.* 2015. V. 119. N 17. P. 9429-9441. DOI: 10.1021/acs.jpcc.5b02111.
117. **Debnath P., Chakraborty S., Deb S., Nath J., Dey B., Bhattacharjee D., Hussain S.A.** *J. Lumin.* 2016. V. 179. P. 287-296. DOI: 10.1016/j.jlumin.2016.07.027.
118. **Bryce M.R., Petty M.C.** *Nature*. 1995. V. 374. N 6525. P. 771-776. DOI: 10.1038/374771a0.
119. **Goldenberg L.M., Bryce M.R., Petty M.C.** *J. Mater. Chem.* 1999. V. 9. N 9. P. 1957-1974. DOI: 10.1039/A901825E.
120. **Siqueira J.R., Caseli L., Crespilho F.N., Zucolotto V., Oliveira O.N.** *Biosens. Bioelectron.* 2010. V. 25. N 6. P. 1254-1263. DOI: 10.1016/j.bios.2009.09.043.
121. **Pavinatto F.J., Caseli L., Oliveira O.N., Jr.** *Biomacromolecules.* 2010. V. 11. N 8. P. 1897-1908. DOI: 10.1021/bm1004838.
122. **Zasadzinski J.A., Viswanathan R., Madsen L., Garnaes J., Schwartz D.K.** *Science*. 1994. V. 263. N 5154. P. 1726-1733. DOI: 10.1126/science.8134836.
123. **Schwartz D.K.** *Surface Sci. Rep.* 1997. V. 27. P. 245-334. DOI: 10.1016/S0167-5729(97)00003-4.
124. **Schwartz D.K., Garnaes J., Viswanathan R., Zasadzinski J.A.N.** *Science*. 1992. V. 257. N 5069. P. 508-511. DOI: 10.1126/science.257.5069.508.
125. **Takamoto D.Y., Aydil E., Zasadzinski J.A., Ivanova A.T., Schwartz D.K., Yang T., Cremer P.S.** *Science.* 2001. V. 293. N 5533. P. 1292-1295. DOI: 10.1126/science.1060018.
126. **Schwartz D.K., Viswanathan R., Garnaes J., Zasadzinski J.A.** *J. Am. Chem. Soc.* 1993. V. 115. N 16. P. 7374-7380. DOI: 10.1021/ja00069a040.
127. **Kurnaz M.L., Schwartz D.K.** *J. Phys. Chem.* 1996. V. 100. N 26. P. 11113-11119. DOI: 10.1021/jp960665g.
128. **Viswanathan R., Schwartz D.K., Garnaes J., Zasadzinski J.A.N.** *Langmuir*. 1992. V. 8. N 6. P. 1603-1607. DOI: 10.1021/la00042a018.
129. **Ybert C., Lu W., Möller G., Knobler C.M.** *J. Phys. Chem. B.* 2002. V. 106. N 8. P. 2004-2008. DOI: 10.1021/jp013173z.
130. **Marshall G., Dennin M., Knobler C.M.** *Rev. Sci. Instr.* 1998. V. 69. N 10. P. 3699-3700. DOI: 10.1063/1.1149162.
131. **Knobler C.M., Schwartz D.K.** *Curr. Opin. Colloid Interface Sci*. 1999. V. 4. N 1. P. 46-51. DOI: 10.1016/S1359-0294(99)00002-3.
132. **Kartashynska E.S., Vollhardt D.** *JCIS Open*. 2022. V. 7. P. 100057. DOI: 10.1016/j.jciso.2022.100057.
133. **Kartashynska E.S., Vollhardt D.** *Phys. Chem. Chem. Phys.* 2021. V. 23. N 44. P. 25356-25364. DOI: 10.1039/D1CP03511H.
134. **Kovtun A.I., Kartashynska E.S., Vollhardt D.** *JCIS Open.* 2021. V. 1. P. 100001. DOI: 10.1016/j.jciso.2021.100001.
135. **Shen Y.R.** *Nature*. 1989. V. 337. N 6207. P. 519-525. DOI: 10.1038/337519a0.
136. **Shen Y.R.** *Annual Rev. Phys. Chem.* 1989. V. 40. N 1. P. 327-350. DOI: 10.1146/annurev.pc.40.100189.001551.
137. **Zhu X.D., Suhr H., Shen Y.R.** *Phys. Rev. B.* 1987. V. 35. N 6. P. 3047. DOI: 10.1103/PhysRevB.35.3047.
138. **Du Q., Superfine R., Freysz E., Shen Y.R.** *Phys. Rev. Lett.* 1993. V. 70. N 15. P. 2313. DOI: 10.1103/PhysRevLett.70.2313.
139. **Prakash M., Peng J.B., Ketterson J.B., Dutta P.** *Thin Solid Films.* 1987. V. 146. N 3. P. L15-L17. DOI: 10.1016/0040-6090(87)90438-X.
140. **Peng J.B., Ketterson J.B., Dutta P.** *Langmuir*. 1988. V. 4. N 5. P. 1198-1202. DOI: 10.1021/la00083a026.
141. **Rapp G., Koch M.H.J., Hoehne U., Lvov Y., Möhwald H.** *Langmuir*. 1995. V. 11. N 7. P. 2348-2351. DOI: 10.1021/la00007a005.
142. **Kaganer V.M., Möhwald H., Dutta P.** *Rev. Modern Phys.* 1999. V. 71. N 3. P. 779-819. DOI: 10.1103/RevModPhys.71.779.
143. **Tippmann-Krayer P., Kenn R.M., Möhwald H.** *Thin Solid Films.* 1992. V. 210. P. 577-582. DOI: 10.1016/0040-6090(92)90346-D.
144. **Lösche M., Rabe J., Fischer A., Rucha B.U., Knoll W., Möhwald H.** *Thin Solid Films.* 1984. V. 117. N 4. P. 269-280. DOI: 10.1016/0040-6090(84)90357-2.
145. **Peng J.B., Prakash M., Macdonald R., Dutta P., Ketterson J.B.** *Langmuir*. 1987. V. 3. N 6. P. 1096-1097. DOI: 10.1021/la00078a037.

146. **Mikrut J.M., Dutta P., Ketterson J.B., MacDonald R.C.** *Phys. Rev. B.* 1993. V. 48. N 19. P. 14479. DOI: 10.1103/PhysRevB.48.14479.
147. **Wydro P., Krajewska B., Hąc-Wydro K.** *Biomacromolecules*. 2007. V. 8. N 8. P. 2611-2617. DOI: 10.1021/bm700453x.
148. **Guzmán E., Liggieri L., Santini E., Ferrari M., Ravera F.** *Colloids Surf. A: Physicochem. Eng. Asp.* 2012. V. 413. P. 280-287. DOI: 10.1016/j.colsurfa.2011.11.023.
149. **Hąc-Wydro K., Wydro P.** *Chem. Phys. Lipids*. 2007. V. 150. N 1. P. 66-81. DOI: 10.1016/j.chemphyslip.2007.06.213.
150. **Ma G., Allen H.C.** *Langmuir*. 2007. V. 23. N 2. P. 589-597. DOI: 10.1021/la061870i.
151. **Goulet P.J.G., Aroca R.F.** *Analyt. Chem.* 2007. V. 79. N 7. P. 2728-2734. DOI: 10.1021/ac062059f.
152. **Liu J., Conboy J.C.** *Langmuir*. 2005. V. 21. P. 9091-9097. DOI: 10.1021/la051500e.
153. **Duffy D.M., Harding J.H.** *Langmuir*. 2004. V. 20. N 18. P. 7630-7636. DOI: 10.1021/la049552b.
154. **DiMasi E., Patel V.M., Sivakumar M., Olszta M.J., Yang Y.P., Gower L.B.** *Langmuir*. 2002. V. 18. N 23. P. 8902-8909. DOI: 10.1021/la0260032.
155. **Price A.D., Schwartz D.K.** *J. Phys. Chem. B.* 2007. V. 111. N 5. P. 1007-1015. DOI: 10.1021/jp066228b.
156. **Kumar N., Wang L., Siretanu I., Duits M., Mugele F.** *Langmuir*. 2013. V. 29. N 17. P. 5150-5159. DOI: 10.1021/la400615j.
157. **Hussain S.A., Paul P.K., Bhattacharjee D.** *J. Phys. Chem. Solids.* 2006. V. 67. N 12. P. 2542-2549. DOI: 10.1016/j.jpcs.2006.07.011.
158. **Hussain S.A., Paul P.K., Bhattacharjee D.** *J. Colloid Interface Sci.* 2006. V. 299. N 2. P. 785-790. DOI: 10.1016/j.jcis.2006.02.036.
159. **Maiorova L.A., Vu T.T., Gromova O.A., Nikitin K.S., Koifman O.I.** *BioNanoScience*. 2018. V. 8. N 1. P. 81-89. DOI: 10.1007/s12668-017-0424-0.
160. **Naselli C., Rabolt J., Swalen J.** *J. Chem. Phys.* 1985. V. 82. P. 2136-2140. DOI: 10.1063/1.448351.
161. **Ahmed I., Haque A., Bhattacharyya S., Patra P., Plaisier J.R., Perissinotto F., Bal J.K.** *ACS Omega.* 2018. V. 3. N 11. P. 15789-15798. DOI: 10.1021/acsomega.8b02235.
162. **Sakai A., Wang S.H., Péres L.O., Caseli L.** *Synthet. Metals.* 2011. V. 161. N 15. P. 1753-1759. DOI: 10.1016/j.synthmet.2011.06.019.
163. **Sakai A., Péres L.O., Caseli L.** *Colloid. Polym. Sci.* 2015. V. 293. N 3. P. 883-890. DOI: 10.1007/s00396-014-3477-4.
164. **Nayak P., Viswanath P.** *Opt. Mater.* 2021. V. 122. P. 111807. DOI: 10.1016/j.optmat.2021.111807.
165. **Meral K., Erbil H.Y., Onganer Y.** *Appl. Surface Sci.* 2011. V. 258. N 4. P. 1605-1612. DOI: 10.1016/j.apsusc.2011.10.008.
166. **Hussain S.A., Chakraborty S., Bhattacharjee D., Schoonheydt R.A.** *Thin Solid Films*. 2013. V. 536. P. 261-268. DOI: 10.1016/j.tsf.2013.03.015.
167. **Wang K.-H., Syu M.-J., Chang C.-H., Lee Y.-L.** *Sensor. Actuat. B: Chem.* 2012. V. 164. N 1. P. 29-36. DOI: 10.1016/j.snb.2012.01.056.
168. **Ahmed I., Dildar L., Haque A., Patra P., Mukhopadhyay M., Hazra S., Kulkarni M., Thomas S., Plaisier J.R., Dutta S.B., Bal J.K.** *J. Colloid. Interface Sci.* 2018. V. 514. P. 433-442. DOI: 10.1016/j.jcis.2017.12.037.
169. **Assunção da Silva E., Rodrigues de Oliveira V.J., Braunger M., Constantino C., Olivati C.** /*Mater. Res.* 2014. V. 17. P. 1442-1448. DOI: 10.1590/1516-1439.288814.
170. **Wang Z., Liu S., Du Z., Zhang H.** /*Mater. Lett.* 2004. V. 58. N 10. P. 1642-1645. DOI: 10.1016/j.matlet.2003.10.041.
171. **Liang L., Fang Y.** *Spectrochim. Acta Part A: Molec. Biomolec. Spectrosc.* 2008. V. 69. N 1. P. 113-116. DOI: 10.1016/j.saa.2007.03.036.
172. **Roy S., Saifuddin M., Mandal S., Hazra S.** *J. Colloid. Interface Sci.* 2022. V. 606. P. 1153-1162. DOI: 10.1016/j.jcis.2021.08.071.
173. **Dey B., Debnath P., Bhattacharjee D., Majumdar S., Arshad Hussain S.** *Mater. Today: Proceed.* 2018. V. 5. N 1. Pt. 2. P. 2287-2294. DOI: 10.1016/j.matpr.2017.09.231.
174. **Singhal R., Gambhir A., Pandey M.K., Annapoorni S., Malhotra B.D.** *Biosens. Bioelectron.* 2002. V. 17. N 8. P. 697-703. DOI: 10.1016/S0956-5663(02)00020-9.
175. **Gorbachev I., Smirnov A., Ivanov G., Avramov I., Datsuk E., Venelinov T., Bogdanova E., Anisimkin V., Kolesov V., Kuznetsova I.** *Sensors*. 2023. V. 23. N 1. P. 100. DOI: 10.3390/s23010100.
176. **Khomutov G.B., Kim V.P., Potapenkov K.V., Parshintsev A.A., Soldatov E.S., Usmanov N.N., Saletsky A.M., Sybachin A.V., Yaroslavov A.A., Migulin V.A., Taranov I.V., Cherepenin V.A., Gulyaev Y.V.** *Colloid. Surf. A: Physicochem. Eng. Asp.* 2017. V. 532. P. 150-154. DOI: 10.1016/j.colsurfa.2017.05.070.
177. **Kang K.H., Kim J.M., Kim D.K., Jung S.B., Chang J.S., Kwon Y.S.** *Sensor. Actuat. B: Chem.* 2001. V. 77. N 1. P. 293-296. DOI: 10.1016/S0925-4005(01)00745-6.
178. **Ohnuki H., Ishizaki Y., Suzuki M., Desbat B., Delhaes P., Giffard M., Imakubo T., Mabon G., Izumi M.** *Mater. Sci. Eng.: C.* 2002. V. 22. N 2. P. 227-232. DOI: 10.1016/S0928-4931(02)00170-4.
179. **Kamilya T., Pal P., Talapatra G.B.** *Colloid. Surf. B: Biointerfaces.* 2007. V. 58. N 2. P. 137-144. DOI: 10.1016/j.colsurfb.2007.02.020.
180. **Furtado F.A.d.S., Caseli L.** *Thin Solid Films.* 2020. V. 709. P. 138253-138253. DOI: 10.1016/J.TSF.2020.138253.
181. **Vu T.T., Kharitonova N.V., Maiorova L.A., Gromova O.A., Torshin I.Y., Koifman O.I.** *Macroheterocycles*. 2018. V. 11. N 3. P. 286-292. DOI: 10.6060/mhc171260m.
182. **Momsen W.E., Smaby J.M., Brockman H.L.** *J. Colloid. Interface Sci.* 1990. V. 135. N 2. P. 547-552. DOI: 10.1016/0021-9797(90)90025-J.
183. **Choudhary K., Kumar J., Taneja P., Gupta R.** *Liquid Crystals.* 2017. V. 44. P. 1-8. DOI: 10.1080/02678292.2017.1306890.
184. **Tao Y.T.** *J. Am. Chem. Soc.* 1993. V. 115. N 10. P. 4350-4358. DOI: 10.1021/ja00063a062.
185. **Chollet P.-A.** *Thin Solid Films.* 1978. V. 52. N 3. P. 343-360. DOI: 10.1016/0040-6090(78)90177-3.
186. **Bettarini S., Bonosi F., Gabrielli G., Martini G.** *Langmuir*. 1991. V. 7. N 6. P. 1082-1087. DOI: 10.1021/la00054a010.
187. **Pomerantz M., Segmüller A.** *Thin Solid Films.* 1980. V. 68. N. 1. P. 33-45. DOI: 10.1016/0040-6090(80)90134-0.
188. **Knobloch H., Peñacorada F., Brehmer L.** *Thin Solid Films.* 1997. V. 295. N 1. P. 210-213. DOI: 10.1016/S0040-6090(96)09401-1.
189. **Lecourt B., Blaudez D., Turlet J.M.** *Thin Solid Films.* 1998. V. 313-314. P. 790-794. DOI: 10.1016/S0040-6090(97)00996-6.
190. **Hasegawa T., Umemura J., Takenaka T.** *J. Phys. Chem.* 1993. V. 97. N 35. P. 9009-9012. DOI: 10.1021/j100137a028.
191. **Umemura J., Kamata T., Kawai T., Takenaka T.** *J. Phys. Chem.* 1990. V. 94. P. 62-67. DOI: 10.1021/J100364A009.
192. **Outka D., Stöhr J., Rabe J., Swalen J.** *J. Chem. Phys.* 1988. V. 88. P. 4076-4087. DOI: 10.1063/1.453862.
193. **Geue T., Ziegler A., Stumpe J.** *Macromolecules.* 1997. V. 30. N 19. P. 5729-5738. DOI: 10.1021/ma9703822.
194. **Araujo F.T., Peres L.O., Caseli L.** *Langmuir*. 2019. V. 35. P. 7294-7303. DOI: 10.1021/acs.langmuir.9b00536.

195. **Paul S., Pearson C., Molloy A., Cousins M.A., Green M., Kolliopoulou S., Dimitrakis P., Normand P., Tsoukalas D., Petty M.C.** *Nano Lett.* 2003. V. 3. N 4. P. 533-536. DOI: 10.1021/nl034008t.
196. **Oliveira O.** *Braz. J. Phys.* 1992. V. 22. P. 60-69.
197. **Kobayashi K., Takaoka K., Ochiai S.** *Thin Solid Films.* 1989. V. 178. N 1. P. 453-458. DOI: 10.1016/0040-6090(89)90337-4.
198. **Zhang Z., Liang Y., Tian Y., Jiang Y.** *Spectrosc. Lett.* 1996. V. 29. N 2. P. 321-336. DOI: 10.1080/00387019608001605.
199. **Zhu J., Dai X., Xiong J.** *AIP Adv.* 2019. V. 9. N 4. P. 45314-45314. DOI: 10.1063/1.5088720/1076701.
200. **Kamata T., Umemura J., Takenaka T.** *Chem. Lett.* 1988. V. 17. N 7. P. 1231-1234. DOI: 10.1246/cl.1988.1231.
201. **Wang S., Li Y.L., Zhao H.L., Liang H., Liu B., Pan S.** *Appl. Surf. Sci.* 2012. V. 261. P. 31-36. DOI: 10.1016/J.APSUSC.2012.07.041.
202. **Kasha M., Rawls H.R., Ashraf El-Bayoumi M.** *Pure Appl. Chem.* 1965. V. 11. N 3-4. P. 371-392. DOI: 10.1351/pac196511030371.
203. **Saikin S.K., Eisfeld A., Valleau S., Aspuru-Guzik A.** *Nanophotonics.* 2013. V. 2. N 1. P. 21-38. DOI: 10.1515/nanoph-2012-0025.
204. **Niu J.Z., Cheng G., Li Z., Wang H., Lou S., Du Z., Li L.S.** *Colloid. Surf. A: Physicochem. Eng. Asp.* 2008. V. 330. N 1. P. 62-66. DOI: 10.1016/j.colsurfa.2008.07.041.
205. **Chakraborty S., Bhattacharjee D., Hussain S.A.** *Appl. Phys. A.* 2013. V. 111. N 4. P. 1037-1043. DOI: 10.1007/s00339-012-7338-z.
206. **Furman I., Whitten D.G., Penner T.L., Ulman A., Geiger H.C.** *Langmuir*. 1994. V. 10. N 3. P. 837-843. DOI: 10.1021/la00015a039.
207. **Dutta A.K., Misra T.N., Pal A.J.** *Langmuir*. 1996. V. 12. N 2. P. 459-465. DOI: 10.1021/la940678q.
208. **Sato T., Ozaki Y., Iriyama K.** *Langmuir*. 1994. V. 10. N 7. P. 2363-2369. DOI: 10.1021/la00019a055.
209. **Alvarez-Puebla R.A., Liz-Marzán L.M.** *Angew. Chem. Int. Ed.* 2012. V. 51. N 45. P. 11214-11223. DOI: 10.1002/anie.201204438.
210. **Moriizumi T.** *Thin Solid Films.* 1988. V. 160. N 1-2. P. 413-429. DOI: 10.1016/0040-6090(88)90088-0.
211. **Kalinina M.A., Arslanov V.V., Vatsadze S.Z.** *Colloid. J.* 2003. V. 65. N 2. P. 177-185. DOI: 10.1023/A:1023365108235.
212. **Schöning M.J., Sauke M., Steffen A., Marso M., Kordos P., Lüth H., Kauffmann F., Erbach R., Hoffmann B.** *Sens. Actuators B: Chem.* 1995. V. 27. N 1. P. 325-328. DOI: 10.1016/0925-4005(94)01611-K.
213. **Bhalla N., Jolly P., Formisano N., Estrela P.** Biosensor Technologies for Detection of Biomolecules. Portland Press. 2016. 131 p.
214. **Haleem A., Javaid M., Singh R.P., Suman R., Rab S.** *Sens. Int.*. 2021. V. 2. P. 100100. DOI: 10.1016/j.sintl.2021.100100.
215. **Cabaj J., Sołoducho J., Nowakowska-Oleksy A.** *Sens. Actuators B: Chem.* 2010. V. 143. N 2. P. 508-515. DOI: 10.1016/j.snb.2009.09.047.
216. **Cabaj J., Sołoducho J., Świst A.** *Sens. Actuators B: Chem.* 2010. V. 150. N 2. P. 505-512. DOI: 10.1016/j.snb.2010.09.008.
217. **Girard-Egrot A.P., Blum L.J.** Langmuir-Blodgett technique for synthesis of biomimetic lipid membranes. In: Nanobiotechnology of biomimetic membranes. 2007. Springer. P. 23-74. DOI: 10.1007/0-387-37740-9_2.
218. **Mirzaei A., Kim J.-H., Kim H.W., Kim S.S.** *Sens. Actuators B: Chem.* 2018. V. 258. P. 270-294. DOI: 10.1016/j.snb.2017.11.066.
219. **Shakeel A., Rizwan K., Farooq U., Iqbal S., Altaf A.A.** *Chemosphere.* 2022. V. 294. P. 133772. DOI: 10.1016/j.chemosphere.2022.133772.
220. **Ding H., Erokhin V., Kumar Ram M., Paddeu S., Nicolini C.** *Mater. Sci. Eng.: C.* 2000. V. 11. N 2. P. 121-128. DOI: 10.1016/S0928-4931(00)00195-8.
221. **Brglez Š.** *J. Clean. Prod*. 2021. V. 312. P. 127746. DOI: 10.1016/j.jclepro.2021.127746.
222. **Ulman A.** An Introduction to Ultrathin Organic Films: From Langmuir-Blodgett to Self-Assembly. Academic press. 2013. 443 p.
223. **Reason M., Smith G., Latham R., Teesdale-Spittle P., Ramsden J., Henry B.** *Int. J. Pharmaceut.* 2000. V. 195. N 1. P. 25-28. DOI: 10.1016/S0378-5173(99)00354-3.
224. **Chang S.M., Ebert B., Tamiya E., Karube I.** *Biosens. Bioelectron.* 1991. V. 6. N 4. P. 293-298. DOI: 10.1016/0956-5663(91)85014-N.
225. **Salamianski A.E., Zhavnerko G.K., Agabekov V.E.** *Surf. Coat. Technol.* 2013. V. 227. P. 62-64. DOI: 10.1016/j.surfcoat.2013.02.024.
226. **Kim D.I., Zhavnerko G.K., Ahn H.S., Choi D.H.** *Tribol. Lett.* 2004. V. 17. N 2. P. 169-177. DOI: 10.1023/B:TRIL.0000032442.03009.21.
227. **Zhang S.-w., Lan H.-q.** *Tribol. Int.* 2002. V. 35. N 5. P. 321-327. DOI: 10.1016/S0301-679X(02)00011-7.
228. **Torrent-Burgués J.** *BioNanoSci*. 2023. V. 13. N 3. P. 1324-1338. DOI: 10.1007/s12668-023-01112-2.
229. **Bland H.C., Moilanen J.A., Ekholm F.S., Paananen R.O.** *Langmuir*. 2019. V. 35. N 9. P. 3545-3552. DOI: 10.1021/acs.langmuir.8b04182.
230. **Eftimov P., Yokoi N., Tsuji K., Peev N., Georgiev G.A.** *Appl. Sci.* 2022. V. 12. N 23. P. 12095. DOI: 10.3390/app122312095.
231. **Olżyńska A., Wizert A., Štefl M., Iskander D.R., Cwiklik L.** *Biochim. Biophys. Acta (BBA) - Biomembr*. 2020. V. 1862. N 9. P. 183300. DOI: 10.1016/j.bbamem.2020.183300.
232. **Castelli F., Sarpietro M.G., Rocco F., Ceruti M., Cattel L.** *J. Colloid. Interface Sci.* 2007. V. 313. N 1. P. 363-368. DOI: 10.1016/j.jcis.2007.04.018.
233. **Brosseau C.L., Leitch J., Bin X., Chen M., Roscoe S.G., Lipkowski J.** *Langmuir*. 2008. V. 24. N 22. P. 13058-13067. DOI: 10.1021/la802201h.
234. **Kurniawan J., Ventrici de Souza J.F., Dang A.T., Liu G.-y., Kuhl T.L.** *Langmuir*. 2018. V. 34. N 51. P. 15622-15639. DOI: 10.1021/acs.langmuir.8b03504.
235. **Pavinatto F.J., Caseli L., Pavinatto A., dos Santos D.S., Nobre T.M., Zaniquelli M.E.D., Silva H.S., Miranda P.B., de Oliveira O.N.** *Langmuir*. 2007. V. 23. N 14. P. 7666-7671. DOI: 10.1021/la700856a.
236. **Jurak M.** *J. Phys. Chem. B.* 2013. V. 117. N 13. P. 3496-3502. DOI: 10.1021/jp401182c.
237. **Hac-Wydro K., Dynarowicz-Latka P.** *Ann.- Univ. Mariae Curie-Sklodowska Sect. AA – Chem.* 2013. V. 63. P. 47-60. DOI: 10.2478/v10063-008-0027-2.
238. **Thanka Rajan S., Subramanian B., Arockiarajan A.** *Ceram. Int.* 2022. V. 48. N 4. P. 4377-4400. DOI: 10.1016/j.ceramint.2021.10.243.
239. **Gonçalves M.C.P., Kieckbusch T.G., Perna R.F., Fujimoto J.T., Morales S.A.V., Romanelli J.P.** *Proc. Biochem*. 2019. V. 76. P. 95-110. DOI: 10.1016/j.procbio.2018.09.016.
240. **Leontidis E.** Langmuir–Blodgett Films: Sensor and Biomedical Applications and Comparisons with the Layer-by-Layer Method. In: Surface Treatments for Biological, Chemical, and Physical Applications. Chap. 5. 2017. P. 181-208. DOI: 10.1002/9783527698813.ch5.

241. **Pompeo G., Girasole M., Cricenti A., Cattaruzza F., Flamini A., Prosperi T., Generosi J., Congiu Castellano A.** *Biochim. Biophys. Acta (BBA) - Biomembr.* 2005. V. 1712. N 1. P. 29-36. DOI: 10.1016/j.bbamem.2005.03.007.
242. **Pereira A.R., de Oliveira Junior O.N.** *Eclética Química.* 2021. V. 46. N 1. P. 18-29. DOI: 10.26850/1678-4618eqj.v46.1SI.2021.p18-29.
243. **Dynarowicz-Łątka P., Kita K.** *Adv. Colloid. Interface Sci.* 1999. V. 79. N 1. P. 1-17. DOI: 10.1016/S0001-8686(98)00064-5.
244. **Nobre T.M., Pavinatto F.J., Caseli L., Barros-Timmons A., Dynarowicz-Łątka P., Oliveira O.N.** *Thin Solid Films.* 2015. V. 593. P. 158-188. DOI: 10.1016/j.tsf.2015.09.047.
245. **Singh A., Iyer A., Amiji M., Ganta S.** Multifunctional nanosystems for cancer therapy. In: Biomaterials for cancer therapeutics. 2013. Elsevier. P. 387-413. DOI: 10.1533/9780857096760.3.387.
246. **Fidalgo Rodríguez J.L., Dynarowicz-Latka P., Miñones Conde J.** *Chem. Phys. Lipids.* 2020. V. 232. P. 104968. DOI: 10.1016/j.chemphyslip.2020.104968.
247. **Kulig W., Cwiklik L., Jurkiewicz P., Rog T., Vattulainen I.** *Chem. Phys. Lipids.* 2016. V. 199. P. 144-160. DOI: 10.1016/j.chemphyslip.2016.03.001.
248. **Sottero B., Gamba P., Gargiulo S., Leonarduzzi G., Poli G.** *Curr. Med. Chem.* 2009. V. 16. N 6. P. 685-705. DOI: 10.2174/092986709787458353.
249. **Vollhardt D.** *J. Phys. Chem. C.* 2007. V. 111. N 18. P. 6805-6812. DOI: 10.1021/jp0704822.
250. **Ng S.C., Zhou X.C., Chen Z.K., Miao P., Chan H.S.O., Li S.F.Y., Fu P.** *Langmuir*. 1998. V. 14. N 7. P. 1748-1752. DOI: 10.1021/la970296v.
251. **Prabhakaran D., Yuehong M., Nanjo H., Matsunaga H.** *Analyt. Chem.* 2007. V. 79. N 11. P. 4056-4065. DOI: 10.1021/ac0623540.
252. **Gür F., Kaya E.D., Gür B., Türkhan A., Onganer Y.** *Colloid. Surf. A: Physicochem. Eng. Asp.* 2019. V. 583. P. 124005. DOI: 10.1016/j.colsurfa.2019.124005.
253. **Zhang T., Zheng B., Li L., Song J., Song L., Zhang M.** *Appl. Surface Sci.* 2021. V. 539. P. 148255. DOI: 10.1016/j.apsusc.2020.148255.
254. **Kang Y., Jang J., Lee Y., Kim I.S.** *Desalination*. 2022. V. 524. P. 115462. DOI: 10.1016/j.desal.2021.115462.
255. **Ma Z., Ren L.-F., Ying D., Jia J., Shao J.** *Desalination*. 2022. V. 539. P. 115952. DOI: 10.1016/j.desal.2022.115952.
256. **Iwamoto M., Shidoh S.-i.** *Jnp. J. Appl. Phys.* 1990. V. 29. N 10R. P. 2031. DOI: 10.1143/JJAP.29.2031.
257. **Seo Y., Jung C., Jikei M., Kakimoto M.-a.** *Thin Solid Films.* 1997. V. 311. N 1-2. P. 272-276. DOI: 10.1016/S0040-6090(97)00680-9.
258. **Ahn D.J., Franses E.I.** *AIChE J.* 1994. V. 40. N 6. P. 1046-1054. DOI: 10.1002/aic.690400615.
259. **Roy D., Nayan D., Ganesan V., Gupta P.** *Synth. Reactiv. Inorg. Metal-Org. Nano-Metal Chem.* 2015. V. 45. P. 560 - 566. DOI: 10.1080/15533174.2014.934572.
260. **Hemakanthi G., Nair B.U., Dhathathreyan A.** *J. Chem. Sci.* 2000. V. 112. N 2. P. 109-118. DOI: 10.1007/BF02704312.
261. **Petty M., Pearson C., Evenson S., Badyal J.** *Adv. Mater.* 1997. V. 9. N 1. P. 58-61. DOI: 10.1002/ADMA.19970090113.
262. **Peng X., Chen H., Kan S., Bai Y., Li T.** *Thin Solid Films.* 1994. V. 242. N 1-2. P. 118-121. DOI: 10.1016/0040-6090(94)90513-4.
263. **Geue T., Schultz M., Englisch U., Stömmer R., Pietsch U., Meine K., Vollhardt D.** *J. Chem. Phys.* 1999. V. 110. N 16. P. 8104-8111. DOI: 10.1063/1.478713.
264. **Prakash M., Ketterson J.B., Dutta P.** *Thin Solid Films.* 1985. V. 134. N 1-3. P. 1-4. DOI: 10.1016/0040-6090(85)90110-5.
265. **Sastry M., Mandale A.B., Badrinarayanan S., Ganguly P.** *Langmuir*. 1992. V. 8. N 10. P. 2354-2356. DOI: 10.1021/la00046a002.
266. **Raja N.S., Sankaranarayanan K., Dhathathreyan A., Nair B.U.** *Biochim. Biophys. Acta (BBA)-Biomembr.* 2011. V. 1808. N 1. P. 332-340. DOI: 10.1016/j.bbamem.2010.09.015.
267. **Yan H., Yang L., Yang Z., Yang H., Li A., Cheng R.** *J. Hazard. Mater.* 2012. V. 229-230. P. 371-380. DOI: 10.1016/j.jhazmat.2012.06.014.
268. **Villanueva M.E., Salinas S.R., Vico R.V., Bianco I.D.** *Colloid. Surf. B: Biointerfaces*. 2023. V. 227. P. 113337. DOI: 10.1016/j.colsurfb.2023.113337.
269. **Szafran K., Jurak M., Mroczka R., Wiącek A.E.** *Molecules*. 2023. V. 28. N 5. P. 2375. DOI: 10.3390/molecules28052375.
270. **Li S.** *Bioresour. Technol.* 2010. V. 101. N 7. P. 2197-2202. DOI: 10.1016/j.biortech.2009.11.044.
271. **Schoondorp M.A., Vorenkamp E.J., Schouten A.J.** *Thin Solid Films.* 1991. V. 196. N 1. P. 121-136. DOI: 10.1016/0040-6090(91)90180-6.
272. **La Fuente Arias C.I., Kubo M.T.K.-n., Tadini C.C., Augusto P.E.D.** *Crit. Rev. Food Sci.Nnutrition*. 2023. V. 63. N 14. P. 2260-2276. DOI: 10.1080/10408398.2021.1973955.
273. **Schoondorp M.A., Schouten A.J., Hulshof J.B.E., Feringa B.L.** *Langmuir*. 1992. V. 8. N 7. P. 1825-1830. DOI: 10.1021/la00043a023.
274. **Álvarez P.M., García-Araya J.F., Beltrán F.J., Masa F.J., Medina F.** *J. Colloid. Interface Sci.* 2005. V. 283. N 2. P. 503-512. DOI: 10.1016/j.jcis.2004.09.014.
275. **Xue H., Wu R., Xie Y., Tan Q., Qin D., Wu H., Huang W.J.A.S.** *Appl. Sci.* 2016. V. 6. N 7. P. 197. DOI: 10.3390/app6070197.
276. **Shi X., Huang L., Pan D.** *J. Power Sources.* 2020. V. 473. P. 228529. DOI: 10.1016/j.jpowsour.2020.228529.
277. **Buckner S.L., Agarwal V.K.** *Solar Energy Mater.* 1985. V. 12. N 2. P. 131-136. DOI: 10.1016/0165-1633(85)90028-0.
278. **Sarkın A.S., Ekren N., Sağlam Ş.** *Solar Energy*. 2020. V. 199. P. 63-73. DOI: 10.1016/j.solener.2020.01.084.
279. **Qi Y., Yaddehige M.L., Green K.A., Moore J., Jha S., Ma G., Wang C., Watkins D.L., Gu X., Patton D., Morgan S.E., Dai Q.** *J. Power Sources.* 2022. V. 536. P. 231518. DOI: 10.1016/j.jpowsour.2022.231518.
280. **Lee H.j., Cho Y.r., Yeo Y.s., Park S.h., Shin W.S., Jin S.h., Lee J.k., Kim M.r.** Dye-Sensitized Solar Cells with P3HT/Fullerene Derivatives. 2006 IEEE 4th World Conference on Photovoltaic Energy Conference. 2006. P. 259-262. DOI: 10.1109/WCPEC.2006.279440.
281. **Katayanagi H., Ohigashi T.** *Annual Rev.* 2016. 2016. P. 44. https://www.ims.ac.jp/en/about/publication/ann_rev_2016.html.
282. **Akhtar N., Gengler R.Y.N., Palstra T.T.M., Rudolf P.** *J. Phys. Chem. C.* 2012. V. 116. N 45. P. 24130-24135. DOI: 10.1021/jp307702k.
283. **Velázquez M.M., Alejo T., López Díaz D., Martín-García B., Merchán Moreno M.D.** Langmuir-Blodgett Methodology: A Versatile Technique to Build 2D Material Films. IntechOpen. 2016. 22 p. DOI: 10.5772/63495.
284. **Minakata T., Nagoya I., Ozaki M.** *Synth. Met.* 1991. V. 42. N 1. P. 1501-1508. DOI: 10.1016/0379-6779(91)91886-F.
285. **Cheung J.H., Rosner R.B., Rubner M.F.** *MRS Online Proceed. Library (OPL).* 1992. V. 247. P. 859. DOI: 10.1557/PROC-247-859.

286. **Goldenberg L.M., Pearson C., Bryce M.R., Petty M.C.** *J. Mater. Chem.* 1996. V. 6. N 5. P. 699-704. DOI: 10.1039/JM9960600699.
287. **Zhou Y., Dong X., Mi Y., Fan F., Xu Q., Zhao H., Wang S., Long Y.** *J. Mater. Chem. A.* 2020. V. 8. N 20. P. 10007-10025. DOI: 10.1039/D0TA00849D.
288. **Wang Y., Runnerstrom E.L., Milliron D.J.** *Annual Rev. Chem. Biomolec. Eng.* 2016. V. 7. N 1. P. 283-304. DOI: 10.1146/annurev-chembioeng-080615-034647.
289. **Paneliya S., Khanna S., Utsav, Singh A.P., Patel Y.K., Vanpariya A., Makani N.H., Banerjee R., Mukhopadhyay I.** *Renew. Energy.* 2021. V. 167. P. 591-599. DOI: 10.1016/J.RENENE.2020.11.118.
290. **Hoppe C.E., Williams R.J.J.** *J. Colloid. Interface Sci.* 2018. V. 513. P. 911-922. DOI: 10.1016/J.JCIS.2017.10.048.
291. **Kim K., Jeong J.H., Kim I.-J., Kim H.-S.** *J. Power Sources.* 2007. V. 167. N 2. P. 524-528. DOI: 10.1016/j.jpowsour.2007.01.097.
292. **Bazzi K., Mandal B.P., Nazri M., Naik V.M., Garg V.K., Oliveira A.C., Vaishnava P.P., Nazri G.A., Naik R.** *J. Power Sources.* 2014. V. 265. P. 67-74. DOI: 10.1016/j.jpowsour.2014.04.069.
293. **Fu M., Yu H., Huang S., Li Q., Qu B., Zhou L., Kuang G.-C., Chen Y., Chen L.** *Nano Lett.* 2023. V. 23. N 8. P. 3573-3581. DOI: 10.1021/acs.nanolett.3c00741.
294. **Razavi S.M.R., Oh J., Haasch R.T., Kim K., Masoomi M., Bagheri R., Slauch J.M., Miljkovic N.** *ACS Sustain. Chem. Eng.* 2019. V. 7. N 17. P. 14509-14520. DOI: 10.1021/ACSSUSCHEMENG.9B02025/SUPPL_FILE/SC9B02025_SI_008.AVI.
295. **Chen L., Meng H., Jiang L., Wang S.** *Chem. – An Asian J.* 2011. V. 6. N 7. P. 1757-1760. DOI: 10.1002/ASIA.201100010.
296. **Xing W., Shan Y., Guo D., Lu T., Xi S.** *Corrosion*. 1995. V. 51. N 1. P. 45-49. DOI: 10.5006/1.3293576.
297. **Sacilotto D.G., Costa J.S., Ferreira J.Z.** *Mater. Res.* 2022. V. 25. P. e20220268-e20220268. DOI: 10.1590/1980-5373-MR-2022-0268.
298. **Kraft A., Grimsdale A.C., Holmes A.B.** *Angew. Chem. Int. Ed.* 1998. V. 37. N 4. P. 402-428. DOI: 10.1002/(SICI)1521-3773(19980302)37:4<402::AID-ANIE402>3.0.CO;2-9.
299. **Hu B., Karasz F.E.** *Synth. Met.* 1998. V. 92. N 2. P. 157-160. DOI: 10.1016/S0379-6779(98)80105-7.
300. **Cheung J.H., Rubner M.F.** *Thin Solid Films.* 1994. V. 244. N 1. P. 990-994. DOI: 10.1016/0040-6090(94)90617-3.
301. **Correia F.C., Wang S.H., Péres L.O., Caseli L.** *Colloid. Surf. A: Physicochem. Eng. Asp.* 2012. V. 394. P. 67-73. DOI: 10.1016/j.colsurfa.2011.11.027.
302. **Mikroyannidis J.A., Fakis M., Spiliopoulos I.K.** *J. Polym. Sci. Part A: Polym. Chem.* 2009. V. 47. N 13. P. 3370-3379. DOI: 10.1002/pola.23412.
303. **Araghi H.Y., Giri N.K., Paige M.F.** *Spectrochim. Acta Part A: Molec. Biomolec. Spectrosc.* 2014. V. 129. P. 339-344. DOI: 10.1016/j.saa.2014.03.042.
304. **Perween S., Khan Z., Singh S., Ranjan A.** *Sci. Rep.* 2018. V. 8. N 1. P. 16038. DOI: 10.1038/s41598-018-34440-5.
305. **Zins D., Cabuil V., Massart R.** *J. Molec. Liq.* 1999. V. 83. N 1-3. P. 217-232. DOI: 10.1016/S0167-7322(99)00087-2.
306. **Zahn M.** *J. Nanopart. Res.* 2001. V. 3. N 1. P. 73-78. DOI: 10.1023/A:1011497813424.
307. **Wang Y.M., Cao X., Liu G.H., Hong R.Y., Chen Y.M., Chen X.F., Li H.Z., Xu B., Wei D.G.** *J. Magn. Magn. Mater.* 2011. V. 323. N 23. P. 2953-2959. DOI: 10.1016/J.JMMM. 2011.05.060.
308. **Shen L., Stachowiak A., Hatton T.A., Laibinis P.E.** *Langmuir.* 2000. V. 16. N 25. P. 9907-9911. DOI: 10.1021/LA0005412.
309. **Bahri A., Khamehchi E.** *Biointerface Res. Appl. Chem.* 2020. V. 10. N 6. P. 6652-6668. DOI: 10.33263/BRIAC106.66526668.
310. **Song J., Wang Q., Shaik I., Puerto M., Bikkina P., Aichele C., Biswal S.L., Hirasaki G.J.** *J. Colloid. Interface Sci.* 2020. V. 563. P. 145-155. DOI: 10.1016/J.JCIS.2019.12.040.
311. **Gmira A., Al Enezi S.M., Yousef A.A.** *SPE Middle East Oil Gas Show Conf, MEOS, Proceed.* 2017. V. 2017-March. P. 1511-1520. DOI: 10.2118/183855-MS.
312. **Caseli L.** *An. Acad. Bras. Ciênc.* 2018. V. 90. N 1. P. 631-644. DOI: 10.1590/0001-3765201720170453
313. **Berzina T.S., Troitsky V.I., Petrigliano A., Alliata D., Tronin A.Y.U., Nicolini C.** *Thin Solid Films.* 1996. V. 284-285. P. 757-761. DOI: 10.1016/S0040-6090(95)08439-8.
314. **Possarle L.H.R.R., Siqueira Junior J.R., Caseli L.** *Colloid. Surf. B: Biointerfaces.* 2020. V. 192. P. 111032. DOI: 10.1016/j.colsurfb.2020.111032.
315. **Kamegawa T., Suzuki N., Che M., Yamashita H.** *Langmuir.* 2011. V. 27. N 6. P. 2873-2879. DOI: 10.1021/la1048634.
316. **Zhong J., Deng Q., Cai T., Li X., Gao R., Wang J., Zeng Z., Dai G., Deng S.** *Fuel*. 2021. V. 292. P. 120248. DOI: 10.1016/j.fuel.2021.120248.
317. **Hague A., Díaz G.D., Hicks D.J., Krajewski S., Reed J.C., Paraskeva C.** *Int. J. Cancer.* 1997. V. 72. N 5. P. 898-905. DOI: 10.1002/(SICI)1097-0215(19970904)72:5%3C898::AID-IJC30%3E3.0.CO;2-2.
318. **Beyer-Sehlmeyer G., Glei M., Hartmann E., Hughes R., Persin C., Böhm V., Schubert R., Jahreis G., Pool-Zobel B.L.** *Br. J. Nutr.* 2003. V. 90. N 6. P. 1057-1070. DOI: 10.1079/BJN20031003.
319. **Reczyńska K., Marchwica P., Khanal D., Borowik T., Langner M., Pamuła E., and Chrzanowski W.** *Mater. Sci. Eng.: C.* 2020. V. 111. P. 110801. DOI: 10.1016/j.msec.2020.110801.
320. **Dałek P., Borowik T., Reczyńska K., Pamuła E., Chrzanowski W., Langner M.** *Langmuir*. 2020. V. 36. N 37. P. 11138-11146. DOI: 10.1021/acs.langmuir.0c02141.
321. **Akrami-Hasan-Kohal M., Eskandari M., Solouk A.** *Colloid. Surf. B: Biointerfaces.* 2021. V. 205. P. 111892. DOI: 10.1016/j.colsurfb.2021.111892.
322. **Nazari M., Safaeijavan R., Vaziri Yazdi A., Moniri E.** *Inorg. Chem. Commun.* 2023. V. 153. P. 110769. DOI: 10.1016/j.inoche.2023.110769.
323. **Овчинников В.В., Кулаков А.А., Григорьева И.Г., Мальцева С.А.** Термодинамические свойства органических кислот и их некоторых производных. *Изв. вузов. Химия и хим. технология.* 2019. Т. 62. Вып. 11. С. 38-45. **Ovchinnikov V.V., Kulakov A.A., Grigor′eva I.G., Maltseva S.A.** *ChemChemTech [Izv. Vyssh. Uchebn. Zaved. Khim. Khim. Tekhnol.]*. 2019. V. 62. N 11. P. 38-45. DOI: 10.6060/ivkkt.20196211.5990.

Поступила в редакцию 24.10.2023
Принята к опубликованию 25.09.2024

Received 24.10.2023
Accepted 25.09.2024